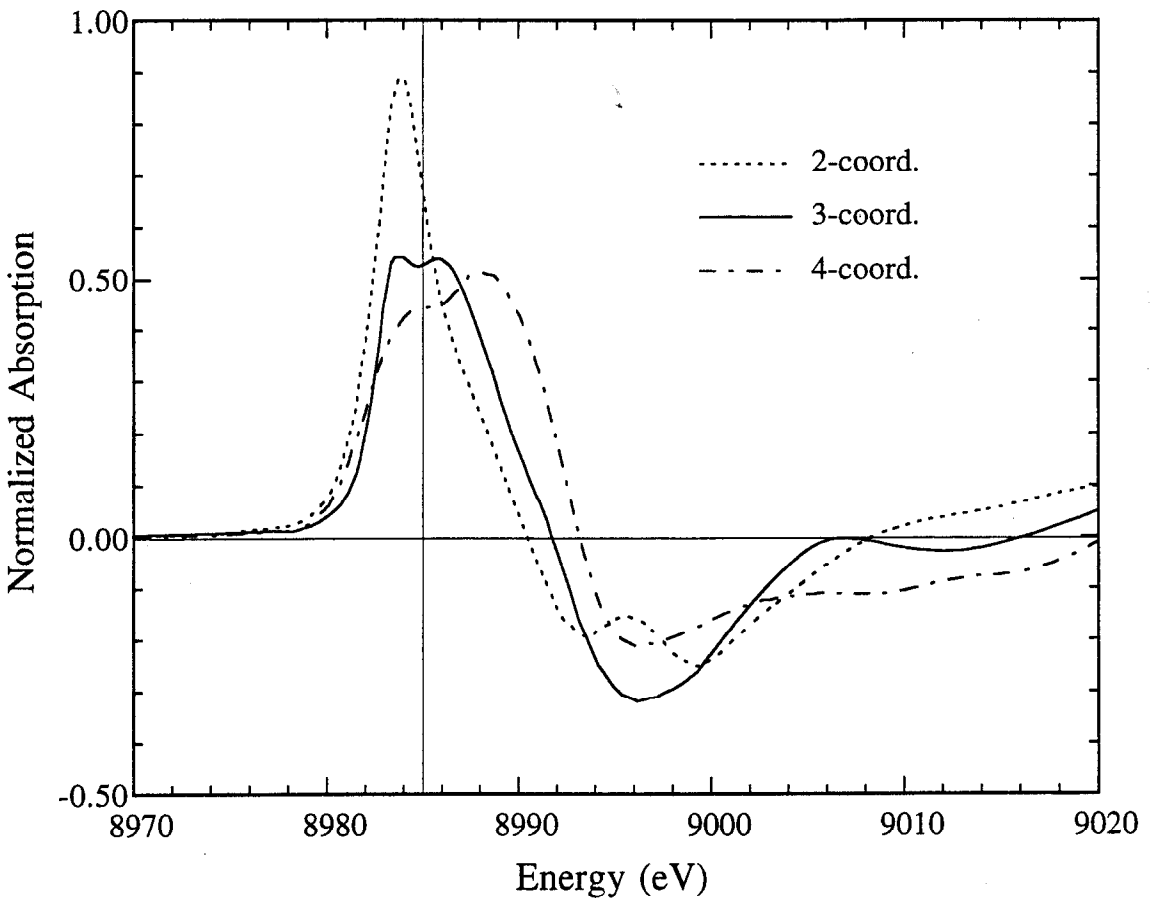

Figure 6.2. Difference edges of Cu(I) compounds when the edge of $[Cu_2(L_8\text{-}Et)(OAc)](ClO_4)_2$[24] (CUL2) is subtracted : Cu(I)(*N*-methylimidazole)$_2BF_4$,[25] linear 2-coordinate (- - - -); $[Cu(I)_2(mxyN_6)](BF_4)_2$,[26] 3-coordinate (——); and Cu(I)(*N*-methylimidazole)$_4ClO_4$,[27] tetrahedral 4-coordinate (— - — - —).

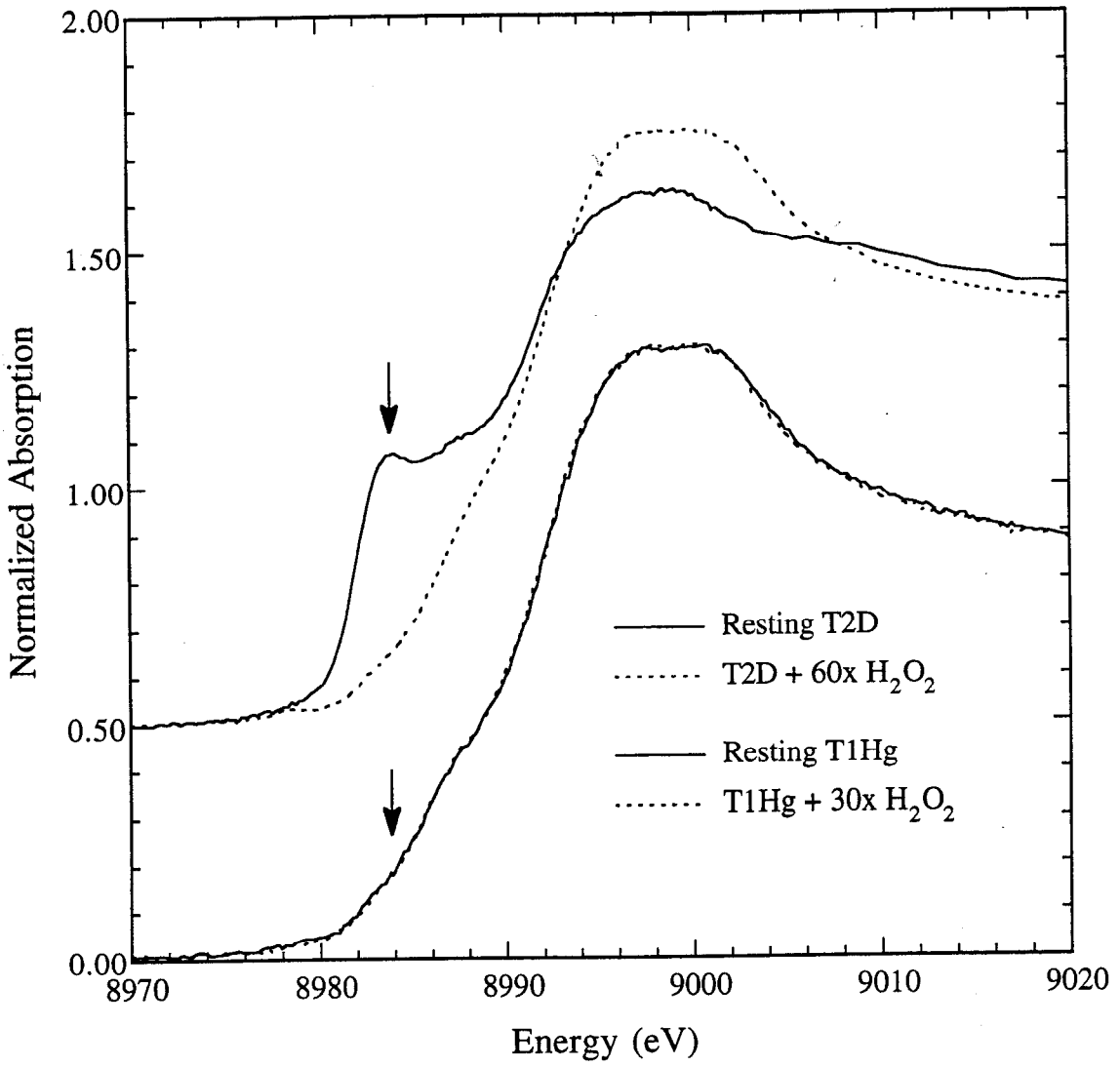

Figure 6.3. Edges of resting (——) and totally oxidized (H_2O_2-treated) (- - - -) laccase. Top : T2D laccase. Resting sample is corrected T2DS, totally oxidized sample is corrected T26A. Bottom : T1Hg laccase. Resting sample is corrected 1ML01, totally oxidized sample is corrected 2ML01.

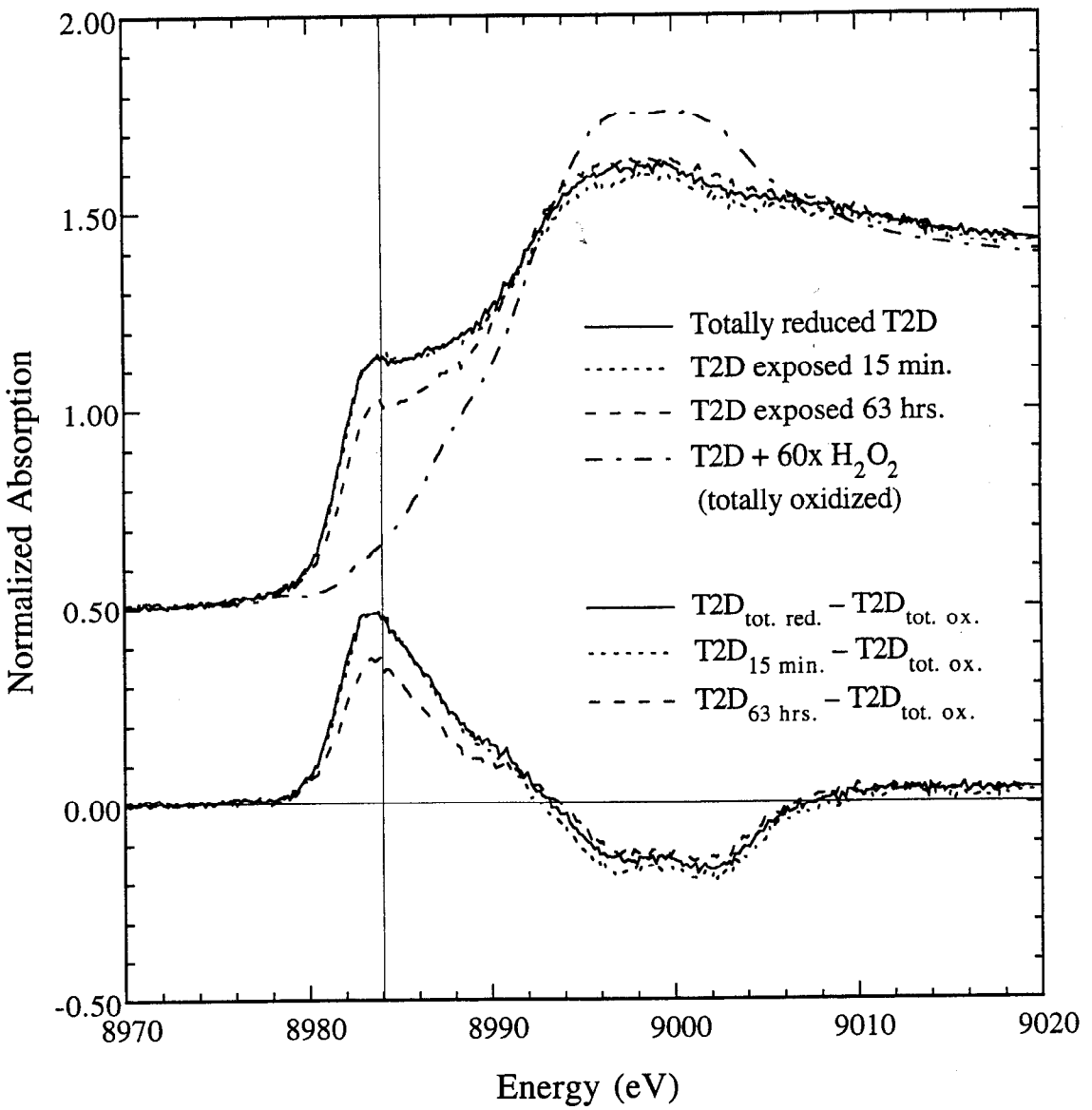

Figure 6.4. T2D laccase sample series showing reactivity with dioxygen. Top : Corrected X-ray absorption edges. Bottom : Difference edges made by subtracting totally oxidized T2D laccase (T26A). Totally reduced T2D (T2D1) (——), T2D exposed to air for 15 minutes (T2D2) (- - - -), T2D exposed for 63 hours (T2D3) (– – –) and totally oxidized T2D (T26A) (— - — - —).

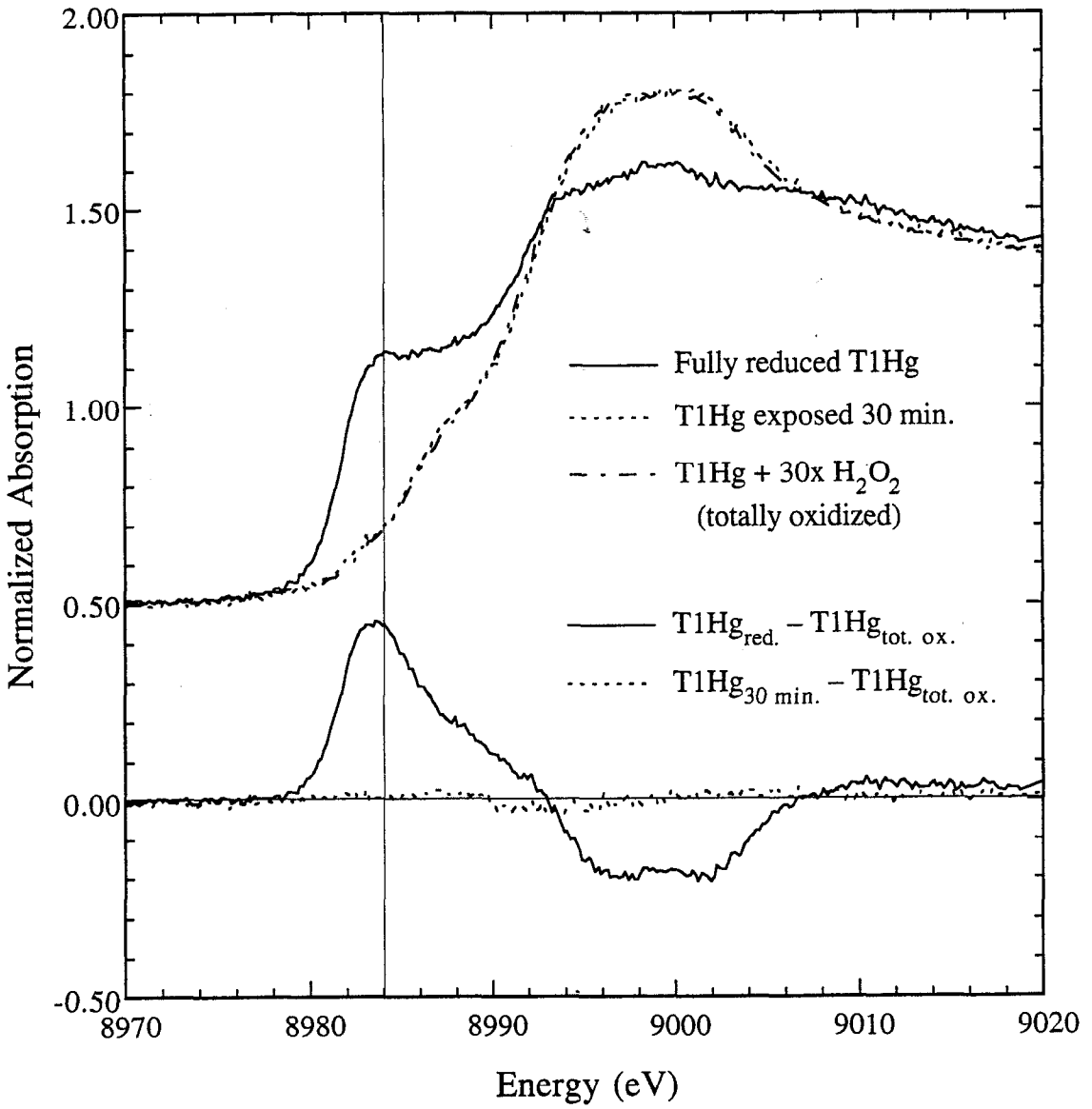

Figure 6.5. T1Hg laccase sample series showing reactivity with dioxygen. Top : Corrected X-ray absorption edges. Bottom : Difference edges made by subtracting totally oxidized T1Hg laccase (2ML01). Totally reduced T1Hg (MLRD) (——), T1Hg exposed to air for 30 minutes (MLOX) (- - - -), and totally oxidized T1Hg (2ML01) (— - — - —).

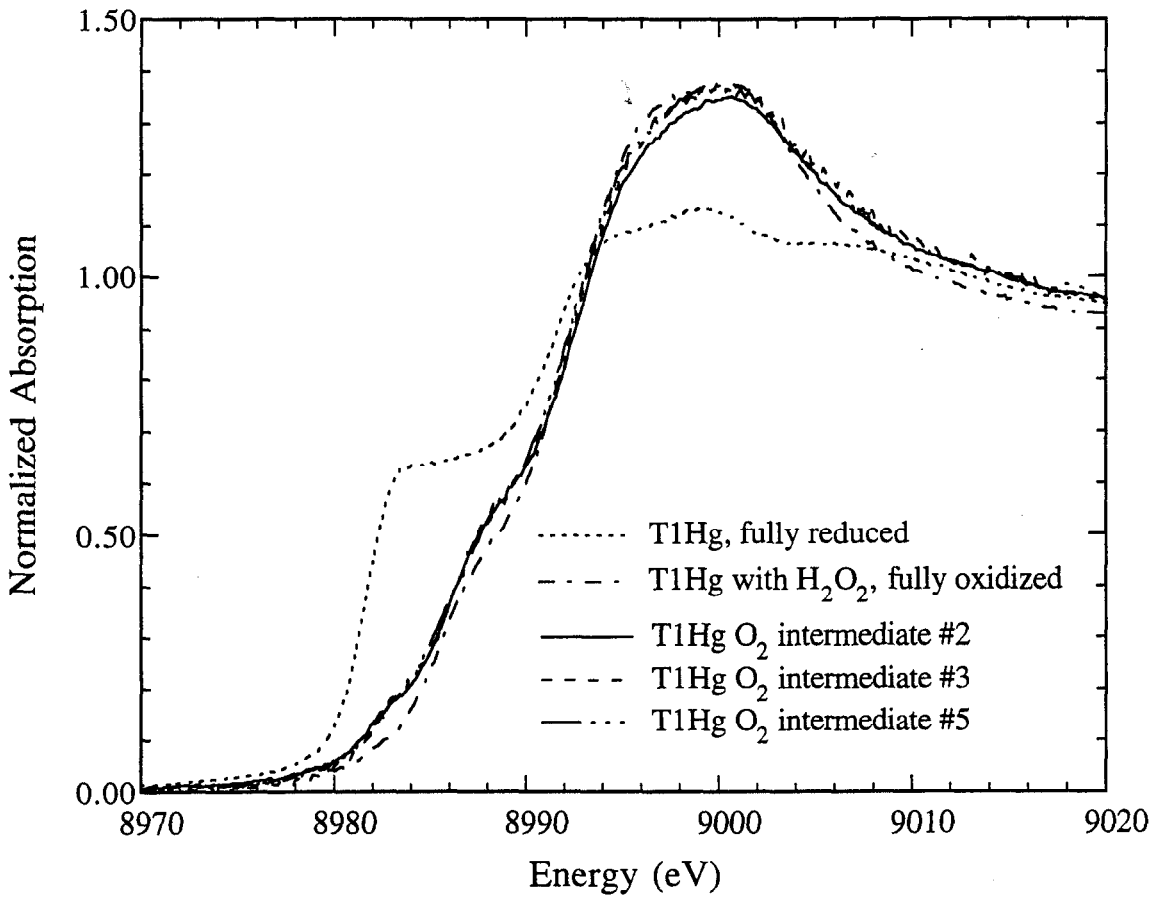

Figure 6.6. X-ray edges of some T1Hg O_2 intermediate samples, with fully reduced and fully oxidized T1Hg laccase. Edges are normalized, but no corrections for either native content or oxidation of T2 have been applied.

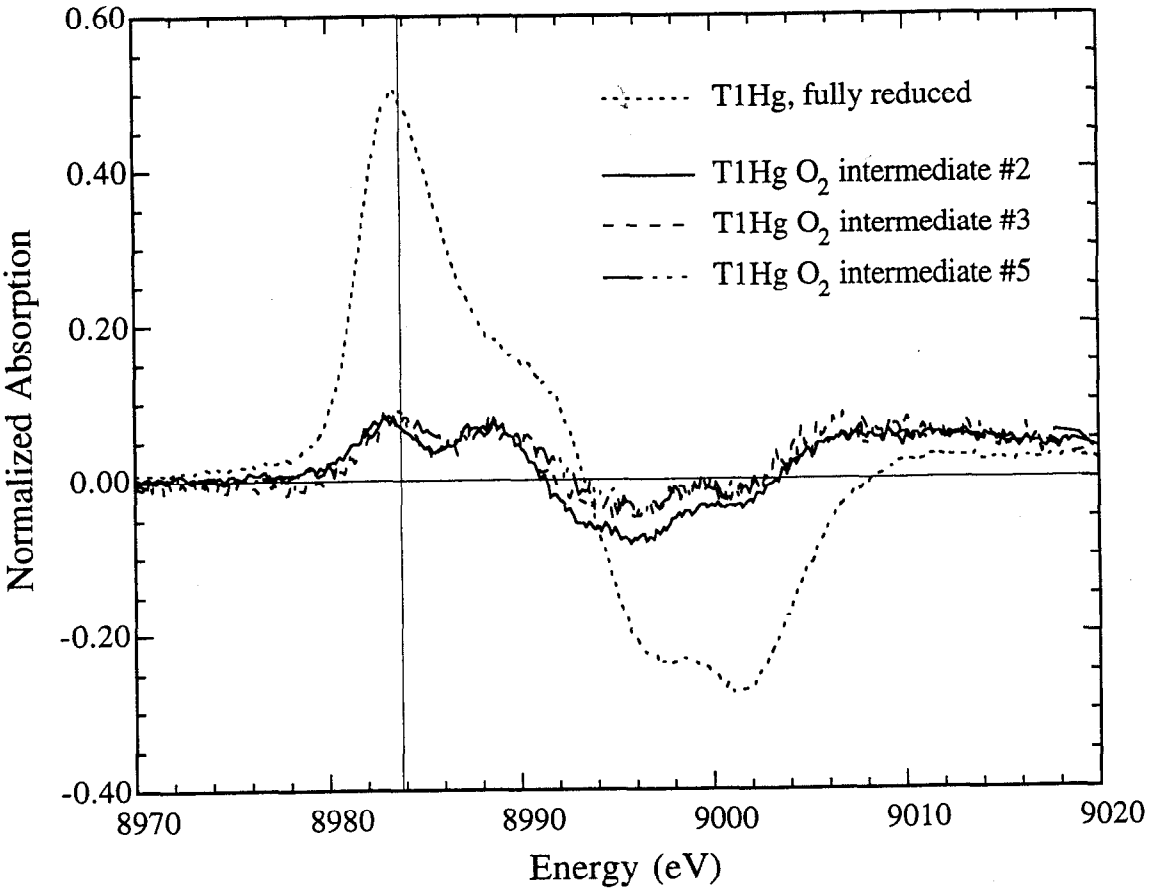

Figure 6.7. Corrected difference edges of "100% reduced ΔT1Hg" (see Table 6.3) and of some T1Hg O_2 intermediates with fully oxidized T1Hg (MLFOX, corrected) subtracted.

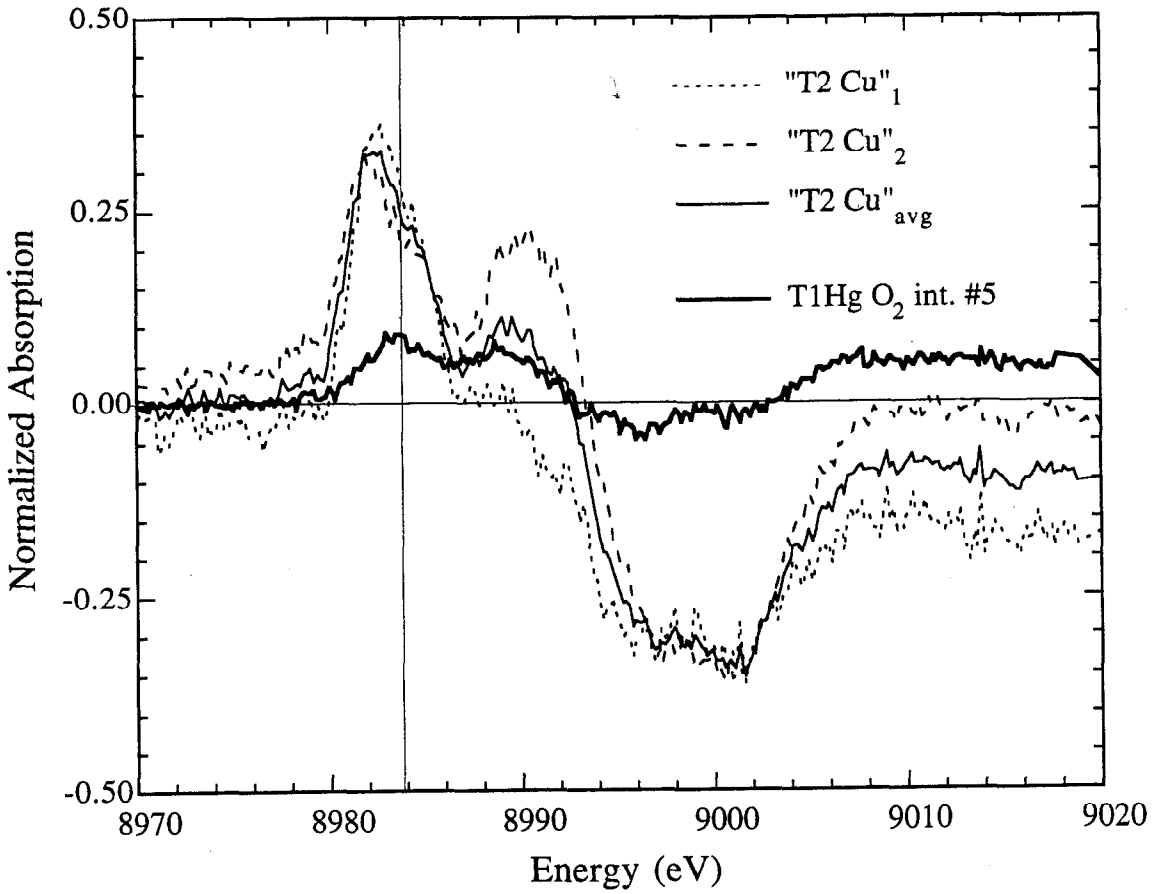

Figure 6.8. Difference edges of "100% reduced ΔT2", constructed by various methods (see Table 6.3), and a corrected difference edge of one sample of T1Hg O_2 intermediate. "ΔT2 $Cu"_1$ (- - - -), "ΔT2 $Cu"_2$ (– – – –), "ΔT2 $Cu"_{avg}$ (——) and T1Hg O_2 intermediate #5 (ML31) (▬▬).

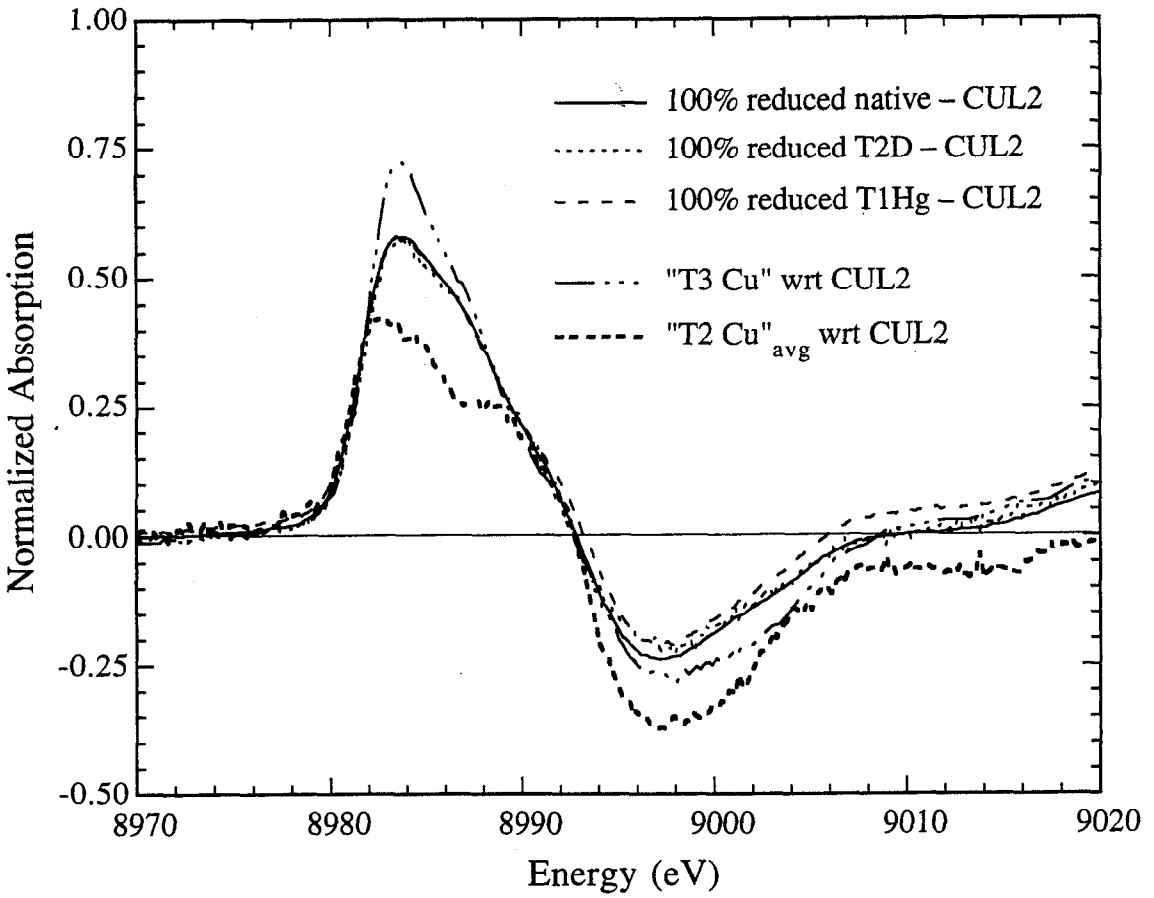

Figure 6.9. Corrected difference edges of various forms of laccase with CUL2 subtracted. Fully reduced native (——), T2D (- - - -) and T1Hg (– – –) laccase, "ΔT3 Cu" (- - - ——) and "ΔT2 Cu"$_{avg}$ (- - - -) with the edge of $[Cu_2(L_8\text{-Et})(OAc)](ClO_4)_2$[24] (CUL2) subtracted (see Table 6.5) for the purpose of determining the geometry of Cu(I) in laccase.

Chapter 7

Edge and EXAFS Studies of *Rhodospirillum rubrum* Nickel Carbon Monoxide Dehydrogenase and Nickel Model Compounds

(A) Brief Overview of *Rhodospirillum rubrum* Ni Carbon Monoxide Dehydrogenase

(1) Information Known From Other Studies

It has been known for some time that trace amounts of nickel are essential for healthy growth in plants and animals,[1] but the first nickel-containing enzyme, urease, was not identified until 1975. Since then, four classes of nickel-containing enzymes have been identified: urease (in plants), hydrogenase (in sulfate-reducing bacteria), methyl-S-coenzyme-M reductase (in methanogenic bacteria) and carbon monoxide dehydrogenase (in photosynthetic and acetogenic bacteria). As yet, no nickel enzymes have been discovered in animals.

The two classes of nickel-containing carbon monoxide dehydrogenase (henceforth CODH) so far characterized both run the following reaction :

$$CO + H_2O \rightleftharpoons CO_2 + 2H^+ + 2e^-$$

In acetogenic bacteria (the most intensively studied of which is *Clostridium thermoaceticum*), CODH is extremely flexible, and this reaction may proceed both ways, with concomitant synthesis (or at times degradation) of acetyl-coenzyme A from either CO or H_2-CO_2 at another site on the CODH enzyme.[2,3] However, in photosynthetic bacteria (including *R. rubrum*), this reaction proceeds only in the forward direction, generating CO_2 and H^+ from CO and H_2O, and the CODH does not itself carry out synthesis of any larger molecules.[4]

R. rubrum Ni CODH is a monomeric protein of 62 kDa containing one Ni, 8 Fe and approximately 8 inorganic S. It is associated *in vivo* with a 22-kDa subunit which contains four Fe in an Fe-S center.[5] *In vitro*, without the 22-kDa subunit, the 62-kDa unit is capable of converting CO to CO_2 in the presence of a low-potential one-electron reductant such as methyl viologen.[6] *In vivo*, the 22-kDa subunit serves to mediate electron transfer from CO to the hydrogenase in *R. rubrum*, thus enabling the latter to generate H_2. Beyond this, the physiological role of Ni CODH in *R. rubrum* is not yet clear.

An apo form of the 62-kDa unit can be obtained by growing *R. rubrum* in the absence of nickel.[7] Studies on this form of the protein show conclusively that Ni is required for the protein to be active, and strongly suggest that Ni is the site where CO binds.[8,9] EPR studies at liquid helium temperatures have been done on both the holo and apo forms, in oxidized and reduced states.[4,7,10] In the reduced state, an Fe_4S_4-type signal (seen at g = 1.90–2.05) due to about two such units was observed in both holo- and apo-Ni CODH. EPR on the oxidized state of the holo-Ni CODH showed two clusters of signals, one with g = 2.04, 1.90 and 1.71 and the other with g = 4.24, 4.32 and 4.40, while oxidized apo-

Ni CODH showed no signals at all. (Fe_4S_4 is EPR-silent when oxidized.) The signals observed in the oxidized holo-Ni CODH are therefore due to the Ni itself. Furthermore, the g = 2.04 feature was observed to broaden upon labelling with either ^{61}Ni or ^{57}Fe. Thus Ni is associated with the Fe-S clusters in some way.

(2) Some Questions About the Ni CODH Active Site

Although the studies mentioned above established that the active site of *R. rubrum* CODH must contain Ni associated with Fe-S clusters in some manner, before we undertook this XAS study nothing was known about the immediate environment of Ni — its geometry, ligation or relation to the Fe-S clusters. Is Ni actually part of a cubane cluster (i.e., $NiFe_3S_4$, shown in Figure 7.1(a))? Or is it instead attached to an Fe_4S_4 cluster through a bridge (Figure 7.1(b))? Also, we wanted to determine the coordination environment about the Ni, as a step towards understanding the structure and function of this enzyme.

(B) Some Results of XAS Studies on Ni Proteins and Model Compounds Carried Out by Other Workers

(1) Edge Studies on Ni Models

Major work in surveying the edges of Ni compounds of various coordination geometries and ligand types has been carried out by Robert A. Scott[11,12] and Michael J. Maroney.[13] Maroney's survey is more extensive, but, unfortunately, the energy resolution of the edge data collected by him is considerably lower than that collected by Scott. All Maroney's data were collected using Si[111] monochromator crystals, whereas Scott used Si[220] crystals and a 1-mm monochromator entrance slit. This means that Scott's edge data reveal more features and details than Maroney's do, and so afford more accurate conclusions.

The first feature of a nickel edge is the selection-rule-forbidden 1s→3d transition, which occurs at 8332-8333 eV, at the onset of the rising edge (Figure 7.2, bottom). This feature is extremely weak for compounds with centrosymmetric geometries (octahedral and square-planar), but grows much larger as the geometry deviates from centrosymmetry, because some mixing of the 3p and 3d orbitals then occurs, and so the transition becomes allowed in some degree. It reaches maximum height (still less than 10% of the total edge jump) with tetrahedral geometry.

For nitrogen-type ligands, octahedral compounds show a steep, featureless rising edge which often peaks sharply at a normalized amplitude of above 1.5 units (the overall

edge jump is scaled to 1 unit, see Chapter 2) and then dips well below 1.0 units (Figure 7.3, bottom). In square-planar compounds, on the other hand, the rising edge is interrupted by a spike at about 8337 eV, variously assigned as 1s→4s, 1s→$4p_z$, or 1s→4p plus shakedown, and the edge does not finally rise much above 1.2 units, or peak sharply at the top (Figure 7.2, top). The rising edge for tetrahedral compounds does not have the characteristic signature of a spike half-way up, nor does it rise to as tall a maximum, but it may show a shoulder half-way up (Figure 7.2, bottom). Five-coordinate compounds, as might be expected, show edges that are intermediate between all these, with medium-sized 1s→3d transitions, a relatively smooth rising edge that is not very steep and, usually, a slightly taller profile than edges of square-planar compounds (Figure 7.3, top). Where Ni(II) and Ni(III) compounds with the same ligands and ligating geometry can be compared, the Ni(III) edge shows similar features to the corresponding Ni(II) edge, only shifted to higher energy by 1–2 eV. However, this shift is not useful for identifying the Ni oxidation state in an unknown compound because the edge position is also affected by the polarizability of the ligands attached to Ni (*vide infra*).

Maroney further observed that rising edges of square-pyramidal compounds have a shoulder about halfway up, while those of trigonal-bipyramidal compounds rise featurelessly to a peak. He also noted that features for the Ni(III) compound edges are generally broader and and less distinct, and the areas of their 1s→3d transitions are about 50% larger, than those for the corresponding Ni(II) compounds.

When compared with edges of nitrogen-ligated compounds, edges of compounds with sulfur-type ligation also show the same characteristic transitions mentioned for the various geometries, but have lower maximum edge amplitudes (Figures 7.2 and 7.3). Thus, octahedral compounds lack a tall sharp peak. Edges of square planar compounds are still distinguished by spikes at 8337 eV, but are generally flatter on top. Another effect of sulfur ligation is that the edge is shifted to lower energy by 1–2 eV, which may be explained as due to the reduction of the positive charge density on the Ni atom by the more polarizable sulfur ligands. For Ni compounds with mixed nitrogen-type and sulfur-type ligands, Maroney found a smooth change in the characteristics the edges displayed as the proportion of sulfur ligation was increased.

(2) XAS Studies on Ni Proteins

EXAFS studies on all four classes of Ni-containing enzymes have been carried out.

In jack bean urease, Ni is coordinated with 5–6 N/O-type ligands, and a Ni-Ni interaction was detected in the 2-mercaptoethanol-inhibited enzyme.[14] In the S-methyl

coenzyme-M reductase of *Methanobacterium thermoautotrophicum*, the nickel "corphin" factor F_{430} has a Ni-tetrapyrrole structure. In free F_{430}, the pyrrole ring is ruffled and the Ni geometry is square-planar, but when the F_{430} is incorporated into the protein the coordination number rises to 5–6 N/O, in an octahedral geometry, and the pyrrole ring lies flat.[11,15]

In the hydrogenases, the most recent results show that Ni is coordinated with a mixture of nitrogen-type and sulfur-type ligands. In *Desulfovibrio baculatus* hydrogenase there are 3–4 N/O, 1–2 S/Cl, and also one selenium, coordinated to Ni in a pseudo-octahedral or pentacoordinate geometry.[16] In *Thiocapsa roseopersicina* hydrogenase, Ni is ligated by ~3 N/O and ~2 S in a trigonal bipyramidal geometry, and the EXAFS Fourier transform furthermore shows peaks at 4.3 Å and 6.2 Å that can be fitted with Fe and S, and so are suggestive of a Ni-Fe-S cluster.[17]

Two independent studies of the *Clostridium thermoaceticum* Ni CODH have also been published.[12,18] Data ranges were rather limited (to k ~10 $Å^{-1}$) in both studies, which may explain why one study (Bastian, *et al.*) suggested Ni–S_4 ligation (S at 2.16 Å) and one Fe at ~3.25 Å, while the other study (Cramer, *et al.*) suggested Ni–N_2S_2 ligation (N/O at 1.97 Å, S at 2.21 Å). Based on the edge of the protein, the latter study also suggested a distorted square-planar or square-pyramidal geometry for Ni. (A complicating factor, however, is that there are six Ni in each $\alpha_3\beta_3$ protein unit, and at least two different Ni sites.[3])

(C) Experimental Details

(1) Preparation of Samples

In all, we collected data on six samples of *R. rubrum* Ni CODH, four oxidized and two reduced, over three years. (Only five of these were subsequently analyzed; see next section.) All samples were provided by Professor Paul W. Ludden of the University of Wisconsin at Madison. *R. rubrum* CODH was purified and assayed as described in the literature.[4,9] The final step of purification, native gel electrophoresis, yielded two bands of CODH with differing activity and Fe content. The majority of CODH purified as peak 1, the more active band, and this band was used in all experiments. Activities were measured in terms of μmol of CO oxidized per minute per mg protein. Samples were prepared for spectroscopy in an anaerobic glove box [Vacuum Atmospheres (Hawthorne, CA) Dri-Lab glove box model HE-493] containing an N_2 atmosphere with <1 ppm O_2. The samples were oxidized with methyl viologen or indigo carmine on a DE52 column, eluted with sodium chloride solution, then concentrated if necessary in a collodion ultrafiltration

apparatus (Schleicher & Schuell). To produce reduced samples, sodium dithionite was added, for a final concentration of 5 or 10 mM dithionite. See Table 7.1 for the final concentrations of the samples and buffers, and for the specific activities of CODH. The redox states of the samples were not characterized by EPR or other spectroscopic methods before XAS data were measured on them.

The oxidized and reduced samples were each loaded into EXAFS cells made of lucite (outer dimensions $2 \times 4 \times 28$ mm^3, volume ~180 μl) with an X-ray-transparent front face of 40 μm Kapton tape for X-ray fluorescence measurements. The samples were stored in liquid nitrogen and also mounted for data collection under liquid nitrogen.

Some of the Ni(II) model compounds we used were obtained commercially, some were provided by collaborators, most notably Professor Richard H. Holm of Harvard University, and some were synthesized by us (see Table 7.2). The solid compounds were ground with boron nitride and packed into aluminum spacers in the manner described in Chapter 2.

(2) Data Collection

Protein data were collected at the unfocussed bending magnet beam line X19A at the National Synchrotron Light Source (NSLS), and at the unfocussed 8-pole wiggler beam line 7-3 at the Stanford Synchrotron Radiation Laboratory (SSRL) (see Table 7.1). (One data set, collected in April 1990 on beam line 4-2 at SSRL, proved much noisier and more glitch-ridden than all the other data sets, and it was not curvefitted, nor is it included in Table 7.1.) Si[220] monochromator crystals were used on all beam lines. For all the edge spectra shown, including those of model compounds and Fe edges measured on two of the protein samples in 1991, the monochromator entrance slit at SSRL BL 7-3 was set at a 1-mm vertical gap. (NSLS BL X19A lacked a monochromator entrance slit, but the hutch slit was set at a 1-mm gap.) EXAFS spectra were collected separately, employing a 2-mm or 1.5-mm gap in the slit (at both beam lines) for increased flux, except in 1992 at SSRL BL 7-3, when a 1-mm gap was maintained for combined edge-and-EXAFS scans (see Table 7.1). Besides the energy resolution of the data, edge scans also differed from EXAFS scans in that 6 motorsteps/eV rather than 3 motorsteps/eV were taken in the edge region of the scan. Edge spectra were measured to $k = 9$ Å^{-1} (Fe K edges were measured to $k = 11$ Å^{-1}) and EXAFS spectra were measured to $k = 15$ Å^{-1}.

All the model compound data were measured at SSRL on unfocussed beam lines, most of them on BL 7-3. All edges and most of the EXAFS were measured with a 1-mm monochromator slit; a few compounds had EXAFS scans measured with a 2-mm slit.

All data that we collected, both protein and model compound, were measured at 10 K. Some model compound data provided to us by Professor Robert A. Scott were measured at 4 K, under the same conditions as our data, at SSRL. Protein data were measured in fluorescence mode, using a 13-element Ge solid-state detector array.[19] Model compound data were measured in transmission mode.

No photoreduction or photooxidation (as seen by a change in the Ni or Fe edge) of any of the samples was observed during data collection.

(3) Data Analysis

Data were reduced and analyzed using XFPAKG, in the manner described in Chapter 2. Scans were calibrated using nickel foil as an internal standard, taking the first inflection point of the foil as 8331.6 eV. We made repeated attempts to obtain protein EXAFS data usable to k = 15 Å^{-1}, but were unable to do so because of a monochromator glitch at k = 12.8 Å^{-1}, which manifested itself as a large step in the two data sets with the lowest noise (CODHX and CODHRX, see Table 7.1). It was less severe in the other data sets, but we still considered it inadvisable to trust data beyond it. Subtraction of the background was done by fitting a polynomial to the EXAFS region and then applying this at the bottom of the "edge step" and extending this into the pre-edge region. A different three-region spline to k = 12.7 Å^{-1} was applied to each protein data set. Model compound data were splined (also with three regions) to the limit of the data (usually k = 14.5 Å^{-1} or 15 Å^{-1}, unless cut short by the monochromator glitch at k = 12.8 Å^{-1}) and then Fourier-transformed over the same range as the protein data for analysis. For all data analyzed in relation to the proteins, a data range of k = 3.0–12.0 Å^{-1} was used for the forward Fourier transform, and the data were then backtransformed to k = 3.25–11.75 Å^{-1} for curvefitting. Parameters were also extracted over the same data ranges. (An earlier analysis over a shorter data range, using only CODHX, has been published.[20])

For comparisons of the edges of the proteins and model compounds, the same one-region spline to k = 9 Å^{-1} was applied to most of the files, since normalization of peak heights can be greatly affected by spline curvature.

(D) Edge Studies

(1) Further Observations About Model Compound Edges

Apart from the observations of trends in Ni edges already made by Scott and Maroney (*vide supra*), it is difficult to pick out systematic trends based on finer details of geometry. We tried correlating features such as the height of the spike at 8337 eV or the

size and location of the 1s→3d transition with details of geometry such as the extent of chelation, bite size of chelating ligands, bond length and degree of saturation in the ligands. We could not find any trends that held for our entire library of edges. However, there were a number intriguing trends, or rather, exceptions to trends observed by Scott and Maroney, in subsets of related compounds.

One such trend may be observed in the edges of Ni($N_2S_2C_2$) (**5**), Ni($N_2S_2C_3$) (**6**) and Ni($N_2S_2C_4$) (**7**) (see Table 7.2 for all compounds discussed), provided to us by Professor Robert D. Bereman of North Carolina State University (Figure 7.4, bottom). These compounds differ only in that the stepwise lengthening of an alkane chain (from C_2 to C_4) in the tetradentate ligand forces increasing deviation from square-planar towards tetrahedral geometry. As we might expect, the progressive deviation from centrosymmetry is accompanied by a corresponding increase in the size of the 1s→3d transition in the edge as the 3d orbitals acquire more p character. We might also expect, based on the appearance of tetrahedral compound edges (*vide ante*), that the ~8337 eV spike should decrease in size or sharpness as the geometry deviated from planarity. However, this clearly does not happen, raising the possibility that the size of the spike does not depend primarily on the geometry of the compound.

On the other hand, we have measured two square-planar compounds where the ~8337 eV spike seems to have been broadened and reduced to a shoulder. Ni(tsalen) (**8**) differs from Ni(ebmba) (**9**) (Figure 7.4, middle) only in that two bonds in the ligand are unsaturated, allowing for conjugation around the bite of the chelate. Both compounds are truly square-planar; in both cases no weakly bonding interactions between molecules perturb the coordination geometry. In the other case, [Ni(SS_2)]$_2$ (**15**) (Figure 7.4, top), the Ni coordination is nominally square-planar, but the two Ni atoms are quite close to each other (2.74 Å), and so there is probably some interaction between them.

From this small sampling, we may hypothesize that delocalization of valence electrons is responsible for broadening of features in the Ni edge spectrum, in particular of the ~8337 eV transition. This is consistent with the appearance of the edges of $NiFe_3S_4$ cubanes (highly delocalized systems) (Figure 7.4, top) which, apart from the 1s→3d transition, do not show sharp features anywhere along the edge.

The edges of a series of tripodal Ni–NS_3L compounds provide another fascinating exception to the trends (Figure 7.5). The edge for [Ni($NS_3{}^{tBu}$)Cl](BPh_4) (**22**) is that of a typical trigonal bipyramidal compound, as described by Maroney. However, edges for all the other compounds in this series (where Cl is replaced by H, Me, CO and COMe respectively (**18–21**)) do not fit this description at all. They all rise at lower energy, have a

much lower profile, and show six transitions from the bottom of the edge (the 1s→3d transition) to the top of the edge (at ~8360 eV). The transition at ~8360 eV changes slightly in energy, but the other transitions remain at about the same energy for all four compounds, varying only in height. Of the five compounds in this series, only [Ni(I)(NS_3^{tBu})CO](BPh_4) is a Ni(I) compound; all the rest are Ni(II) compounds. Thus, the difference between L = Cl and all the rest cannot be explained by the Ni oxidation state, nor in terms of the spectrochemical series, which would predict a splitting in the 1s→3d feature for L = Cl (Ni should be high-spin in this case) rather than H, as we observed. Clearly, there are complex electronic effects at play, which cannot easily be accounted for by a simple ligand field theory.

Therefore, besides geometry and hardness of binding atoms, the appearance of Ni edges is affected by other electronic effects. The presence of a spike at ~8337 eV does not always mean that a compound is square-planar, nor does its absence always mean that the compound is not square-planar. However, in all the compounds we examined, the 1s→3d feature still proved a reliable indicator of centrosymmetry, so that it is still quite easy to distinguish square-planar compounds from tetrahedral compounds. Edges of trigonal bipyramid compounds can vary considerably in appearance, and we have no explanation that accounts for all of our data.

(2) Ni K and Fe K Edges of Ni CODH

The Ni edge of oxidized Ni CODH has the same sort of "smeared-out, low resolution" appearance as the edges of the $NiFe_3S_4$ cubanes and $[Ni(SS_2)]_2$ (Figure 7.6, top), though not the same precise shape. It has a 1s→3d feature of the same size as the cubane edges, which suggests that it may, like the cubanes, have a distorted tetrahedral coordination about Ni. Also, the edge rises at the same energy as the cubane edges. However, further up the edge rise, the Ni CODH edge does not resemble the cubane edge so closely. The $[Ni(SS_2)]_2$ edge does not match the CODH edge as closely even as the cubanes do, since the 1s→3d transition is a lot smaller and the edge rises at lower energy. We were not able to find any compounds that resembled the Ni CODH edge more closely than the cubanes or $[Ni(SS_2)]_2$. All the mononuclear compound edges that we compared the Ni CODH edge with had steeper edge rises and more sharply resolved transitions (Figure 7.6, bottom). All this suggests that, consistent with findings from EXAFS analysis,[20] Ni is not part of a $NiFe_3S_4$ cubane (*vide infra*), and also that the Ni atom is part of a highly delocalized electronic environment. Also, the coordination geometry of Ni is clearly not centrosymmetric, but is distorted four-coordinate (possibly tetrahedral) or perhaps five-coordinate.

A highly delocalized electronic environment would also explain why no shift in the edge could be observed when the Ni CODH was reduced (Figure 7.7). Indeed, the edges of oxidized and reduced Ni CODH, especially for the samples measured in 1992 (CDHOX and CDHRD), are practically identical. There is a small difference in the spectra for the oxidized and reduced samples measured in 1991 (CODHOX and CODHRX). However, there is just as much variation in the edges for the three oxidized samples measured in different years (Figure 7.8). Thus, all the Ni edges show that the Ni environment undergoes no major changes when the protein is reduced (despite indications to the contrary from EXAFS analysis, *vide infra*). The Ni atom may in fact be in the same oxidation state for both oxidized and reduced forms of the protein, rapidly tranferring any electrons it receives to the Fe-S units it is associated with.

We also measured Fe K edges (Figure 7.9) on oxidized and reduced CODH in 1991 (samples CODHOX and CODHRX). Consistent with results from EPR spectra, the Fe's in Ni CODH are definitely shown to be in an Fe_4S_4-cubane-like environment. Again, we could not observe any shift with redox state in these edges. The edge of the reduced protein is a little more "smeared out" in appearance, possibly reflecting the presence of two extra electrons (for two reduced Fe_4S_4 units). It is unlikely that a difference of two electrons spread out over 9 metal and 8 S atoms would be detectable by a shift in the X-ray edges, though it can be detected by EPR.

Thus the Ni K and Fe K edges of Ni CODH show that Ni in CODH has a distorted four-coordinate or five-coordinate environment, and that it is unlikely to be occupying one corner of a cubane. They also show that there is no significant change in the effective oxidation state of Ni, or the Ni ligand environment, upon changing the redox state of the protein.

(E) EXAFS Analysis of Ni CODH Samples and Related Model Compounds

(1) Extraction and Testing of Parameters on Model Compounds

Parameters extracted over a range of $k = 3.25–11.75$ Å^{-1} (*vide infra*) were thoroughly tested on model compounds in order to gauge their reliability. One-, two- and three-wave fits were carried out on filtered data from model compounds as shown in Tables 7.3 and 7.5–7.8. (See also Appendix III for complete fit results.)

The relative Debye-Waller factor is represented by the parameter c_2, which is always negative (see Chapter 2). A larger negative value of c_2 indicates more disorder in the distances of scatterers, or more vibrational disorder and a weaker Ni–X bond.

Coordination numbers and c_2 values were evaluated together to determine the most reasonable fit to a data set.

Fits were done either by floating coordination numbers and fixing c_2 (Type 2 fits), or varying c_2 and fixing coordination numbers (Type 3 fits), or occasionally by varying both coordination numbers and Debye-Waller factors (Type 1 fits). In all fits, the Ni–X distances of all waves were varied. In two- or three-wave Type 1 fits, there is considerable correlation between the coordination numbers and c_2 values, and so these fits do not have much physical significance as such. However, they can be useful in finding out what minimum the data tend towards.

(a) Extraction of Parameters and Tests on "Single-Shell" Compounds

Parameters over k = 3.25–11.75 $Å^{-1}$ were extracted from Ni(dmegly)$_2$ (**2**), (Ni–N = 1.85 Å), Ni(dedtc)$_2$ (**14**) (average Ni–S = 2.201 Å) and $(Et_4N)_2[NiFe_3S_4(PPh_3)(SEt)_3]$ (**10**) (average Ni··Fe = 2.689 Å).

In order to gauge a reasonable range of values for the Debye-Waller factors, the Ni–N and Ni–S parameters were fitted to several "single-shell" compounds, i.e. compounds with only one type of ligand, all occurring within a narrow range of distances. Testing was carried out on 12 compounds with Ni–N ligation and 5 with Ni–S ligation. The results are summarized in Table 7.3 and listed in full in Appendix III.

Distances were obtained with good accuracy, within 0.014 Å at worst and often within 0.006 Å. Also, the shorter the Ni–X bond, the lower the magnitude of the Debye-Waller factor (as shown by c_2). (The square-pyramidal Ni–N appears to be an exception to this trend. However, this compound has a cyclam-like ring ligated to the Ni, with a pyridine molecule in the apical position, probably at a longer distance. It is quite likely that we are seeing mainly the contribution from the cyclam ring nitrogens, and that the apical nitrogen actually interferes destructively with this signal, especially at higher values of *k*.) These fits also showed that the Ni–S parameters give much more reliable coordination numbers than the Ni–N parameters, with coordination numbers within 0.4 units (as opposed to 1.5 units) of the correct value. The range of reasonable c_2 values for four-coordinate Ni–N compounds is -0.0221 to -0.0265. For octahedral Ni–N compounds this range is -0.0253 to -0.0280. For Ni–S compounds, the corresponding ranges in reasonable c_2 values are -0.0201 to -0.0214 and -0.0217 (for one octahedral compound) respectively.

It can be seen that there is considerable latitude in the coordination numbers and relative Debye-Waller factors obtained, and that it would be hard to make a reliable judgement of the true coordination number from these alone. It is therefore helpful to also

take the length of the Ni–L bond into account when estimating a coordination number. To give us criteria for making such judgements, we surveyed 126 crystallographically determined model compounds with various geometries and ligand combinations, and the results are summarized in Table 7.4. As can be seen, square-planar compounds have the shortest bond lengths (e.g., Ni–N = 1.85–2.066 Å in Ni–N_4 compounds) and octahedral compounds the longest (e.g., Ni–N = 2.035–2.151 Å in Ni–N_6 compounds), and tetrahedral and five-coordinate compounds are somewhere in between. Also, the length of Ni–N does not seem to depend on whether there are S ligands also coordinated to Ni (e.g., Ni–N = 1.857–2.003 Å in square-planar Ni–N_2S_2 compounds), or how many S there are. The same is true of Ni–S with respect to the presence of N ligands. Rather, bond lengths are more affected by the steric and electronic character of the ligand for each compound. For square-planar Ni–S_4 compounds, the bond length shortens from 2.165–2.240 Å to 2.101–2.122 Å as the formal oxidation state of Ni increases from +2 to +4. This trend is also present, but not so well-substantiated, in Ni–N_2S_4 compounds.

The only compound available for testing the Ni–Fe parameters was $(Et_4N)_3[NiFe_3S_4(SEt)_4]$ (**11**). When the data for it were Fourier transformed, we obtained two peaks that were not very well separated and thus not optimal for testing the Ni–Fe parameters. Nevertheless, the second peak was windowed out and fitted with the Ni–Fe parameters. A good fit was obtained, with 2.6 Fe at 2.75 Å. A Type 3 fit (*vide supra*) with 3 Fe's gave a c_2 value of -0.0169 (result in Table 7.3).

(b) Further Testing of Parameters on Ni–N,S Compounds

Next, the Ni–N and Ni–S parameters were tested on compounds with mixed N,S ligation, namely Ni(tsalen) (**8**), $[Ni(NS_3{}^{tBu})H](BPh_4)$ (**18**) and $[Ni(N_3S_2)]$ (**16**). Ni(tsalen) is a fairly regular compound, with Ni–N = 1.85 Å, 1.86 Å and Ni–S = 2.174 Å, 2.139 Å. $[Ni(NS_3{}^{tBu})H](BPh_4)$ has a different ratio of N and S ligands, but is still fairly regular (Ni–N = 2.02 Å, Ni–S = 2.234, 2.227, 2.218 Å). $[Ni(N_3S_2)]$ is ligated by a strained terpyridine, and it also has two crystallographically inequivalent molecules, both of which make for more disorder in the ligand distances (Ni–N = 1.968–2.125 Å, Ni–S = 2.274–2.332 Å).

For all three compounds, the main Fourier transform peak was filtered out, and fits of Type 1, 2 and 3 (*vide supra*), using various combinations of N and S waves, were done on the backtransformed data (see Tables 7.5–7.7, and Appendix III for a complete list of fit results). For N+S and S+S' combinations, several Type 3 fits were made, exploring several possible combinations of N-type and S-type ligation. Results agreed with those of

the Type 2 fits, and also showed how shallow or deep the minimum was for numbers of N and S coordinated. In the case of [Ni(NS_3^{tBu})H](BPh_4), the main Fourier transform peak was narrower than that for the other two compounds, so fits were tried on data from two Fourier transform windows, one of the same width as for the other two compounds, and including a small low-R' peak, and the other narrower, including only the main peak. Results from both these windows were quite similar. The wider window showed somewhat less of undesirable correlation between coordination numbers (CN's) and relative Debye-Waller factors, so only the results from this window will be discussed. A summary of the results of the Type 2 fits is in Table 7.6, selected Type 3 fits are listed in Table 7.7, and results for all fits done are in Appendix III.

As in Chapter 5, fits using incorrect combinations of N and S waves as well as correct combinations were done. As expected, fits using one or two N waves were extremely poor, with either a high fit index, or unreasonable R, CN or c_2 values. Fits using one or two S waves do better. In Ni(tsalen) and [Ni(N_3S_2)], which have two S ligated to Ni, one S wave alone could not produce a reasonable fit, that is, no fit produces a combination of R, CN and c_2 that is physically reasonable (as judged from the results in Tables 7.3 and 7.4). Only 2 S are found, and they by themselves cannot constitute a coordination shell. However, in [Ni(NS_3^{tBu})H](BPh_4), which has three S ligated to Ni, 4 S at 2.22 Å gives a very reasonable fit, with a good fit index (F = 0.492). Again, for S+S' fits, a reasonable fit could not be obtained in Ni(tsalen) and [Ni(N_3S_2)], but [Ni(NS_3^{tBu})H](BPh_4) gave reasonable fits with a two-wave total of 3 or 4 S.

For all three compounds, reasonable N+S fits had a fit index which was 25% lower than reasonable S+S' fits. Also, distances obtained for Ni–N and Ni–S are all within 0.03 Å of the averaged crystallographic bond distances.

For Ni(tsalen) and [Ni(NS_3^{tBu})H](BPh_4), Type 2 fits produced the correct coordination numbers (2N/2S and 1N/3S respectively), and, of the various Type 3 fits tried, the most reasonable c_2 values were also obtained when the correct combination of CN's was used. However, the most reasonable Type 3 fit did not produce the lowest fit index. A slightly (less than 5%) lower fit index was achieved by fixing a larger CN for the N wave (3N/2S and 2N/3S respectively), which also resulted in a more negative c_{2N} value. Nevertheless, applying the criteria in Table 7.3 in a straightforward manner gives us the correct distances and coordination numbers.

In the case of [Ni(N_3S_2)], however, the Type 2 fit gives 1.9 N and 1.9 S. There is no Type 3 fit in which the c_2 values fit within the criteria listed in Table 7.3. A fit with 2N/2S comes the closest to being "reasonable", with c_2 values just barely outside the range

given in Table 7.3 (c_{2N} = -0.0270, c_{2S} = -0.0220). The fit with the correct CN's (3N/2S) gives c_{2N} = -0.0340, c_{2S} = -0.0233, while the fit with the lowest fit index (4N/2S) gives c_{2N} = -0.0406, c_{2S} = -0.0244. All three fits have fit indices within 10% of each other. From CN and c_2 values alone, then, we can tell that there are two S in the coordination shell, but the number of N is anywhere between two and four. If we take the Ni–S bond length (2.30 Å) into account, we can eliminate an octahedral 4N/2S geometry as highly unlikely, and then the shape of the edge spectrum (which is in this case typically trigonal bipyramidal) tips the balance towards the correct answer of three N and two S (although we cannot totally eliminate the possibility of tetrahedral coordination).

In summary, Ni–N and Ni–S distances can be obtained with a high degree of accuracy (within 0.03 Å for Ni–N and 0.01 Å for Ni–S). The number of S in a coordination shell can also be ascertained with some accuracy (within 0.1 units in these compounds), but the number of N was less accurate (being within 0.1 units for Ni(tsalen) and [Ni(NS_3^{tBu})H](BPh_4), but off by 1 unit for [Ni(N_3S_2)]). It can be seen from the fits to [Ni(N_3S_2)] that static disorder in the bond distances raises the Debye-Waller factor considerably, so that we have to exercise care in using Table 7.3 to eliminate possible geometries, especially with regard to N coordination. The c_2 values in Table 7.3 can be used to set a lower bound for the possible number of N or S coordinated to Ni. The bond distances in Table 7.4 can also be used to confirm or eliminate octahedral coordination. There is less difference in Ni–N and Ni–S bond distances between four and five-coordinated compounds of various geometries, but the variation in distances (together with the appearance of the edge) can still be useful in judging the more likely geometry.

(c) Testing for the Presence of Fe Using $(Et_4N)_3[NiFe_3S_4(SEt)_4]$

Since a major question about the Ni site in CODH is whether it is part of a cubane, we carried out EXAFS analysis on such a cubane, namely $(Et_4N)_3[NiFe_3S_4(SEt)_4]$ (**11**). For a more complete comparison with the fits done on the protein data (*vide infra*), reverse Fourier transforms were calculated including only the two major peaks (R' = 1.37–2.85 (0.1) Å — Window 2) and also including the two major peaks with a substantial shoulder to lower R (R' = 1.00–2.85 (0.1) Å — Window 3). S+Fe, S+S'+Fe and N+S+Fe fits were carried out on data from both backtransforms. A summary of selected fits is given in Table 7.8, with the complete results being listed in Appendix III. Results of fits to Window 2 are discussed first, then compared with results from Window 3.

S+Fe fits show that $(Et_4N)_3[NiFe_3S_4(SEt)_4]$ (**11**) has more disorder in Ni–scatterer distances than $(Et_4N)_2[NiFe_3S_4(PPh_3)(SEt)_3]$ (**10**) (from which Ni–Fe parameters were

extracted), showing only 2.3 Fe at a longer distance (2.75 Å vs. 2.689 Å). Unfortunately, no crystal structure of (**11**) is available with which to compare this result, which seems to indicate that (**11**) is a slightly less rigid or regular cubane than (**10**). A Type 3 fit of (**11**) with 4S/3Fe gives c_{2Fe} = -0.0184. The first shell (i.e., the scatterers directly coordinated to Ni) is also somewhat disordered, since a Type 2 fit gives 2.9 S, rather than 4 S, at 2.25 Å. A certain amount of disorder is expected, since the Ni–S(Et) distance is certainly different from the Ni–S(cubane) distance.

We hoped to distinguish the Ni–S(Et) and the Ni–S(cubane) bond distances with three-wave S+S'+Fe fits. We obtained two minima. One had S and S' at exactly the same distance (2.25 Å) with a total CN of 2.9, being in effect the same as the two-wave S+Fe fit. The other minimum had 3.5 S at 2.26 Å and 1.0 S' at 2.47 Å. It is possible that Ni–S(Et) is 2.47 Å long, and that we really are seeing the two Ni–S distances present in this compound. However, as Table 7.4 shows, the typical Ni–S bond in a tetrahedral compound is 2.25–2.30 Å long, so Ni–S(Et) would then be unusually long.

The N+S+Fe fits were carried out to make a comparison with the N+S+Fe fits done on the protein data (*vide infra*). We wished to see whether the N detected in the protein EXAFS spectra is real, or whether it is just filling in spaces, as it would be in fits to $(Et_4N)_3[NiFe_3S_4(SEt)_4]$. The N+S+Fe fits have higher fit indices than the S+S'+Fe fits. In these fits, the N-wave correlates with the S-wave, so that S is shifted to shorter distance (2.7 S at 2.22 Å), and N makes a rather large contribution (3.7 N at 2.16 Å). The Fe-wave, being at much longer distance, is not affected by this correlation. In the corresponding Type 3 fit with 2N/3S/1Fe, the N-wave shifts to 2.26 Å, but it is clear from the too-low c_2 values (c_{2N} = -0.0140, c_{2S} = -0.0153) that the same type of correlation is going on.

Results from fits on Window 3 were very similar to those from Window 2. In general CN's for S and N were a little higher, but not to any significant degree, and CN's for Fe were very slightly lower. In the S+S'+Fe fits, starting from the same initial values as in Window 2, we did not obtain the minimum wherein the two S waves go to exactly the same R. For both initial values, the other minimum, with 3.7 S at 2.26 Å and 1.2 S' at 2.47 Å, was obtained. (CN_S = 3.7 is rather high, since we expect to find only 3 S(cubane) atoms. This may indicate that some correlation occurs between the two S-waves.) The N+S+Fe fits once again did not match the data as closely as the S+S'+Fe fits. They also behaved in the same way as for Window 2, with the Type 2 fit giving 4.4 N at 2.19 Å and 3.4 S at 2.22 Å. The shift in R_N in the Type 3 fit with 2N/3S/1Fe is less dramatic this time, with R_N = 2.23 Å. The $|c_2|$ values are still too low (c_{2N} = -0.0184, c_{2S} = -0.0171), but they

are closer to the reasonable values set forth in Table 7.3. Thus, while the Type 2 fit would suggest that Window 3 contains more N than Window 2, the Type 3 fit suggests the opposite. We conclude that there really is the same amount of "N-wave contribution" in both windows.

In summary, fits to $(Et_4N)_3[NiFe_3S_4(SEt)_4]$ all show a strong Fe contribution, as expected for fits to a cubane, even though the contribution has been lessened by disorder in the Ni–Fe distances. Results from fitting Fourier Windows 2 and 3 turned out to be very similar. It is rather disconcerting that such a large N-wave should be obtained when no N is in fact present, but its effect on the S-wave, and the long Ni–N distance, are signs that it is not modelling any real presence of N ligands. Neither the number of S present, nor the number of N found, was much affected by the inclusion or exclusion of the "left shoulder of the main peak". It is also important to note that the N+S+Fe fits do not fit the data as closely as the S+S'+Fe fits in both windows. This is significant when compared with the different results obtained by including the "left shoulder" of the main peak in CODH data.

(2) EXAFS Analysis of *Rhodospirillum rubrum* Ni CODH Data

The EXAFS spectra for the five protein data sets are shown in Figure 7.10. It can be seen that the data for all the oxidized samples, and for CDHRD, have a beat node at k ~7–8 $Å^{-1}$. However, the EXAFS of CODHRX is qualitatively different, being much larger and not showing the beat node, although the presence of more than one shell of scatterers is shown by shoulders in the EXAFS. The Fourier transforms for the five data sets (Figure 7.11) show that CODHRX does indeed have a much taller peak than the other data sets, and that it alone also has three peaks above the noise at R' = 3–5 Å. However, all five Fourier transforms can be considered in terms of one main peak with "shoulders" on either side. These shoulders can be quite large compared with the main peak, and they are not in most cases easily separable from the main peak. Since we were not sure what contribution these shoulders might make to the EXAFS of the coordinating shell of Ni, various Fourier windows were used, both including and excluding the shoulders on either side, to obtain backtransformed data for curvefitting (see Table 7.9 and Figures 7.12 and 7.13). In particular, CODHX, the first data set to be collected and analyzed, shows a large, well-separated peak to the left of the main peak, which could not be reduced by splining. This peak was analyzed separately, as well as together with the main peak, and parallel fits were also done on the other data sets. The types of fits done for each window are shown in Table 7.10.

Results of some Type 2 and Type 3 fits are shown in Tables 7.11 and 7.12 respectively, and complete fit results are listed in Appendix III. Once again, for N+S and S+S' combinations, several Type 3 fits were made, exploring several possible combinations of N-type and S-type ligation. Again, Type 3 fit results generally agreed with those of the Type 2 fits, and also showed how shallow or deep the minimum was for numbers of N and S coordinated. Some variation in the Ni–X distance (usually Ni–N) with differing contributions of N and S was observed. Those fits for which the Ni–X distance differs by more than 0.02 Å from the corresponding Type 2 fit are considered to be less sound. These fits always also have c_2 values that are well outside the range set forth in Table 7.3. Generally, discussion of results will first be in terms of Type 2 fits, followed by additional insights from Type 3 fits, if any.

When using the fit index F (defined in Chapter 2) to evaluate the goodness of a fit to the data, we have to bear in mind that the fit index is not adjusted for the size of the signal. Thus, for equally good fits, we would expect the fit indices for fits to CODHRX to be larger than those for fits to the smaller signals in other data sets. The fit index is also affected by the noise level in a data set. So the fit index should only be used to compare different fits made on the same data. However, it can be seen from comparing Figures 7.14 and 7.15 (and also Figures 7.18 and 7.19) that the fits to CODHRX do in general achieve a worse match in phase and amplitude than corresponding fits in the other data sets.

(a) Results of One-Wave Fits

One-wave fits were performed on data from Windows 1 and 2. No attempt was made to fit data from Windows 3 or 6 with one wave because these had a beat node in the EXAFS (see Figure 7.13), and one wave clearly would not give a good fit.

Even though the Fourier transform peak of CODHX Window 1 looked quite different from that for the other data sets, when curvefitted with N or S all five data sets gave much the same result : either 1 N at about 1.9 Å, or less than 0.5 S at about 1.6 Å. In all cases it was obvious that the parameters did not match the signal in the backtransform at all, either in phase or in amplitude, and so this peak really does not contain either an N-type or an S-type wave. And so, even for CODHX, it is clear that the "first peak" or "left shoulder" cannot stand on its own.

For one-wave fits to data from Window 2 (see Table 7.11), N fits fared poorly, but S fits were able to give a fairly close fit of the data. Between 1.3 S and 1.8 S at 2.23 Å or 2.24 Å were obtained, except for CODHRX, which had 2.3 S at 2.25 Å. This suggests that the "main peak" does contain S.

(b) Results of Two-Wave Fits to Window 2

We turn to two-wave fits for a better indication of whether the "main peak" in Window 2 can account for a complete coordination of Ni by itself. N+N', S+S' and N+S fits were done on this window.

N+N' could not achieve a close fit of the data, and the fits achieved often had a total coordination number of more than six, which is chemically unlikely.

Of the two-wave fits tried, S+S' fits achieved the closest match to the Window 2 data. One of the S-waves was found at about the same distance (2.24–2.25 Å) and slightly higher CN (1.5–2.1 S, 3.1 S for CODHRX) as in the one-wave S fit. However, in all five data sets, the other S-wave was found at R < 2.1 Å. This is true for all Type 3 fits with reasonable c_2 values as well as for Type 2 fits. Since no Ni–S bond length of less than 2.1 Å has been found even for Ni^{IV}–S compounds (see Table 7.4), we reject S+S' as being a physically reasonable fit of the data.

In the N+S fits, two initial distances for N were tried: 2.1 Å and 1.9 Å. In the former case, the coordination number for N always refined to a negative value, so these fits will not be considered further. In the latter case, the S wave reached more or less the same R and CN as it did in the S only fit, and the contribution of the N wave varied between 0.4 N to 0.7 N (1.1 N for CODHRX). Except for CODHX, the N wave was at 1.89–1.91 Å. In CODHX, N was at 1.82 Å, which is shorter than Ni–N distances found for any model compound (see Table 7.4). In this case, especially when compared with fits done on other windows of CODHX (*vide infra*), it is doubtful that this represents a true N-wave. For CODHOX, the Type 3 1N/2S fit has a Ni–N distance of 1.84 Å (see Table 7.12), which is substantially different from the result for the Type 2 fit (0.4 N at 1.91 Å), and so it is also doubtful that this window contains a true N-wave. For the other three samples, some component of a true N-wave may be present. For CDHOX and CDHRD, the total coordination adds up to 1N and 2S, which is not quite sufficient for a complete coordination shell. For CODHRX, we observe 1N and 3S, which may indeed comprise a complete coordination shell.

(c) Results of Two-Wave Fits to Window 3

Window 3 includes both the major peaks in CODHX or, in the other data sets, the main peak plus its left shoulder. Again, N+N, S+S' and N+S fits were done on the data.

N+N' fits were actually able to achieve the closest fits to the data in the cases of CODHX and CODHOX (see Figure 7.14). However, these fits had total CN's of 11 (CODHX) or 8 (CODHOX), so they are not physically reasonable. For the other three data

sets, N+N' had the worst match to the data (see Figure 7.15), and total CN's ranged from 9 to 12. Once again, N+N' may be dismissed as physically implausible for the coordination shell of Ni.

In contrast to Window 2, S+S' fits were generally a poorer match to the data than N+S fits (see Figure 7.14). The one exception to this is CODHRX, where S+S' provides a slightly (15–20%) better match (see Figure 7.15). However, for all five data sets we again find that while one of the S-waves is at 2.25–2.27 Å, the other is always found at < 2.1 Å, both in Type 2 fits and in Type 3 fits with reasonable c_2 values. So S+S' is again not a reasonable coordination shell for this Fourier window.

N+S fits are the only ones wherein the R, CN and c_2 values of both waves used are all physically reasonable at the same time. With the exception of CODHRX, these fits also provide the closest match to the data. Again, CODHRX is different from the other data sets in that it shows a contribution of 3 S (2.8 S at 2.25 Å), while the rest show 2 S (2.0–2.1 S at 2.23–2.24 Å). (CODHOX shows 1.6 S, but a 1N/2S Type 3 fit gives c_{2S} = -0.0252, which is more reasonable than c_{2S} = -0.0162, which was obtained using 1N/1S.)

The contribution from the N-wave is rather weak by comparison, and so it is harder to firmly establish the number of N coordinated to Ni. It is possible that the presence of N is merely an artifact of the Fourier transform, an effect of including the left shoulder of the main Fourier peak in the backtransform. However, the tests done on $(Et_4N)_3[NiFe_3S_4(SEt)_4]$ (*vide ante*), with Fourier windows both excluding and including the left shoulder, showed that where no N's were ligated to Ni, no extra N's were found when the left shoulder was included in the transform. On the other hand, we found in all the CODH data sets that the amount of N-wave contribution was doubled or tripled when the left shoulder was included. We believe that this indicates the real presence of Ni–N coordination at ≤ 1.9 Å.

Our analysis also suggests a reason for the large, well-separated first peak in the CODHX Fourier transform. The Ni–N distance in CODHX was found to be 1.85 Å, while for the other data sets it was 1.89 Å (1.87 Å in CDHRD). Perhaps a greater spacing between the N and S distances in CODHX is the cause of the more pronounced beat pattern in the EXAFS of CODHX, which manifested itself as the split between the two peaks when the Fourier transform was applied.

In CODHX, we found 2.1 N at 1.85 Å. In the other two oxidized samples, we found 1.3 N at 1.89 Å. In Type 3 fits (Table 7.12), 2N/2S gave c_{2N} = -0.0216 for CODHX and c_{2N} = -0.0314 for both CODHOX and CDHOX. A Type 3 fit with 1N/2S gave c_{2N} =

-0.0219 and c_{2N} = -0.0218 for CODHOX and CDHOX respectively. Yet the edges of all three samples look very similar, so we do not expect a major change in the Ni geometry. It could be argued that, since the Ni–N bond length for CODHX (1.85 Å) is 0.04 Å shorter than those for CODHOX and CDHOX (1.89 Å), we would expect the bond to be stiffer and the c_2 value to be less negative for CODHX. This would allow us to interpret the low c_{2N} magnitude of -0.0216 as reasonable for CODHX. We may also further argue, based on Table 7.4, that a Ni–N distance of 1.85 Å is extremely unlikely with five-coordinate ligation, which we would have to accept if we concluded that 3 N's were present in CODHX. To accept a value of c_{2N} = -0.0314 as reasonable for the other two oxidized samples, however, we would also have to postulate a certain amount of static disorder in the Ni–N distances. If all this is true, then we can reconcile the differences in the EXAFS of these three samples with the similarity in their edges, and conclude that the most likely ligation for oxidized *R. rubrum* Ni CODH is two nitrogens and two sulfurs.

Reconciliation of edge and EXAFS data is even more difficult when the reduced CODH samples are considered. Besides the difference in the number of S coordinated, we find in CODHRX 1.9 N at 1.89 Å, while in CDHRD we find only 1.2 N at 1.87 Å. A Type 3 fit to CODHRX with 2N/3S gives c_{2N} = -0.0245, while a fit to CDHRD with 1N/2S gives c_{2N} = -0.0242. Yet the edges of both samples are almost identical, not only with each other, but with the edges of all the oxidized samples. In this case, it is not possible to reconcile this discrepancy, and so we have no definite conclusion about the numbers of N or S coordinated to Ni in reduced CODH from EXAFS analysis.

Instead, we have to conclude that either CODHRX or CDHRD is not a good reduced Ni CODH sample. Since CDHRD has exactly the same edge (see Figure 7.7), and also almost exactly the same EXAFS results as CDHOX, it may be that CDHRD is in fact an oxidized sample of Ni CODH. In this case, then, there is a real change in the Ni environment upon reduction, with Ni now being coordinated to 2 N at 1.89 Å and 3 S at 2.25 Å. It is amazing, though, that the addition of one sulfur ligand (or two, *vide infra*) should have made so little difference to the Ni edge of CODHRX. Alternatively, it may be CODHRX that is unreliable — perhaps denatured — and if so then the Ni site in Ni CODH shows no change upon reduction that is perceivable by EXAFS spectroscopy. A third reduced CODH sample, redox-characterized by optical or EPR spectroscopy, should be measured in the future to resolve this problem.

(d) Results of Two- and Three-Wave Fits to Window 6

The Fourier backtransform Window 6 includes the main peak, with both left and right shoulders. Since fits to Window 3 sufficiently proved N+S as the only plausible ligation for all data sets, N+N' and S+S' fits were not repeated on Window 6. However, N+S fits were carried out to see if including the right shoulder would have any effect on the coordination numbers or distances for N or S. As Table 7.11 shows, there is no significant difference in R's or CN's for either N or S. The fit indices are a little higher, but that is normal when more data are included in a Fourier window.

Three-wave fits to Window 6 were made in order to search for any Fe present within 3 Å of Ni, specifically in the "right shoulder" of the main peak, which is quite large for CODHOX, CDHOX and CDHRD (see Figure 7.11). It is pretty obvious, simply from visual inspection of the EXAFS and Fourier transforms of $(Et_4N)_2[NiFe_3S_4(PPh_3)(SEt)_3]$ and $(Et_4N)_3[NiFe_3S_4(SEt)_4]$ compared with those of any CODH data set (Figures 7.16 and 7.17), that Ni in *R. rubrum* CODH does not reside in an $NiFe_3S_4$ cubane. This is confirmed by the results of fits done on $(Et_4N)_3[NiFe_3S_4(SEt)_4]$, where at least 2 Fe were always found (*vide ante*), and the fits following. Note that, except for CODHRX, Window 6 does not include data above R' = 2.6 Å, meaning that we should not expect scatterers found at distances above 2.7 Å to have much physical meaning. The next peak at higher R in the Fourier transforms was not included because in most of the data sets this peak was barely above noise (see Figure 7.11).

N+S+S', N+S+Fe and N+S+N' fits were performed (see Figures 7.18 and 7.19). The N+S+S' and N+S+N' fits are control fits, to estimate the significance of "finding" any Fe with the N+S+Fe fits. In evaluating all these fits, we do not have any firm criteria for the maximum likely c_2 value for N' and S', since we have no model data for "second-shell" N or S. Since CODHRX has a right shoulder that is much less distinct than those for the other data sets, the results for it differ from the results for the rest.

With the N+S+S' fits, it was possible to obtain a minimum which was basically the same as the N+S fit, with the two S waves at the same distance having a total S coordination of the same magnitude as in the N+S fit. This fit is not shown in Table 7.11 or 7.12 (except for CODHX), since it adds no new information. The other minima that were obtained had N+S at about the same R's and CN's as in the two-wave N+S fits, with S' occurring at various distances. In all five data sets, 0.3–0.5 S' could be found at ~2.9 Å. In other fits, it was also possible to find about 0.4–0.6 S' at 2.43–2.48 Å (CODHOX and CDHOX) or 0.8 S' at 2.62 Å (CODHRX), or 0.7 S' at 2.16 Å (CDHRD).

The minimum with S' at ~2.9 Å was the closest fit to the data in the cases of CODHX, CDHOX and CDHRD. For CODHOX and CODHRX S' at ~2.4–2.6 Å produced a closer fit. However, in all the data sets except CODHRX S' at ~2.9 Å was better able to fit the right shoulder of the main peak (see Figure 7.20, top). For CODHRX, the best fit was obtained with S' at 2.6 Å (Figure 7.20, bottom). Considering both Type 2 and Type 3 fits, another minimum can be obtained in the reduced CODH data sets, in which the 2 S-waves correlate and one of them refines to R ≤ 2.18 Å, while the other is found at R ~2.3 Å. CODHRX and CDHRD also have one more minima in the Type 3 fits: in CODHRX, S' finds a minimum at 3.23 Å (but the fit to the data is poor), while in CDHRD, S' finds a minimum at 2.31 Å, with c_2 = -0.0612, which means that it makes essentially no contribution to the EXAFS signal.

In the N+S+Fe fits, two minima were again found. In both cases, N+S had the same R's and CN's as they did in the two-wave N+S fits, and were essentially unaffected by the location of the Fe-wave. The closer fit was achieved with 0.3–0.4 Fe at 2.70–2.76 Å (except for CODHRX, with 0.6 Fe at 2.80 Å). This minimum also produced the better fit of the right shoulder of the main peak (see Figure 7.21, top), except in CODHRX, where both minima fail to achieve a good fit to the right shoulder (Figure 7.21, bottom). Type 3 fits with 1 Fe gave c_{2Fe} values between -0.0256 and -0.0333 (except c_{2Fe} = -0.0184 for CODHRX). These values are well above those obtained with the $NiFe_3S_4$ cubanes (where c_{2Fe} = -0.0153 to -0.0194, from both (**10**) and (**11**)). However, since a single Fe connected by a single bridge to Ni would not be in as rigid a structure as Fe's in a cubane, these c_2 values are not improbable. Another minimum, with 0.1–0.2 Fe (0.6 Fe for CODHRX) at 3.06–3.09 Å, could also be obtained. Not surprisingly (since this is outside the range included in Window 6, except for CODHRX), the contribution of Fe is so slight as to be below the noise level (except in CODHRX), and also this fit does not manage to reproduce the right shoulder of the main peak in the Fourier transform (except, again, in CODHRX, where it actually produces a slightly better match in this region).

N+S+N' fits were carried out because N-waves are known to have phase shifts very similar to Fe-waves, and so it is easy to mistake one for the other when curvefitting. In this case, the N-wave parameters were so similar to the Fe-wave parameters that N+S+N' fits were almost indistinguishable from N+S+Fe fits. The N and S waves in these fits gave almost exactly the same R's, CN's and c_2's in corresponding fits. The CN's for the N'-wave were of course higher than those for the Fe wave, since N' is a lower *Z* scatterer; about 3 N's correspond to 1 Fe. We thus found a minimum with 1.1–1.3 N' at 2.71–2.76 Å, and another with 0.2–0.5 N' at 3.09–3.11 Å. (CODHRX is again different from the

rest, with 1.2 N' at 2.81 Å and 1.3 N' at 3.09 Å respectively, so that only 2 N's correspond to 1 Fe.)

Comparing the three classes of fits overall, we find that N+S+S', N+S+Fe and N+S+N' achieved comparably close fits to the data (as shown by the fit indices), except for CODHRX, where N+S+S' fitted a little more closely (see Tables 7.11 and 7.12).

Thus, for the four data sets giving similar results, while there may very well be 1 Fe at ~2.7 Å, there may equally well be 1 S at ~2.5 Å or more likely ~2.9 Å (since this fits the "right shoulder"), or several N at ~2.7 Å. Second-shell N-type scatterers (as, for instance, in imidazole rings) usually occur at 2.9–3.1 Å. Ni is most probably four-coordinate and thus would not have any ligating S further away than 2.3 Å (though we cannot rule out an unusual structure such as that found in plastocyanin, see Chapter 5). At ~2.7 Å, therefore, Fe is chemically the most plausible scatterer. Since N or Fe at ~2.7 Å rather than ~3.1 Å accounts better for the "right shoulder" in the Fourier transforms, and it is more likely that we see Fe than N at 2.7 Å, it is possible that 1 Fe is present in Ni CODH at ~2.7 Å from Ni. However, this conclusion is tentative.

For CODHRX, the best three-shell fit is N+S+S', with S' at 2.61–2.62 Å. Even so, this three-shell fit does not match the data as closely as the three-shell fits for the other data sets. However, if we accept this as the most plausible fit, then we have six-coordinate ($Ni\text{-}N_2S_4$) ligation, in which five of the bonds (Ni–N = 1.88–1.89 Å, Ni–S = 2.25 Å) are much shorter than Ni–N or Ni–S bonds in any octahedral model compound surveyed (see Table 7.4). It does not seem likely that so many ligands could crowd within such a short distance from Ni, and furthermore it is unlikely that a change from four-coordinate to six-coordinate geometry should have so little impact on the appearance of the edge. This suggests that, of the two reduced samples, it is CODHRX that is unreliable.

(e) Fits to the Fourier Peaks at R' = 3–5 Å From Ni in CODHRX

Since one possible model for the Ni site in *R. rubrum* CODH involves Ni bridged to a Fe_4S_4 cubane, we investigated whether the three peaks seen at R' = 3–5 Å in CODHRX might be due to backscattering from atoms in a cubane-like array.

Each peak was individually windowed and backtransformed (R' = 2.85–3.60 (0.1) Å — Window 7, R' = 3.52–4.20 (0.1) Å — Window 8, R' = 4.10–5.07 (0.1) Å — Window 9) and all three peaks were also included in a wide backtransform (R' = 2.85–5.07 (0.1) Å — Window 10). Fits using S-waves and Fe-waves were carried out on all four windows. (Fits using N-waves were not performed because N-waves and Fe-waves have such similar phase shifts.) Since the S and Fe parameters are being used at distances far larger

than the distances in the compounds from which they were extracted, the results from these fits are not definitive. At such distances, the CN values obtained would be only a rough indication of the presence or absence of S or Fe. The intrinsic EXAFS backscattering from atoms at longer distances is less than from shorter distances, so that CN values found would be lower than the actual number of scatterers present (e.g. 1 S found at 4 Å would suggest the presence of more than 1 S at that distance, but, without calibration on models of known structure, we cannot tell how many there in fact are). Results for some of these fits are shown in Table 7.13, and listed in full in Appendix III.

On each of Windows 7–9, fits were done using an S-wave only, an Fe-wave only, and S+Fe. In all cases, whether one- or two-wave, the parameters were able to achieve a fair-to-good match to the phase of the data above k ~8 Å^{-1}, where the amplitude was greatest, but at lower values of k the phase match was worse, being quite poor in some cases. In the one-wave fits, R_S was usually ~0.2 Å longer than R_{Fe}. In the S+Fe fits, it was possible to obtain two minima, one with R_S about the same as R_{Fe} and the other with R_S being ~0.2 Å longer than R_{Fe}.

On Window 7, S and Fe parameters both performed about as well as each other on the data, and combining them did not solve the problem of poorly matching phases at lower k. This suggests that Window 7 does not in itself completely contain either S or Fe, but does have elements of both, at ~3.5 Å (both S and Fe possible) or ~3.7 Å (for S). On Window 8, there were still problems with phase matching at lower values of k, but the S-wave did match the data better than the Fe-wave, and so we may conclude that Window 8 probably does contain the equivalent of 1.5 S at 4.19 Å, and not much Fe (particularly since CN_{Fe} becomes negative in one of the S+Fe fits). On Window 9, the Fe-wave matched the data much better than the S-wave, so in this case it is obvious that the dominant signal is an Fe-type signal, with the equivalent of 2.3 Fe at 4.87 Å.

On Window 10, only Type 2 fits were carried out. Between three and six waves were used at one time. When so many waves are used to fit EXAFS data, the risk of correlation between different waves is high, and, once again, the results should not be regarded as conclusive. Not all the possible combinations were explored, but, of the fits tried, we can make the following observations. We found five waves to be the minimum necessary to reproduce all the oscillations in the data. These had either S or Fe in the region of the first peak and both S and Fe for each of the other two peaks. Two solutions obtained were : (0.5 Fe at 3.54 Å, 1.8 S at 4.18 Å, 0.6 Fe at 3.83 Å, 1.1 S at 4.65 Å, 1.8 Fe at 4.88 Å) and 0.8 S at 3.73 Å, 2.0 S at 4.17 Å, 1.1 Fe at 3.82 Å, 1.0 S at 4.66 Å, 1.9 Fe at 4.87 Å). The latter is a slightly closer fit to the data.

To see whether S's and Fe's at the above distances could be due to a cubane, we used the crystal structure coordinates[21] for $[Fe_4S_4(SPh)_4]^{3-}$ as a model Fe_4S_4 cubane. Ni was attached by a bond 2.21 Å long to one of the S from SPh, such that the Ni–S–Fe angle was 103° and Ni··Fe was 3.52 Å. Ni was then rotated around the cubane by rotating the S–Fe bond (Figure 7.22). With Ni in various positions, the distances from Ni to the other Fe's and S's in the cubane were then measured. Apart from the Fe fixed at 3.52 Å, the other Fe's in the cubane were found at distances ranging from 4.7 Å to 6.3 Å, and the cubane S's at distances between 3.4 Å and 5.7 Å (not including the apical S furthest from Ni, which is at 6.7–7.2 Å from Ni), depending on the orientation of the cubane towards Ni.

This exercise makes it obvious that the Fe_4S_4 cubane is far too large a moiety to fit within the three high-R Fourier peaks in CODHRX. It is possible that we are seeing EXAFS signals from only one face of such a cubane. At certain orientations, our model shows as many as 2 Fe and 2 S within R = 3.5–4.9 Å. However, no orientation of the model shows 2 S at 4.2 Å or 2 Fe at 4.9 Å (these being the most stable waves in the fits to Window 10); at most only one atom occurs at each of these distances.

We may thus conclude that the Fourier peaks observed at R' = 3–5 Å are probably not due to an Fe_4S_4 cubane bridged to Ni through a terminal S, such as is shown in Figure 7.1(b), and probably not even due to two such cubane units. The origin of the Fourier peaks is in any case doubtful, since this sample shows contradictory results for its edge and its Ni coordination shell.

(F) Conclusion

Edge and EXAFS investigations of five samples of *Rhodospirillum rubrum* Ni CODH were carried out. Results from four of these samples (three oxidized and one of two reduced samples) show consistently that the nickel in the active site is most probably coordinated with two nitrogens (or oxygens) at 1.85–1.89 Å and two sulfurs at 2.23–2.25 Å, in a geometry that is considerably distorted from planarity, perhaps pseudo-tetrahedral. If this reduced sample is truly reduced, these four samples suggest that there is no significant change in ligation upon reduction of Ni CODH. Data from the other reduced sample were best fitted with two nitrogens (or oxygens) at 1.89 Å, but three sulfurs at 2.25 Å and a fourth sulfur at 2.61 Å. Most of these Ni–ligand distances are extremely short for a six-coordinate compound and suggest that this sample is unreliable. Otherwise, there is a major change in Ni ligation upon reduction of Ni CODH.

This, however, would not be consistent with the Ni and Fe K edges, which show no significant change with redox state, suggesting not only that the Ni ligation remains the

same, but also that there is extensive delocalization of electrons throughout the Ni/Fe/S cluster. The latter is also consistent with the "smeared-out, low-resolution" appearance of the Ni edge. The Fe edge of CODH shows a strong resemblance to the Fe edge of a $NiFe_3S_4$ cubane, confirming the presence of Fe_4S_4-type moieties in the protein.

Leaving aside the reduced sample that is most likely unreliable, edge and EXAFS results together suggest that the oxidation state and coordination shell of Ni do not change upon reduction or oxidation.

It is established beyond doubt that Ni is not part of an $NiFe_3S_4$ cubane. There is a possibility that 1 Fe was detected at ~2.7 Å in four of the samples, but this is by no means certain. It was found that a group of peaks at R' = 3–5 Å in the Fourier transform of one of the samples (whose reliability is doubtful) could not be fitted by modelling an Fe_4S_4 cubane ligated to Ni through a thiolate S. Thus, EXAFS analysis gives no firm evidence for an Fe_4S_4 cubane or two near Ni (as suggested by EPR and other studies), but does not preclude their existence.

Studies on more samples of Ni CODH, especially in the reduced state, would be desirable, to resolve the discrepancies that we have found. It would also be extremely interesting to interpret the edge and EXAFS spectra of Ni CODH with CO or CN^- bound to the site. Ni edges have many intriguing features, and these would also be worth investigating in the future.

References

(1) Ankel-Fuchs, D.; Thauer, R. K. In *The Bioinorganic Chemistry of Nickel*; J. R. Lancaster Jr., Ed.; VCH: New York, 1988; pp 93-110.

(2) Ragsdale, S. W.; Wood, H. G.; Morton, T. A.; Ljungdahl, L. G.; DerVartanian, D. V. In *The Bioinorganic Chemistry of Nickel*; J. R. Lancaster Jr., Ed.; VCH: New York, 1988; pp 311-332.

(3) Shin, W.; Lindahl, P. A. *Biochemistry* **1992**, *31*, 12870-12875.

(4) Bonam, D.; Ludden, P. W. *J. Biol. Chem.* **1987**, *262*, 2980-2987.

(5) Ensign, S. A.; Ludden, P. W. *J. Biol. Chem.* **1991**, *266*, 18395-18403.

(6) Ensign, S. A.; Campbell, M. J.; Ludden, P. W. *Biochem.* **1990**, *29*, 2162-2168.

(7) Bonam, D.; McKenna, M.-C.; Stephens, P. J.; Ludden, P. W. *Proc. Natl. Acad. Sci. USA* **1988**, *85*, 31-35.

(8) Ensign, S. A.; Bonam, D.; Ludden, P. W. *Biochem.* **1989**, *28*, 4968-4973.

(9) Ensign, S. A.; Hyman, M. R.; Ludden, P. W. *Biochem.* **1989**, *28*, 4973-4979.

(10) Stephens, P. J.; McKenna, M.-C.; Ensign, S. A.; Bonam, D.; Ludden, P. W. *J. Biol. Chem.* **1989**, *264*, 16347-16350.

(11) Eidsness, M. K.; Sullivan, R. J.; Scott, R. A. In *The Bioinorganic Chemistry of Nickel*; J. R. Lancaster Jr., Ed.; VCH: New York, 1988; pp 73-91.

(12) Cramer, S. P.; Eidsness, M. K.; Pan, W.-H.; Morton, T. A.; Ragsdale, S. W.; DerVartanian, D. V.; Ljungdahl, L. G.; Scott, R. A. *Inorg. Chem.* **1987**, *26*, 2477-2479.

(13) Colpas, G. J.; Maroney, M. J.; Bagyinka, C.; Kumar, M.; Willis, W. S.; Suib, S. L.; Baidya, N.; Mascharak, P. K. *Inorg. Chem.* **1991**, *30*, 920-928.

(14) Clark, P. A.; Wilcox, D. E.; Scott, R. A. *Inorg. Chem.* **1990**, *29*, 579-581.

(15) Eidsness, M. K.; Sullivan, R. J.; Schwartz, J. R.; Hartzell, P. L.; Wolfe, R. S.; Flank, A.-M.; Cramer, S. P.; Scott, R. A. *J. Am. Chem. Soc.* **1986**, *108*, 3120-3121.

(16) Eidsness, M. K.; Scott, R. A.; Prickril, B. C.; DerVartanian, D. V.; Legall, J.; Moura, I.; Moura, J. J. G.; Peck, H. D., Jr. *Proc. Natl. Acad. Sci. USA* **1989**, *86*, 147-151.

(17) Maroney, M. J.; Colpas, G. J.; Bagyinka, C.; Baidya, N.; Mascharak, P. K. *J. Am. Chem. Soc.* **1991**, *113*, 3962-3972.

(18) Bastian, N. R.; Diekert, G.; Niederhoffer, E. C.; Teo, B.-K.; Walsh, C. T.; Orme-Johnson, W. H. *J. Am. Chem. Soc.* **1988**, *110*, 5581-5582.

(19) Cramer, S. P.; Tench, O.; Yocum, M.; George, G. N. *Nucl. Instr. Methods Phys. Res.* **1988**, *A266*, 586-591.

(20) Tan, G. O.; Ensign, S. A.; Ciurli, S.; Scott, M. J.; Hedman, B.; Holm, R. H.; Ludden, P. W.; Korszun, Z. R.; Stephens, P. J.; Hodgson, K. O. *Proc. Natl. Acad. Sci. USA* **1992**, *89*, 4427-4431.

(21) Carney, M. J.; Papaefthymiou, G. C.; Whitener, M. A.; Spartalian, K.; Frankel, R. B.; Holm, R. H. *Inorg. Chem.* **1988**, *27*, 346-352.

(22) Stavropoulos, P.; Muetterties, M. C.; Carrié, M.; Holm, R. H. *J. Am. Chem. Soc.* **1991**, *113*, 8485-8492.

(23) Vannerberg, N.-G. *Acta Chem. Scand.* **1964**, *18*, 2385-2391.

(24) Godycki, L. E.; Rundle, R. E. *Acta Cryst.* **1953**, *6*, 487-495.

(25) Williams, D. E.; Wohlauer, G.; Rundle, R. E. *J. Am. Chem. Soc.* **1959**, *81*, 755-756.

(26) Kratky, C.; Waditschatka, R.; Angst, C.; Johansen, J. E.; Plaquevent, J. C.; Schreiber, J.; Eschenmoser, A. *Helv. Chim. Acta* **1985**, *68*, 1312-1337.

(27) Waditschatka, R.; Kratky, C.; Jaun, B.; Heinzer, J.; Eschenmoser, A. *J. Chem. Soc., Chem. Commun.* **1985**, 1604-1607.

(28) Davis, W. M.; Roberts, M. M.; Zask, A.; Nakanishi, K.; Nozoe, T.; Lippard, S. J. *J. Am. Chem. Soc.* **1985**, *107*, 3864-3870.

(29) Martin, E. M.; Bereman, R. D.; Singh, P. *Inorg. Chem.* **1991**, *30*, 957-962.

(30) Yamamura, T.; Tadokoro, M.; Kuroda, R. *Chem. Lett.* **1989**, 1245-1246.

(31) Yamamura, T.; Tadokoro, M.; Hamaguchi, M.; Kuroda, R. *Chem. Lett.* **1989**, 1481-1484.

(32) Ciurli, S.; Ross, P. K.; Scott, M. J.; Yu, S.-B.; Holm, R. H. *J. Am. Chem. Soc.* **1992**, *114*, 5415-5423.

(33) Ciurli, S.; Yu, S.-b.; Holm, R. H.; Srivastava, K. K. P.; Münck, E. *J. Am. Chem. Soc.* **1990**, *112*, 8169-8171.

(34) Swenson, D.; Baenziger, N. C.; Coucouvanis, D. *J. Am. Chem. Soc.* **1978**, *100*, 1932-1934.

(35) Kobayashi, A.; Sasaki, Y. *Bull. Chem. Soc. Jpn.* **1977**, *50*, 2650-2656.

(36) Bonamico, M.; Dessy, G.; Mariani, C.; Vaciago, A.; Zambonelli, L. *Acta Cryst.* **1965**, *19*, 619-626.

(37) Baker, D. J.; Goodall, D. C.; Moss, D. S. *J. Chem. Soc., Chem. Commun.* **1969**, 325.

(38) Barclay, G. A.; McPartlin, E. M.; Stephenson, N. C. *Acta Cryst.* **1969**, *B25*, 1262-1273.

(39) Baidya, N.; Olmstead, M.; Mascharak, P. K. *Inorg. Chem.* **1991**, *30*, 929-937.

(40) Shetty, P. S.; Fernando, Q. *J. Am. Chem. Soc.* **1970**, *92*, 3964-3969.

(41) Zompa, L. J.; Margulis, T. N. *Inorg. Chim. Acta* **1978**, *28*, L157-L159.

(42) Setzer, W. N.; Ogle, C. A.; Wilson, G. S.; Glass, R. S. *Inorg. Chem.* **1983**, *22*, 266-271.

(43) Ferrari, A.; Braibanti, A.; Bigliardi, G. *Acta Cryst.* **1963**, *16*, 846-847.

Table 7.1. Samples of Ni CODH on which data were collected (does not include one sample collected in April 1990, which was not analyzed).

Data Set Name	**CODHX**	**CODHOX***	**CDHOX**	**CODHRX***	**CDHRD**
Redox State	oxidized	oxidized	oxidized	reduced	reduced
$[Ni^{2+}]$	0.85 mM	1.4 mM	1.5 mM	1.4 mM	1.5 mM
Buffer	50 mM Mops/D_2O with 1 mM indigo carmine, pH 7.5	100 mM Mops, pH 7.5, in 10% glycerol	25 mM Mops, pH 7.5, 15% glycerol, 400 mM NaCl	100 mM Mops, pH 7.5, in 10% glycerol, 5 mM $Na_2S_2O_4$	25 mM Mops, pH 7.5, 15% glycerol, 400 mM NaCl, 10 mM $Na_2S_2O_4$
Activity†	~4000 units/mg	5200 units/mg	3600 units/mg	5200 units/mg	3600 units/mg
Date measured	June 1989	July 1991	July 1992	July 1991	July 1992
Beam Line	NSLS X19A	SSRL 7-3	SSRL 7-3	SSRL 7-3	SSRL 7-3
Ring Current	92-170 mA	24-39 mA	50-92 mA	19-52 mA	38-77 mA
Good scans	6 edge 16 EXAFS	10 edge 29 EXAFS (9 good detectors)	11 edge/EXAFS 20 EXAFS	13 edge 34 EXAFS	30 edge/EXAFS

* — Fe K edges were also measured, to $k = 11$ Å^{-1}.

† — Activity was measured in μmol CO oxidized per minute per mg protein

Table 7.2. Ni model compounds used in this study (continued on next page).

No.	Short name	Full name	Ni ligation	Supplier	Ref.
1	$K_2Ni(CN)_4$	Potassium tetracyanonickelate(II)	C_4	commercial	23
2	$Ni(dmegly)_2$	Bis(dimethylglyoximato)nickel(II)	N_4	commercial	24,25
3	Ni(corphin)	Nickel(II) *ccccc*-octaethyl-pyrrocorphinate	N_4	Scott	26,27
4	[Ni(TC-6,6)]	[Ni(tropocoronand-6,6)]	N_4	Scott	28
5	$Ni(N_2S_2C_2)$	[*N,N'*-ethylenebis(methyl-2-amino-1-cyclopentene-dithiocarboxylato)]nickel(II)	N_2S_2	Bereman	29
6	$Ni(N_2S_2C_3)$	[*N,N'*-trimethylenebis(methyl-2-amino-1-cyclopentene-dithiocarboxylato)]nickel(II)	N_2S_2	Bereman	29
7	$Ni(N_2S_2C_4)$	[*N,N'*-tetramethylenebis-(methyl-2-amino-1-cyclopentene-dithiocarboxylato)]nickel(II)	N_2S_2	Bereman	29
8	Ni(tsalen)	[*N,N'*-ethylenebis-(thiosalicylidenaminato)]nickel(II)	N_2S_2	Holm	30
9	Ni(ebmba)	[*N,N'*-ethylenebis-(*o*-mercaptobenzylaminato)]nickel(II)	N_2S_2	Holm	31
10	$(Et_4N)_2[NiFe_3S_4(PPh_3)(SEt)_3]$	$(Et_4N)_2[NiFe_3S_4(PPh_3)(SEt)_3]$	PS_3	Holm	32,33
11	$(Et_4N)_3[NiFe_3S_4(SEt)_4]$	$(Et_4N)_3[NiFe_3S_4(SEt)_4]$	S_4	Holm	32
12	$[Ni(SPh)_4]^{2-}$	$[(C_6H_5)_4P]_2Ni(SC_6H_5)_4$	S_4	Scott	34
13	$(Bu_4N)_2[Ni(mnt)_2]$	$((C_4H_9)_4N)_2$[Ni(maleonitrile-dithiolate)$_2$]	S_4	Scott	35
14	$Ni(dedtc)_2$	Bis(*N,N'*-diethyldithiocarbamato)-nickel(II)	S_4	Hodgson	36
15	$[Ni(SS_2)]_2$	Di-μ-(bis-2-mercaptoethyl sulfide)-dinickel(II)	S_4	Hodgson	37,38
16	$[Ni(N_3S_2)]$	[Ni(terpyridine)(S-2,4,6-(*i*-Pr)$_3$-C_6H_2)$_2$]·1.5CH_3CN	N_3S_2	Hodgson	39
17	$[Ni(N_2S_3)]$	$Ni[S_2P(OMe)_2]_2$(2,9-dimethyl-1,10-phenanthroline)	N_2S_3	Hodgson	40

Bereman — Prof. Robert D. Bereman of North Carolina State University supplied these compounds

Holm — Prof. Richard H. Holm of Harvard University supplied these compounds

Scott — Prof. Robert A. Scott of the University of Georgia at Athens supplied data for these compounds

Hodgson — Synthesized by Grace Tan in the Hodgson Group

Table 7.2. Ni model compounds used in this study (continued)

No.	Short name	Full name	Ni ligation	Supplier	Ref.
18	$[Ni(NS_3^{tBu})H](BPh_4)$	$\{Ni^{II}[N(CH_2CH_2S\text{-}t\text{-}Bu)_3]H\}(BPh_4)$	NS_3H	Holm	22
19	$[Ni(NS_3^{tBu})Me](BPh_4)$	$\{Ni^{II}[N(CH_2CH_2S\text{-}t\text{-}Bu)_3]Me\}(BPh_4)$	NS_3C	Holm	22
20	$[Ni(NS_3^{iPr})COMe](BPh_4)$	$\{Ni^{II}[N(CH_2CH_2S\text{-}i\text{-}Pr)_3]COMe\}(BPh_4)$	NS_3C	Holm	22
21	$[Ni(NS_3^{tBu})CO](BPh_4)$	$\{Ni^{I}[N(CH_2CH_2S\text{-}t\text{-}Bu)_3]CO\}(BPh_4)$	NS_3C	Holm	22
22	$[Ni(NS_3^{tBu})Cl](BPh_4)$	$\{Ni^{II}[N(CH_2CH_2S\text{-}t\text{-}Bu)_3]Cl\}(BPh_4)$	NS_3Cl	Holm	22
23	$[Ni([9]aneN_3)]^{2+}$	Bis(1,4,7-triazacyclononane) nickel(II)	N_6	Scott	41
24	$[Ni([9]aneS_3)]^{2+}$	Bis(1,4,7-trithiacyclononane) nickel(II)	S_6	Scott	42
25	$NiCl_2$	Nickel(II) chloride, anhydrous	Cl_6	commercial	43

Holm — Prof. Richard H. Holm of Harvard University supplied these compounds

Scott — Prof. Robert A. Scott of the University of Georgia at Athens supplied data for these compounds

Table 7.3. Results from tests of Ni–N, Ni–S and Ni–Fe parameters on "single-shell" compounds (data range k = 3.25–11.75 Å^{-1}).

Coordination geometry	$R(cryst)_{av}$*	R_{EXAFS}#	$\Delta R_{cryst,EXAFS}$†	CN_{EXAFS}§	c_2 value‡	No. of cpds. curve-fitted
Ni-N compounds :						
Approx. sq. planar	1.861–1.921◊	1.859–1.961	0.009–0.014◊	3.3–5.4	-0.0221 to -0.0265	6
Tetrahedral	1.947	1.931	0.016	3.8–4.6	-0.0242	1
Sq. pyramidal	---	1.856–1.857	---	3.2–3.7	-0.0269	1
Octahedral	2.090–2.124◊	2.070–2.118	-0.002 to 0.011◊	4.3–7.5	-0.0253 to -0.0280	4
Ni-S compounds :						
Approx. sq. planar	2.175–2.18	2.170–2.175	0.000–0.010	3.7–4.1	-0.0201 to -0.0214	2
Sq. planar, Ni^{III}	2.149	2.143	0.006	4.2–4.3	-0.0193	1
Tetrahedral	2.288	2.287	0.001	4.0–4.2	-0.0207	1
Octahedral	2.386	2.380	0.006	5.6–6.4	-0.0217	1
Ni-Fe compound :						
Dist. tetrahedral	---	2.755	---	2.5–2.6	-0.0169	1

* — The $R(cryst)_{av}$ values are the averaged crystallographic bond distances for each compound. The range shown is the range of $R(cryst)_{av}$ seen over different compounds.

\# — Similarly, R_{EXAFS} is shown as a range where more than 1 compound was fitted. The R_{EXAFS} values shown are from Type 1, 2 and 3 fits. The 3 types of fits produce practically identical R_{EXAFS} values.

† — $\Delta R_{cryst,EXAFS}$ is calculated for each compound, and is also given as a range of values to indicate the possible goodness of fit for different compounds.

§ — The CN values shown were obtained from fits of both Type 1 and Type 2. (Although Type 1 fits are generally less reliable, in fits to compounds with regular, simple coordination spheres, better CN values can sometimes be obtained.)

‡ — The c_2 values shown were obtained from Type 3 fits.

◊ — Only two of the six square-planar and three of the four octahedral Ni-N compounds fitted have had their crystal structures determined.

Table 7.4. Crystallographic bond distances for some Ni compounds of various coordination geometries (continued on next page). Unless otherwise noted, compounds have a formal Ni oxidation state of +2.

Coordination geometry		$R(Ni–N)_{av}$†	$R(Ni–S)_{av}$†	No. of cpds
$Ni–N_4$	sq. pl.	1.85–2.066	-----	24
$Ni–N_4$	T_d	1.9470	-----	1
$Ni–N_5$	sq. py.	1.871(eq), 2.663(ax)	-----	1
$Ni–N_6$	O_h	2.035–2.151	-----	8
$Ni–N_2O_2$	sq. pl.	1.826–1.92	1.817–1.85 (O)	4
$Ni–N_2O_2$	T_d	1.960	1.896 (O)	1
$Ni–N_3O_3$	O_h	2.059	2.131 (O)	1
$Ni–O_6$	O_h	2.028–2.053	-----	3
$Ni^{I}–N_3S$	sq. pl.	1.980	2.143	1
$Ni–N_2S_2$	app. sq. pl.	1.857–2.003	2.151–2.204	11
$Ni–N_2S_2$	app. D_{2d}	1.913–1.985	2.152–2.167	4
$Ni–NOS_2$	sq. pl.	1.848–1.917 1.865–1.904 (O)	2.178–2.184 (S)	2
$Ni–NS_3$	sq. pl.	1.901–1.953	2.170–2.184	3
$Ni–OS_3$	sq. pl.	1.852 (O)	2.189	1
$Ni–N_4Cl$	tbpy.	2.123	2.295 (Cl)	1
$Ni–N_3S_2$	tbpy.	2.057	2.302	1
$Ni–N_2S_3$	tbpy.	2.00	2.30, 2.42, 2.58*	1
$Ni–NS_3L$‡	tbpy.	2.02–2.208	2.226–2.368	5
$Ni–N_3SCl$	sq. py.	2.047	2.296(S), 2.275(Cl)	1
$Ni–NS_4$	sq. py.	2.06	2.42	1

† — Averages of the crystallographic bond distances were calculated for each compound, and the range shown encompasses the possible values that these averaged bond distances can take for the different compounds surveyed.

* — no averages made in this case

‡ — These compounds are the $[Ni(NS_3^R)L](BPh_4)$ compounds (**18–22**) listed in Table 7.2. Since the character of L varies so widely (L = H^-, CH_3^-, CO, CH_3CO^-, Cl^-), distances for the Ni–L bond are not given.

Table 7.4. Crystallographic bond distances for some Ni compounds of various coordination geometries (continued from previous page). Unless otherwise noted, compounds have a formal Ni oxidation state of +2.

Coordination geometry		$R(Ni–N)_{av}$†	$R(Ni–S)_{av}$†	No. of cpds
$Ni–N_3OS_2$	O_h	2.110(N), 2.249(O)	2.378	1
$Ni–N_4S_2$	O_h	2.041–2.050	2.413–2.516	5
$Ni–N_3S_3$	O_h	2.065–2.118	2.452–2.476	2
$Ni–N_2S_4$	O_h	2.047–2.11	2.412–2.50	6
$Ni^{III}–N_2S_4$	O_h	2.037	2.279	1
$Ni^{II}–S_4$	sq. pl.	-----	2.165–2.240	19
$Ni^{III}–S_4$	sq. pl.	-----	2.135–2.149	4
$Ni^{IV}–S_4$	sq. pl.	-----	2.101–2.122	2
$Ni–S_4$	T_d	-----	2.281–2.292	4
$Ni–PS_3$	T_d	2.174 (P)	2.258	1
$Ni–PS_4$	sq. py.	2.114 (P)	2.281	1
$Ni–S_5$	sq. py.	-----	2.200(eq), 2.741(ax)	1
$Ni–S_6$	O_h	-----	2.386–2.438	4

† — Averages of the crystallographic bond distances were calculated for each compound, and the range shown encompasses the possible values that these averaged bond distances can take for the different compounds surveyed.

Table 7.5. Fits made to Ni–N,S compounds : Ni(tsalen) (**8**), [Ni($NS_3{}^{tBu}$)H](BPh_4) (**18**) and [Ni(N_3S_2)] (**16**). The same fits were performed on all three compounds.

Waves used	Fit Type†
N	1,2,3
S	1,2,3
N + S	1,2,3*
N + N'	1,2,3
S + S'	1,2,3*

1 — Distances, coordination numbers and Debye-Waller factors are varied

2 — Distances, coordination numbers are varied while Debye-Waller factors (c_2 in the EXAFS equation) are fixed at initial (model) values

3 — Distances and Debye-Waller factors are varied while coordination numbers are fixed at various sets of values

3* — Several possible combinations of N and/or S coordination numbers were explored

Table 7.6. Results of Type 2 fits (varying CN's and fixing c_2's) made to Ni–N,S models. Fixed c_{2N} = -0.0230, c_{2S} = -0.0204.

Crystallographic distances	**EXAFS results**			
Ni(tsalen) (**8**) :	**Window :** 0.95–2.35 (0.1) Å			
				Fit Index
Ni–N = 1.85 Å	3.8 N	@	1.97 Å	1.628
1.86 Å				
	1.9 S	@	2.14 Å	1.032
Ni–S = 2.174 Å				
2.139 Å	1.9 N	@	1.87 Å	0.324
	2.0 S	@	2.16 Å	
avg. 2 N @ 1.86 Å	3.4 N	@	1.96 Å	1.226
2 S @ 2.157 Å	2.8 N'	@	2.39 Å	
	1.2 S	@	2.04 Å	0.438
	2.3 S'	@	2.17 Å	
[Ni($NS_3{}^{tBu}$)H](BPh_4) (**18**) :	**Window :** 0.95–2.35 (0.1) Å			
				Fit Index
Ni–N = 2.02 Å	6.7 N	@	2.06 Å	1.719
Ni–S = 2.234 Å	3.2 S	@	2.22 Å	0.575
2.227 Å				
2.218 Å	1.0 N	@	1.99 Å	0.454
	3.0 S	@	2.23 Å	
Ni–H = 2.0 Å				
	3.4 N	@	1.88 Å	0.929
	9.8 N'	@	2.06 Å	
avg. 1 N @ 2.02 Å				
3 S @ 2.226 Å	-0.3 S	@	1.94 Å	0.441
(1 H @ 2.0 Å)	3.2 S'	@	2.22 Å	
[Ni(N_3S_2)] (**16**) :	**Window :** 1.00–2.30 (0.1) Å			
Mol. 1 Mol. 2				Fit Index
Ni–N = 2.113 Å 2.075 Å	4.1 N	@	2.11 Å	1.258
1.974 Å 1.968 Å				
2.086 Å 2.125 Å	1.9 S	@	2.28 Å	0.879
Ni–S = 2.274 Å 2.298 Å	1.9 N	@	2.03 Å	0.461
2.332 Å 2.302 Å	1.9 S	@	2.30 Å	
	3.1 N	@	1.97 Å	0.382
avg. 3 N @ 2.057 Å	6.5 N'	@	2.13 Å	
2 S @ 2.302 Å				
	1.4 S	@	2.21 Å	0.571
	1.8 S'	@	2.33 Å	

Table 7.7. Results of some Type 3 fits (fixing CN's and varying c_2's) made to Ni–N,S model compounds.

Crystallographic distances	**EXAFS results**			
Ni(tsalen) (**8**) :	**Window :** 0.95–2.35 (0.1) Å			
			c_2	Fit Index
Ni–N = 1.85 Å	2 N @	1.87 Å	-0.0242	0.319
1.86 Å	2 S @	2.16 Å	-0.0206	
Ni–S = 2.174 Å	3 N @	1.88 Å	-0.0309	0.303
2.139 Å	2 S @	2.16 Å	-0.0217	
avg. 2 N @ 1.86 Å 2 S @ 2.157 Å				
$[Ni(NS_3{}^{tBu})H](BPh_4)$ (**18**) :	**Window :** 0.95–2.35 (0.1) Å			
			c_2	Fit Index
Ni–N = 2.02 Å	1 N @	1.99 Å	-0.0232	0.456
	3 S @	2.23 Å	-0.0203	
Ni–S = 2.234 Å 2.227 Å 2.218 Å	2 N @	2.00 Å	-0.0359	0.449
	3 S @	2.23 Å	-0.0209	
Ni–H = 2.0 Å				
avg. 1 N @ 2.02 Å 3 S @ 2.226 Å (1 H @ 2.0 Å)				
$[Ni(N_3S_2)]$ (**16**) :	**Window :** 1.00–2.30 (0.1) Å			
Mol. 1 Mol. 2			c_2	Fit Index
Ni–N = 2.113 Å 2.075 Å	1 N @	2.02 Å	-0.0182	0.520
1.974 Å 1.968 Å	2 S @	2.29 Å	-0.0207	
2.086 Å 2.125 Å	2 N @	2.03 Å	-0.0270	0.437
Ni–S = 2.274 Å 2.298 Å	2 S @	2.30 Å	-0.0220	
2.332 Å 2.302 Å	3 N @	2.04 Å	-0.0340	0.404
	2 S @	2.30 Å	-0.0233	
avg. 3 N @ 2.057 Å 2 S @ 2.302 Å				

Table 7.8. Results of Type 2 (varying CN's and fixing c_2's) and Type 3 (fixing CN's and varying c_2's) fits made to $(Et_4N)_3[NiFe_3S_4(SEt)_4]$ (**11**). For the Type 2 fits, values of fixed c_{2N} = -0.0230, c_{2S} = -0.0204, and c_{2Fe} = -0.0153. No crystal structure was available for comparison.

	Window 2 (1.37–2.85 Å)			**Window 3** (1.00–2.85 Å)		
Type 2 fits			Fit Index			Fit Index
	2.9 S @	2.25 Å	0.634	3.0 S @	2.25 Å	0.948
	2.3 Fe @	2.75 Å		2.3 Fe @	2.75 Å	
	0.7 S @	2.25 Å	0.634			
	2.3 S' @	2.25 Å				
	2.3 Fe @	2.75 Å				
	3.5 S @	2.26 Å	0.298	3.7 S @	2.26 Å	0.687
	1.0 S' @	2.47 Å		1.2 S' @	2.47 Å	
	2.2 Fe @	2.76 Å		2.1 Fe @	2.76 Å	
	3.7 N @	2.16 Å	0.399	4.4 N @	2.19 Å	0.780
	2.7 S @	2.22 Å		3.4 S @	2.22 Å	
	2.4 Fe @	2.76 Å		2.4 Fe @	2.76 Å	
Type 3 fits	R	c_2	Fit Index	R	c_2	Fit Index
4 S	2.26 Å	-0.0244	0.750	2.26 Å	-0.0243	0.962
3 Fe	2.75 Å	-0.0184		2.75 Å	-0.0185	
3 S	2.25 Å	-0.0187	0.222	2.25 Å	-0.0185	0.694
1 S'	2.44 Å	-0.0283		2.43 Å	-0.0283	
3 Fe	2.76 Å	-0.0194		2.76 Å	-0.0194	
2 N	2.26 Å	-0.0140	0.272	2.23 Å	-0.0184	0.744
3 S	2.25 Å	-0.0153		2.24 Å	-0.0171	
3 Fe	2.76 Å	-0.0190		2.76 Å	-0.0193	

Table 7.9. Fourier transform windows for R' < 3 Å used for curvefitting of Ni CODH data.

Data set	Window 1	Window 2	Window 3	Window 6
CODHX*	1.00–1.58 Å	1.50–2.25 Å	1.00–2.25 Å	1.00–2.55 Å
CODHOX	0.80–1.60 Å	1.45–2.20 Å	0.80–2.20 Å	0.80–2.60 Å
CDHOX	1.05–1.60 Å	1.40–2.25 Å	1.05–2.25 Å	1.05–2.60 Å
CODHRX	1.00–1.60 Å	1.45–2.60 Å	1.00–2.60 Å	1.00–2.95 Å
CDHRD	1.00–1.57 Å	1.40–2.25 Å	1.00–2.25 Å	1.00–2.60 Å

Window 1 : left (or low-R) shoulder of main peak only

Window 2 : main peak only

Window 3 : main peak + left shoulder

Window 6 : main peak + left shoulder + right shoulder

* — The "left shoulder" in CODHX is in fact a well-separated peak of substantial height.

Table 7.10. Fits made to Ni CODH data for R' < 3 Å. Except where noted, the same fits were performed on all five data sets

	Window 1	Window 2	Window 3	Window 6
N	1,2,3*	1,2,3*		
S	1,2,3*	1,2,3		
N+S		(1,2,3)x2†	1,2,3	1,2,3
N+N'		1,2,3	1,2,3	
S+S'		1,2,3#	1,2,3	
N+S+S'				(2,3)x3§
N+S+Fe				(2,3)x2
N+S+N'				(2,3)x2

1 — Distances, coordination numbers and Debye-Waller factors are varied

2 — Distances, coordination numbers are varied while Debye-Waller factors (c_2 in the EXAFS equation) are fixed at initial (model) values

3 — Distances and Debye-Waller factors are varied while coordination numbers are fixed at various sets of values

( )x2 — Two fit minima are explored

* — Type 3 fit not done for CODHX and CODHOX

† — Only one minimum explored for Window 2 of CDHRD

— Two minima explored for (1,2,3) for CODHRX only

§ — Four minima found for CODHRX and CDHRD, three minima found for the rest

Table 7.11. Results of some of the Type 2 fits (varying CN and fixing c_2) for R' < 3 Å made to five Ni CODH data sets (continued on the next page). Values of fixed c_{2N} = -0.0230, c_{2S} = -0.0204, and c_{2Fe} = -0.0153.

	CODHX			CODHOX			CDHOX			CODHRX			CDHRD		
	CN	R(Å)	F	CN	R(Å)	F	CN	R(Å)	F	CN	R(Å)	F	CN	R(Å)	F
Window 2															
N only	3.1 N	2.08	1.139	2.5 N	2.08	0.917	3.0 N	2.07	1.206	4.2 N	2.10	2.177	3.5 N	2.08	1.240
S only	1.6 S	2.23	0.481	1.3 S	2.24	0.360	1.6 S	2.23	0.449	2.3 S	2.25	1.186	1.8 S	2.24	0.379
N+S	0.6 N 1.7 S	1.82 2.23	0.261	0.4 N 1.4 S	1.91 2.24	0.257	0.7 N 1.8 S	1.91 2.23	0.236	1.1 N 2.6 S	1.89 2.25	0.989	0.5 N 1.9 S	1.89 2.24	0.253
N+N'	1.4 N 1.7 N'	2.08 2.07	1.139	1.8 N 4.1 N'	1.89 2.08	0.529	2.3 N 5.2 N'	1.89 2.07	0.701	3.3 N 7.2 N'	1.90 2.09	1.667	2.4 N 5.7 N'	1.89 2.08	0.738
S+S'	0.4 S 1.8 S'	1.99 2.26	0.143	0.3 S 1.5 S'	2.08 2.25	0.203	0.4 S 2.0 S'	2.07 2.24	0.136	0.8 S 3.1 S'	2.05 2.25	0.827	0.3 S 2.1 S'	2.06 2.24	0.184
Window 3															
N+S	2.1 N 2.1 S	1.85 2.23	0.438	1.3 N 1.6 S	1.89 2.24	0.558	1.3 N 2.0 S	1.89 2.23	0.299	1.9 N 2.8 S	1.89 2.25	0.859	1.2 N 2.1 S	1.87 2.24	0.430
N+N'	4.3 N 6.5 N'	1.86 2.07	0.380	3.1 N 5.1 N'	1.89 2.08	0.473	3.3 N 6.0 N'	1.88 2.07	0.508	4.4 N 8.0 N'	1.89 2.09	1.523	3.4 N 6.5 N'	1.88 2.07	0.600
S+S'	1.0 S 2.5 S'	2.01 2.22	0.781	0.7 S 1.9 S'	2.07 2.25	0.641	0.7 S 2.2 S'	2.06 2.23	0.388	1.2 S 3.4 S'	2.05 2.25	0.704	0.6 S 2.4 S'	2.05 2.24	0.513
Window 6															
N+S	2.2 N 2.1 S	1.85 2.23	0.527	1.4 N 1.7 S	1.88 2.24	0.616	1.4 N 2.0 S	1.88 2.23	0.474	1.9 N 2.8 S	1.89 2.25	0.897	1.3 N 2.2 S	1.87 2.24	0.520

Table 7.11. Results of some of the Type 2 fits (varying CN and fixing c_2) for R' < 3 Å made to five Ni CODH data sets (continued from previous page). Values of fixed c_{2N} = -0.0230, c_{2S} = -0.0204, and c_{2Fe} = -0.0153.

	CODHX			CODHOX			CDHOX			CODHRX			CDHRD		
	CN	R(Å)	F	CN	R(Å)	F	CN	R(Å)	F	CN	R(Å)	F	CN	R(Å)	F
Window 6															
N+S+S'	2.2 N	1.85	0.523	1.8 N	1.88	0.488	1.6 N	1.89	0.416	1.7 N	1.89	0.544	1.2 N	1.85	0.482
	8.8 S	2.24		2.2 S	2.24		2.2 S	2.24		2.6 S	2.25		2.1 S	2.26	
	-6.8S'	2.25		0.6 S'	2.43		0.4 S'	2.48		0.8 S'	2.62		0.7 S'	2.16	
	2.2 N	1.85	0.455	1.4 N	1.88	0.522	1.4 N	1.88	0.277	1.9 N	1.89	0.872	1.3 N	1.87	0.375
	2.1 S	2.22		1.7 S	2.24		2.0 S	2.23		2.8 S	2.25		2.2 S	2.24	
	0.4 S'	2.88		0.4 S'	2.89		0.5 S'	2.90		0.3 S'	2.94		0.5 S'	2.92	
N+S+Fe	2.1 N	1.85	0.441	1.4 N	1.89	0.549	1.3 N	1.88	0.278	1.9 N	1.89	0.755	1.3 N	1.87	0.399
	2.1 S	2.23		1.7 S	2.24		2.0 S	2.23		2.8 S	2.25		2.2 S	2.24	
	0.3 Fe	2.70		0.3 Fe	2.71		0.4 Fe	2.74		0.6 Fe	2.80		0.4 Fe	2.76	
	2.2 N	1.85	0.522	1.4 N	1.88	0.606	1.4 N	1.88	0.440	2.0 N	1.89	0.789	1.3 N	1.87	0.494
	2.1 S	2.23		1.7 S	2.24		2.0 S	2.23		2.8 S	2.25		2.2 S	2.24	
	0.1 Fe	3.06		0.1 Fe	3.08		0.2 Fe	3.07		0.6 Fe	3.09		0.2 Fe	3.09	
N+S+N'	2.2 N	1.85	0.403	1.4 N	1.89	0.499	1.4 N	1.89	0.245	1.9 N	1.89	0.830	1.3 N	1.87	0.383
	2.1 S	2.23		1.7 S	2.24		2.0 S	2.23		2.8 S	2.25		2.2 S	2.24	
	1.1 N'	2.71		1.2 N'	2.71		1.3 N'	2.74		1.2 N'	2.81		1.2 N'	2.76	
	2.2 N	1.85	0.525	1.4 N	1.88	0.611	1.4 N	1.88	0.458	1.9 N	1.89	0.841	1.3 N	1.87	0.509
	2.1 S	2.23		1.7 S	2.24		2.0 S	2.23		2.8 S	2.25		2.2 S	2.24	
	0.2 N'	3.09		0.3 N'	3.10		0.5 N'	3.09		1.3 N'	3.09		0.4 N	3.11	

Table 7.12. Results of some of the Type 3 fits (fixing CN and varying c_2) for R' < 3 Å made to five Ni CODH data sets (continued on the next page)

	CODHX			CODHOX			CDHOX			CODHRX			CDHRD		
Window 2	**R**	**c_2**	**F**	**R**	**c_2**	**F**	**R**	**c_2**	**F**	**R**	**c_2**	**F**	**R**	**c_2**	**F**
3 (6)† N							2.07	-0.0235	1.205	2.09	-0.0276	2.247	2.08	-0.0209	1.248
2 S	2.23	-0.0228	0.612	2.24	-0.0276	0.331	2.23	-0.0240	0.403	2.26	-0.0179	1.162	2.24	-0.0220	0.361
4 S										2.25	-0.0280	1.495			
1 N	1.82	-0.0277	0.334	1.84	-0.0393	0.170	1.89	-0.0320	0.224	1.93	-0.0199	0.947	1.88	-0.0384	0.199
2 S	2.23	-0.0223		2.24	-0.0265		2.23	-0.0227		2.26	-0.0163		2.24	-0.0213	
2 N	1.81	-0.0417	0.341	1.84	-0.0580	0.161	1.88	-0.0490	0.230	1.92	-0.0318	0.937	1.88	-0.0547	0.167
2 S	2.23	-0.0219		2.24	-0.0266		2.24	-0.0231		2.26	-0.0166		2.24	-0.0215	
2 N										1.88	-0.0314	1.030			
3 S										2.25	-0.0219				
Window 3															
1 N	1.84	-0.0128	0.390	1.87	-0.0219	0.470	1.88	-0.0218	0.299	1.91	-0.0179	0.998	1.87	-0.0242	0.450
2 S	2.22	-0.0216		2.24	-0.0252		2.23	-0.0217		2.25	-0.0165		2.24	-0.0207	
2 N	1.85	-0.0216	0.428	1.88	-0.0314	0.402	1.89	-0.0314	0.202	1.91	-0.0266	0.889	1.88	-0.0341	0.358
2 S	2.22	-0.0199		2.24	-0.0245		2.24	-0.0215		2.26	-0.0162		2.24	-0.0203	
3 N	1.86	-0.0278	0.522	1.89	-0.0381	0.379	1.90	-0.0385	0.182	1.91	-0.0327	0.822	1.89	-0.0412	0.309
2 S	2.23	-0.0193		2.25	-0.0245		2.24	-0.0217		2.26	-0.0162		2.24	-0.0204	
2 N										1.88	-0.0245	0.858	1.85	-0.0304	0.239
3 S										2.25	-0.0214		2.24	-0.0259	

† — The number in brackets refers to the fixed-CN value for CODHRX only.

Table 7.12. Results of some of the Type 3 fits (fixing CN and varying c_2) for R' < 3 Å made to five Ni CODH data sets (continued from previous page)

	CODHX			CODHOX			CDHOX			CODHRX			CDHRD		
	R	c_2	F	R	c_2	F	R	c_2	F	R	c_2	F	R	c_2	F
Window 6															
2 N	1.85	-0.0208	0.492	1.88	-0.0294	0.560	1.89	-0.0288	0.460	1.88	-0.0242	0.900	1.89	-0.0319	0.490
2 (3)† S	2.22	-0.0192		2.24	-0.0233		2.24	-0.0203		2.25	-0.0213		2.24	-0.0194	
2 N	1.86	-0.0196	0.316	1.88	-0.0267	0.427	1.89	-0.0269	0.395	1.82	-0.0275	0.578	1.87	-0.0303	0.423
2 (3)† S	2.22	-0.0181		2.23	-0.0215		2.23	-0.0195		2.18	-0.0236		2.24	-0.0197	
1 S'	2.38	-0.0318		2.40	-0.0378		2.40	-0.0506		2.31	-0.0080		2.31	-0.0612	
2 N	1.85	-0.0208	0.420	1.88	-0.0295	0.451	1.89	-0.0290	0.291	1.88	-0.0241	0.869	1.88	-0.0319	0.350
2 (3)† S	2.22	-0.0192		2.24	-0.0233		2.23	-0.0203		2.25	-0.0212		2.24	-0.0195	
1 S'	2.90	-0.0390		2.90	-0.0328		2.90	-0.0300		3.23	-0.0279		2.92	-0.0325	
2 N										1.88	-0.0280	0.444			
3 S										2.25	-0.0236				
1 S'										2.61	-0.0186				
2 N	1.85	-0.0210	0.386	1.88	-0.0301	0.391	1.89	-0.0300	0.196	1.88	-0.0246	0.826	1.89	-0.0326	0.333
2 (3)† S	2.22	-0.0194		2.24	-0.0236		2.24	-0.0208		2.25	-0.0216		2.24	-0.0197	
1 Fe	2.72	-0.0333		2.72	-0.0273		2.74	-0.0256		2.80	-0.0184		2.75	-0.0289	
2 N	1.85	-0.0208	0.492	1.88	-0.0294	0.560	1.89	-0.0288	0.458	1.88	-0.0240	0.830	1.89	-0.0319	0.488
2 (3)† S	2.22	-0.0192		2.24	-0.0233		2.24	-0.0203		2.25	-0.0212		2.24	-0.0194	
1 Fe	3.50	-0.1115		3.47	-0.1072		3.56	-0.1084		3.09	-0.0193		3.52	-0.0982	

† — The number in brackets refers to the fixed-CN value for CODHRX only.

Table 7.13. Some Type 2 fits (varying CN's and fixing c_2's) made to signals at R' = 3–5 Å in CODHRX. Values of fixed c_{2N} = -0.0230, c_{2S} = -0.0204, and c_{2Fe} = -0.0153.

Window 7 (2.85–3.60 Å)			
			Fit Index
0.8 S	@	3.68 Å	0.183
0.7 Fe	@	3.53 Å	0.203
0.5 S	@	3.64 Å	0.164
0.4 Fe	@	3.56 Å	
0.6 S	@	3.53 Å	0.155
1.1 Fe	@	3.54 Å	

Window 8 (3.52–4.20 Å)			
			Fit Index
1.44 S	@	4.19 Å	0.234
1.0 Fe	@	4.04 Å	0.364
2.1 S	@	4.18 Å	0.203
-0.7 Fe	@	4.00 Å	
1.7 S	@	4.08 Å	0.216
1.9 Fe	@	4.08 Å	

Window 9 (4.10–5.07 Å)			
			Fit Index
2.3 S	@	5.03 Å	0.418
2.3 Fe	@	4.87 Å	0.178
-1.3 S	@	4.88 Å	0.073
1.6 Fe	@	4.85 Å	
0.6 S	@	4.66 Å	0.107
2.0 Fe	@	4.88 Å	

Window 10 (2.85–5.07 Å)			
			Fit Index
0.5 Fe	@	3.54 Å	0.072
1.8 S'	@	4.18 Å	
0.6 Fe'	@	3.83 Å	
1.1 S"	@	4.65 Å	
1.8 Fe"	@	4.88 Å	

			Fit Index
0.8 S	@	3.73 Å	0.080
2.0 S'	@	4.17 Å	
1.1 Fe'	@	3.82 Å	
1.0 S"	@	4.66 Å	
1.9 Fe"	@	4.87 Å	

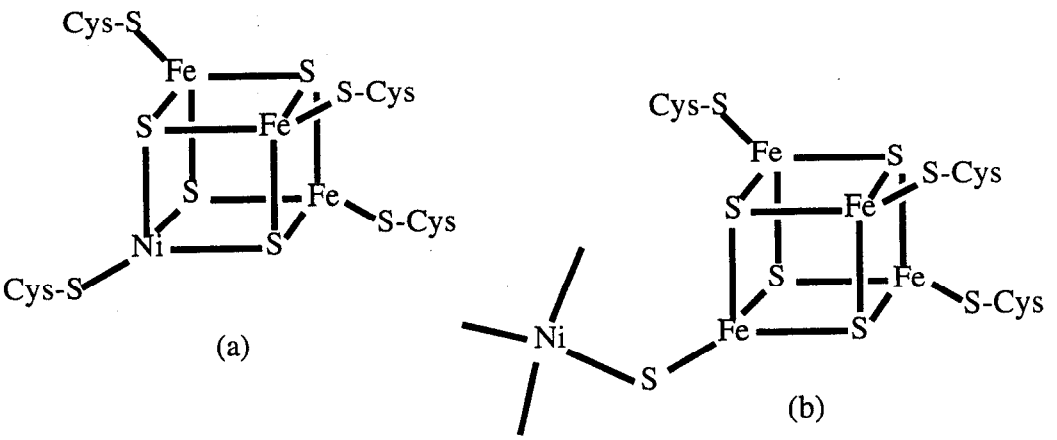

Figure 7.1. Possibilities for the Ni environment in *Rhodospirillum rubrum* Ni CODH: (a) $NiFe_3S_4$ cubane and (b) Ni ligated to Fe_4S_4 cubane.

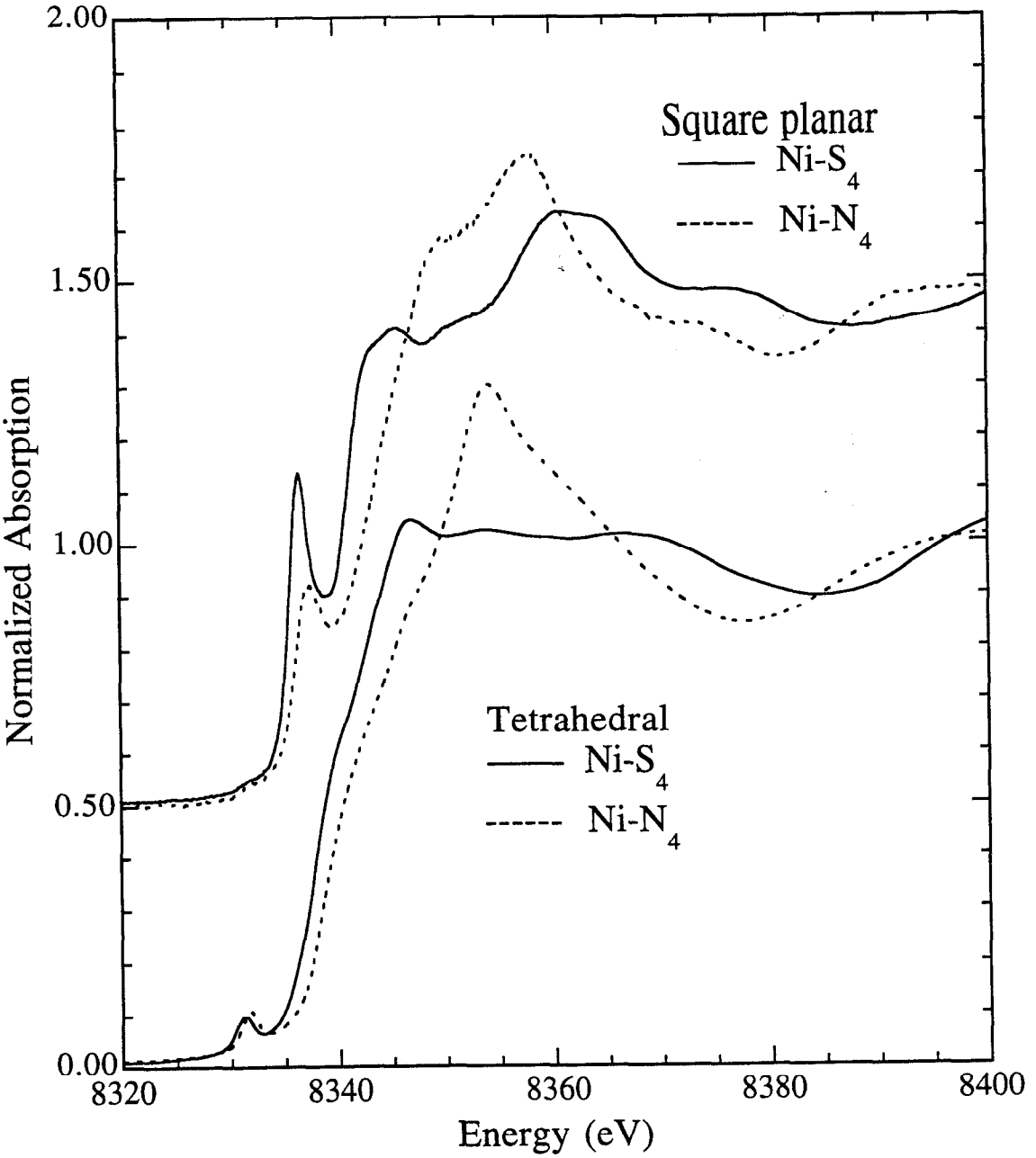

Figure 7.2. Edges of square-planar and tetrahedral Ni compounds. Square planar (top) : $(Bu_4N)_2[Ni(mnt)_2]$ (**13**) (—), and Ni(corphin) (**3**) (----). Tetrahedral (bottom) : $[Ni(SPh)_4]^{2-}$ (**12**) (—), and [Ni(TC-6,6)] (**4**) (----).

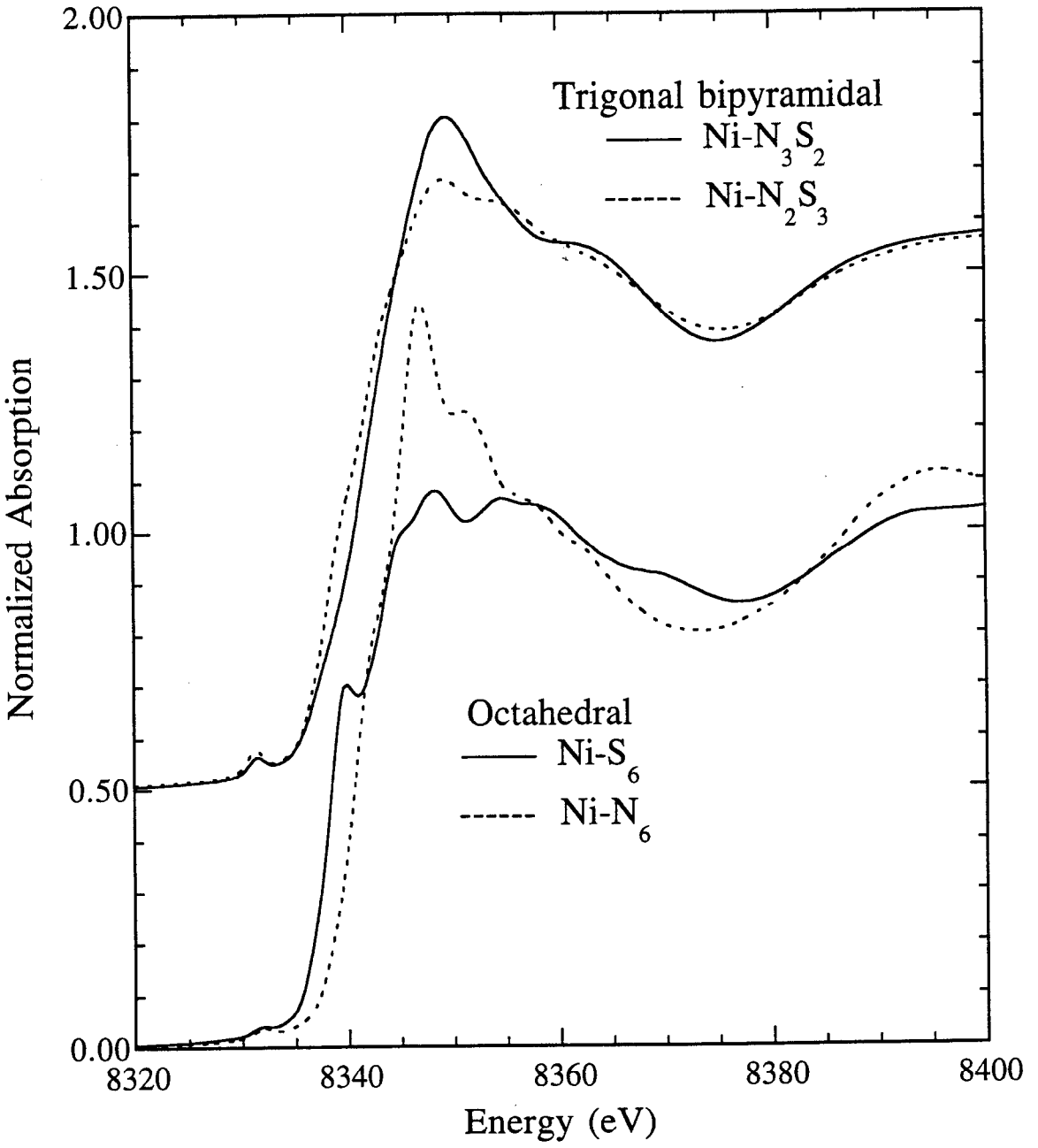

Figure 7.3. Edges of trigonal bipyramidal and octahedral Ni compounds. Trigonal bipyramidal (top) : $[Ni(N_3S_2)]$ (**16**) (—), and $[Ni(N_2S_3)]$ (**17**) (----). Octahedral (bottom) : $[Ni([9]aneS_3)]^{2+}$ (**24**) (—), and $[Ni([9]aneN_3)]^{2+}$ (**23**) (----).

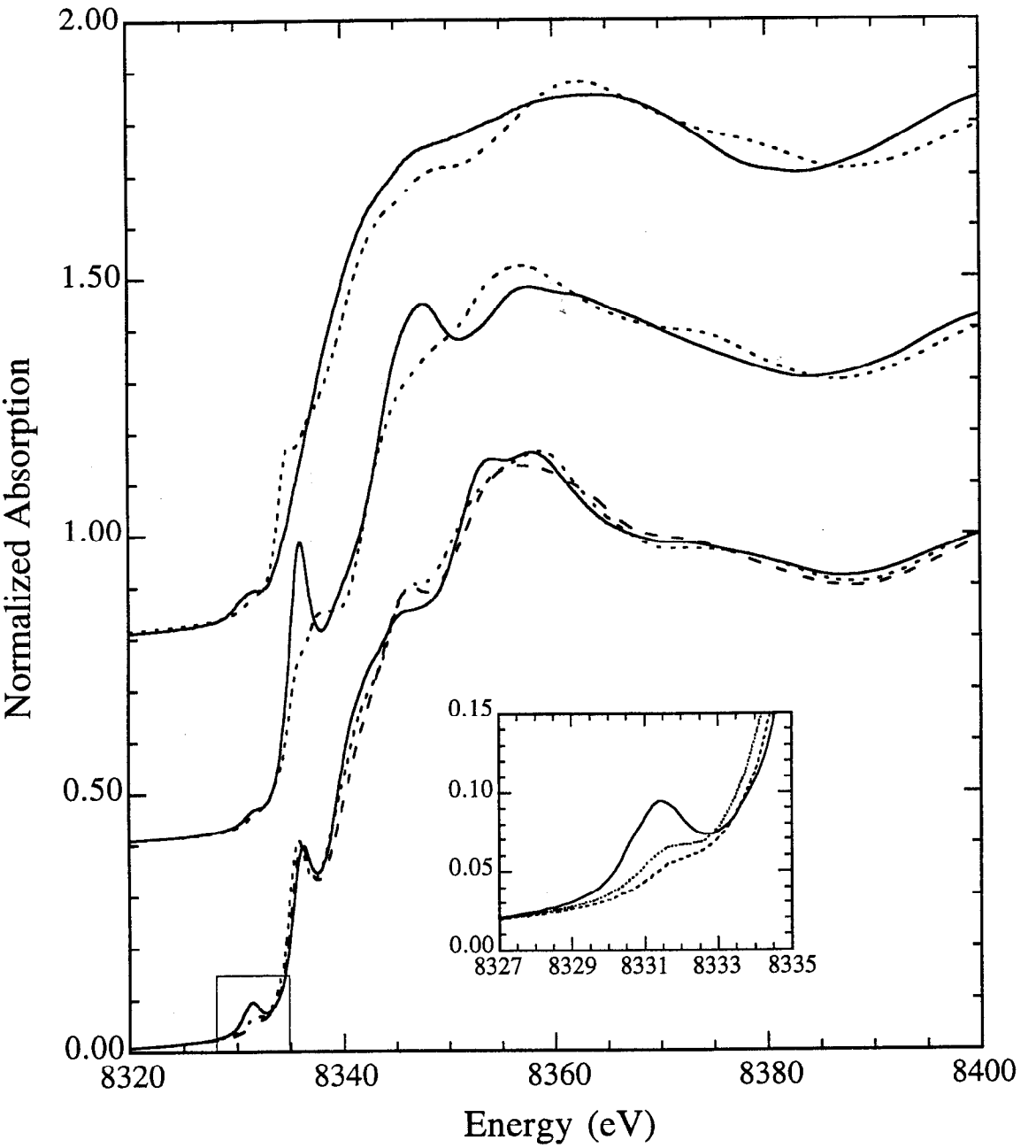

Figure 7.4. Ni compounds with edges of unusual appearance. Top : Ni in a multinuclear cluster. $[Ni(SS_2)]_2$ (**15**) (——), and $(Et_4N)_3[NiFe_3S_4(SEt)_4]$ (**11**) (- - -). Middle : Ni–N_2S_2 square planar. Ni(ebmba) (**9**) (ligand not conjugated) (——), and Ni(tsalen) (**8**) (conjugated ligand) (- - -). Bottom : Ni–N_2S_2 stepwise distortion from square planar towards tetrahedral geometry. Ni($N_2S_2C_2$) (**5**) (distorted 3.4° from planarity) (- - -), Ni($N_2S_2C_3$) (**6**) (distorted 18.6°) (----), and Ni($N_2S_2C_4$) (**7**) (distorted 38.6°) (——). Inset shows 1s→3d feature in compounds (**5**), (**6**) and (**7**).

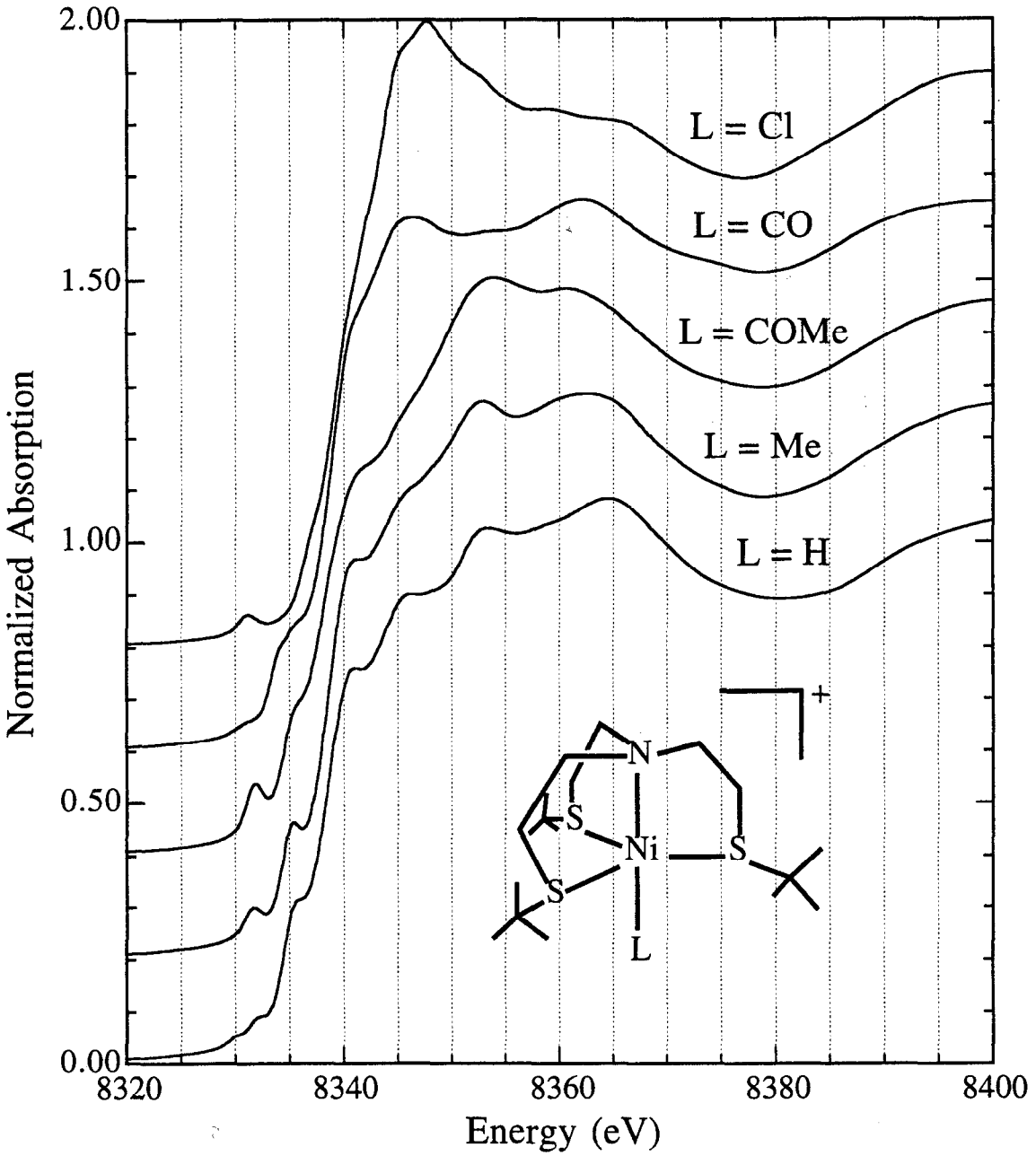

Figure 7.5. Edges of a series of trigonal bipyramid compounds with Ni–NS_3L ligation. Top to bottom : [Ni(NS_3^{tBu})Cl](BPh_4) (**22**), [Ni(NS_3^{tBu})CO](BPh_4) (**21**), [Ni(NS_3^{iPr})COMe](BPh_4) (**20**), [Ni(NS_3^{tBu})Me](BPh_4) (**19**) and [Ni(NS_3^{tBu})H](BPh_4) (**18**). The vertical grid lines aid in comparing the six transitions discernible in these edges.

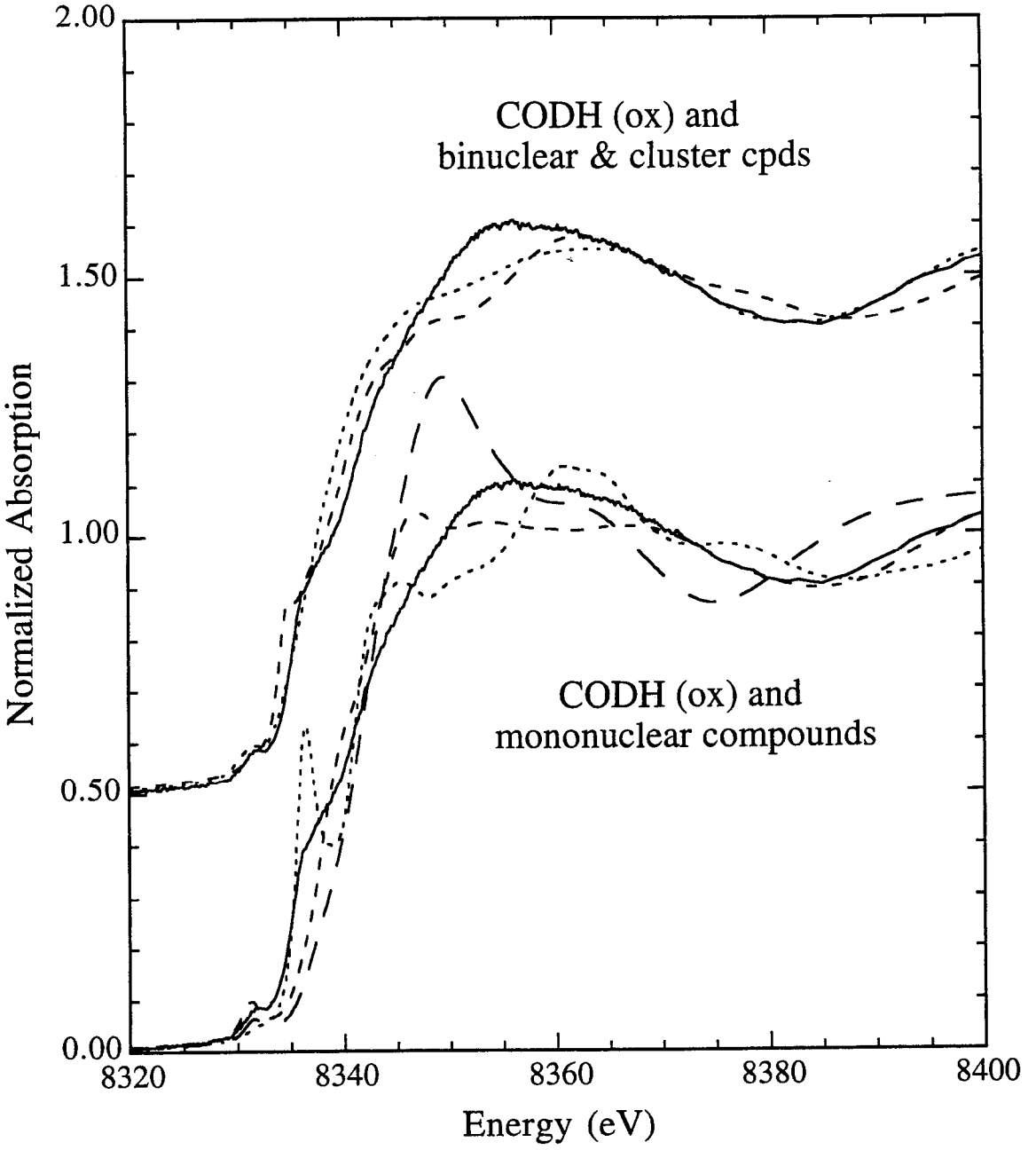

Figure 7.6. Edge of CODH (ox) (1992) (—— in both top and bottom) compared with model compound edges. Top (Ni in clusters) : $(Et_4N)_3[NiFe_3S_4(SEt)_4]$ (**11**) (----) and $[Ni(SS_2)]_2$ (**15**) (– – –). Bottom : $(Bu_4N)_2[Ni(mnt)_2]$ (**13**) (square planar) (----), $[Ni(SPh)_4]^{2-}$ (**12**) (tetrahedral) (– – –), and $[Ni(N_3S_2)]$ (**16**) (trigonal bipyramidal) (— —).

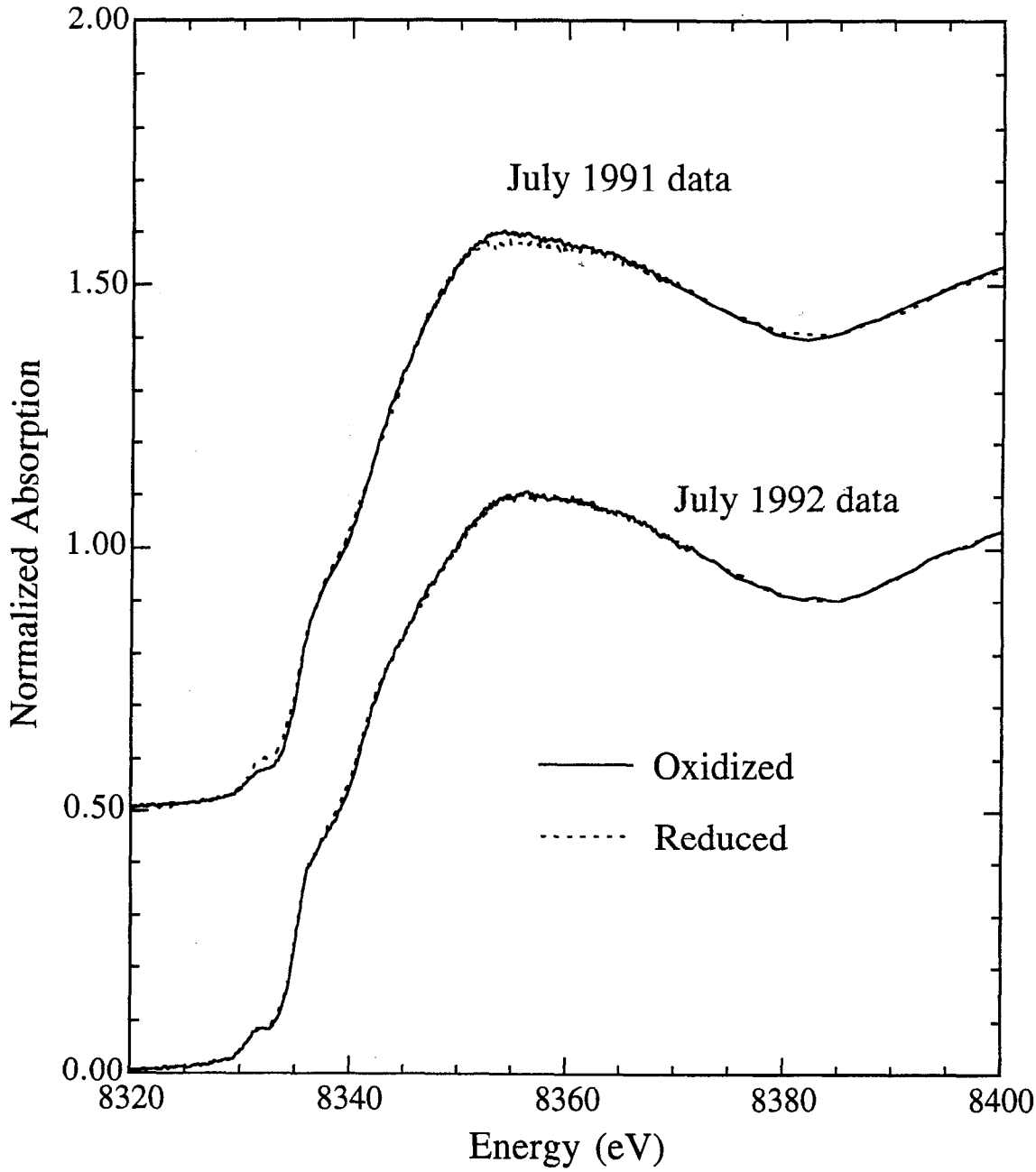

Figure 7.7. Ni K edges of oxidized and reduced Ni CODH samples measured in 1991 and 1992.

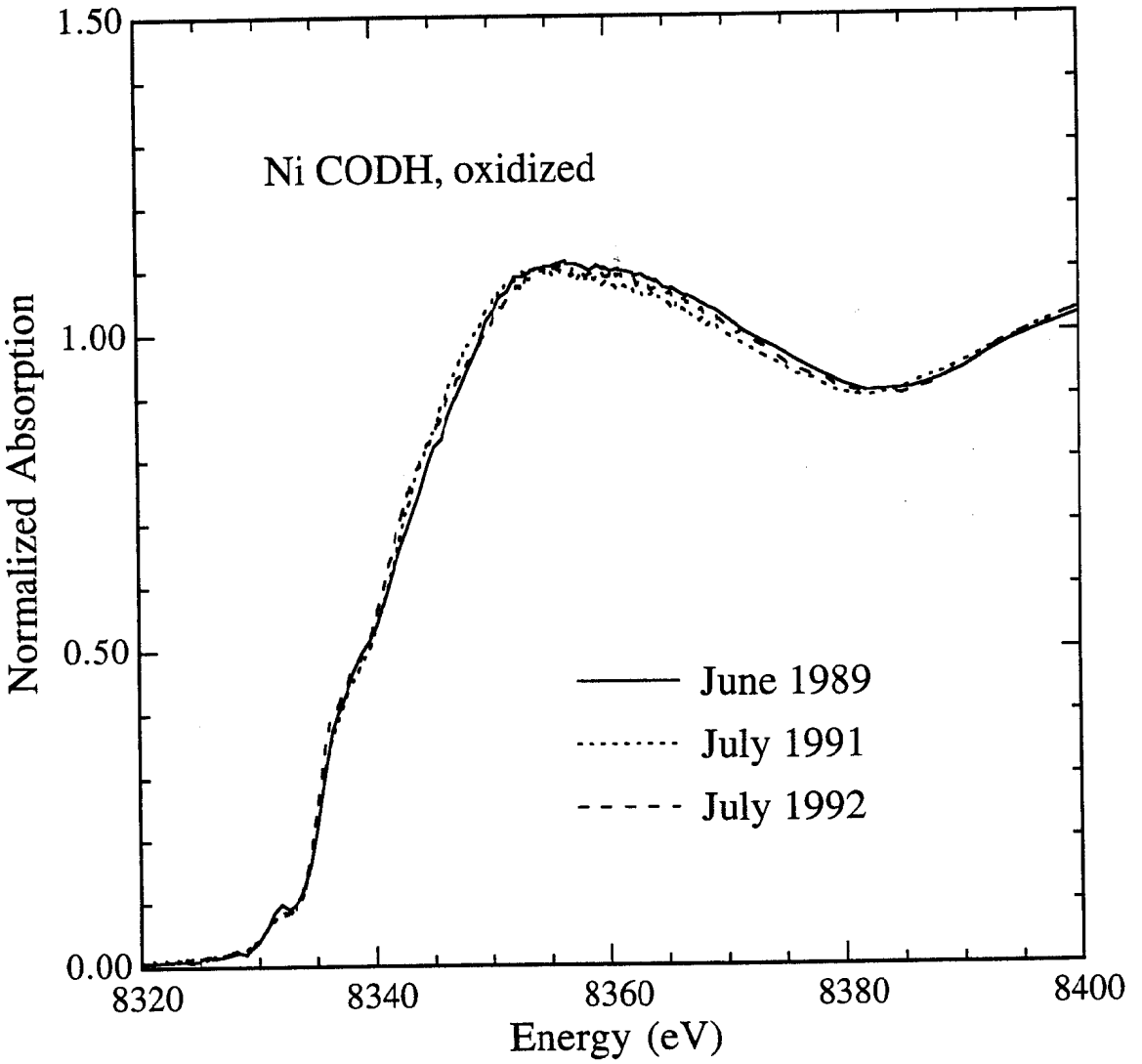

Figure 7.8. Ni K edges of oxidized CODH samples measured in 1989, 1991 and 1992.

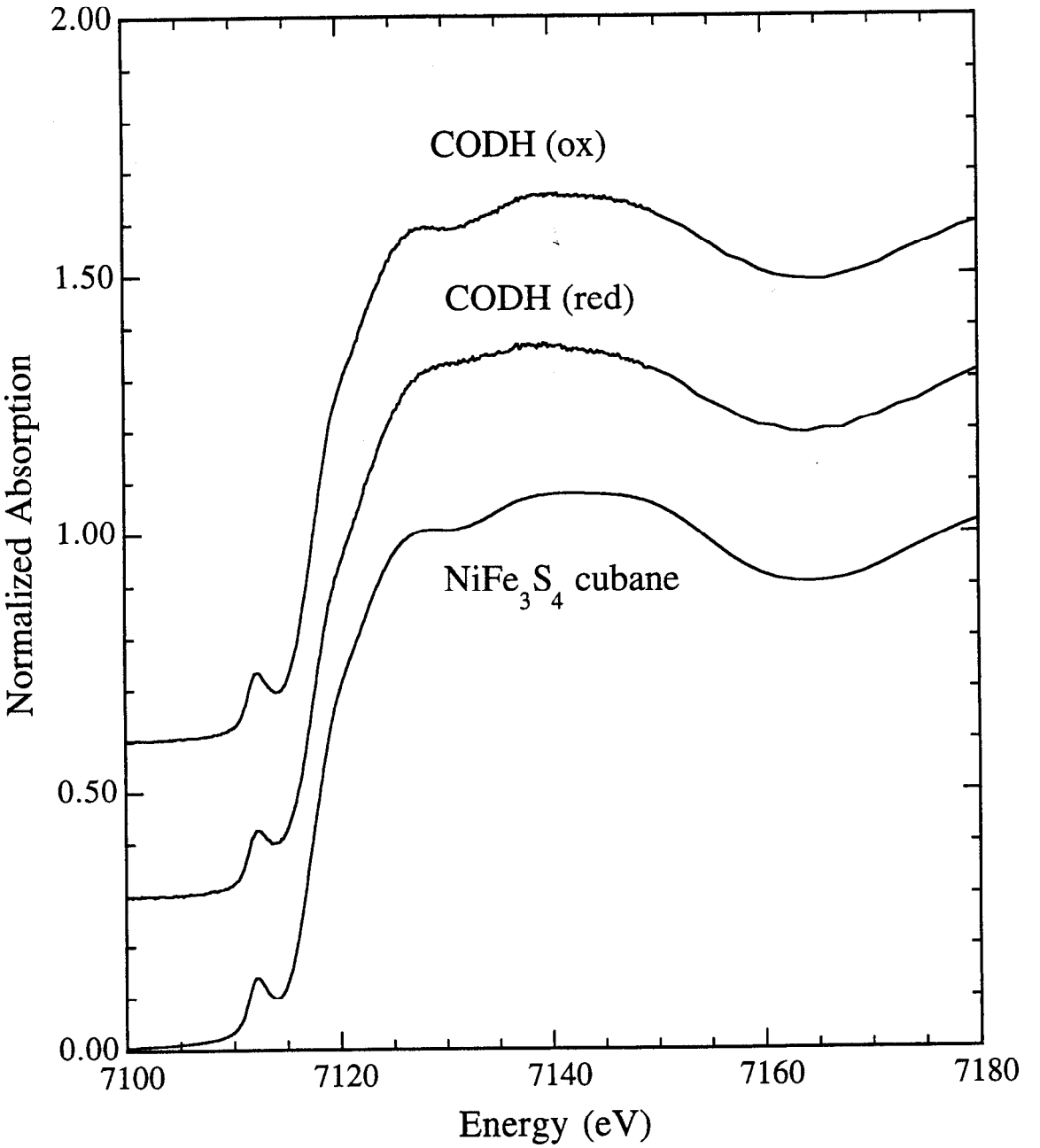

Figure 7.9. Fe K edges of oxidized and reduced Ni CODH (1991 data), and $(Et_4N)_3[NiFe_3S_4(SEt)_4]$ (**11**).

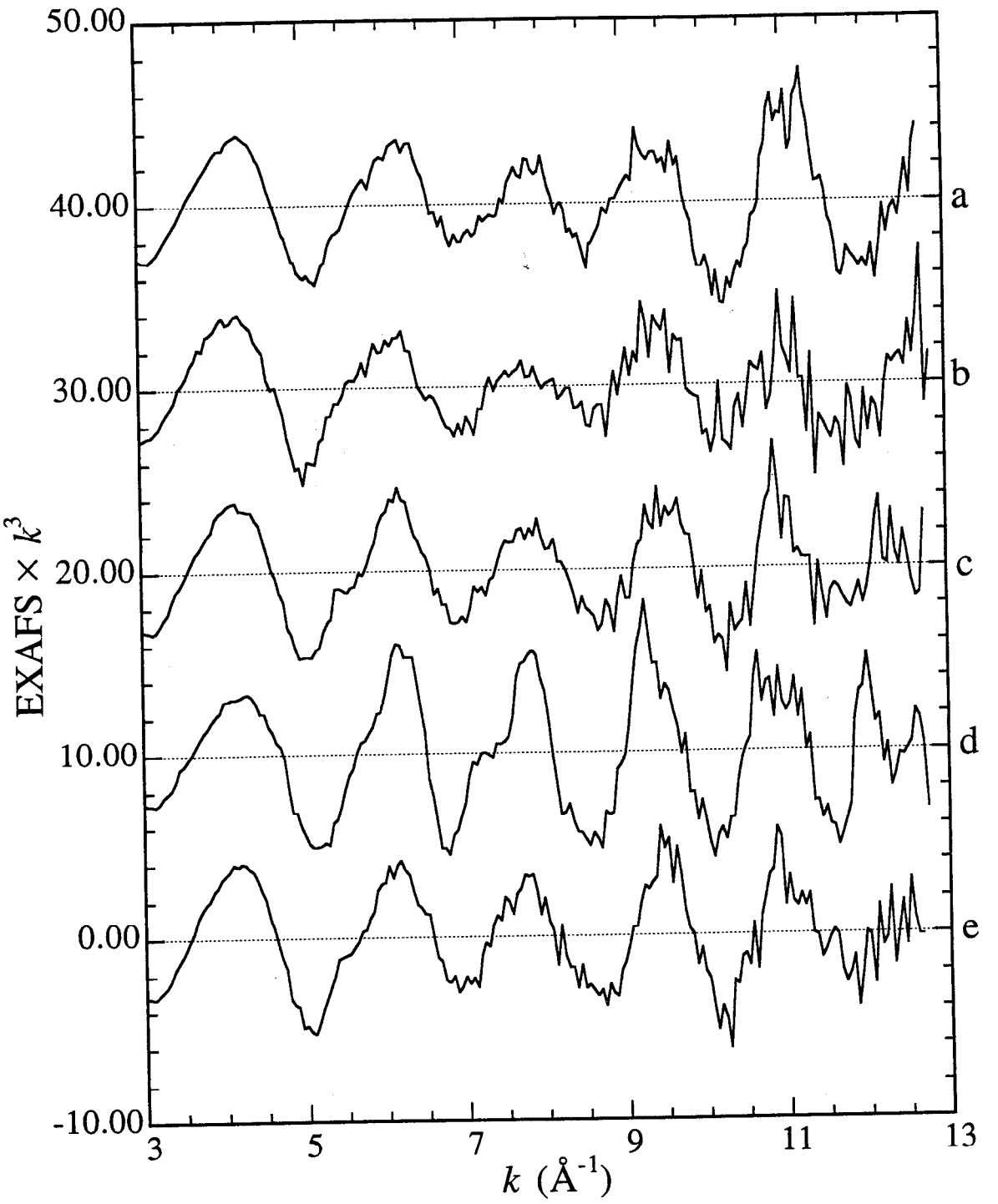

Figure 7.10. EXAFS spectra of Ni CODH protein. (a) CODHX (oxidized, June 1989), (b) CODHOX (oxidized, July 1991), (c) CDHOX (oxidized, July 1992), (d) CODHRX (reduced, July 1991), (e) CDHRD (reduced, July 1992).

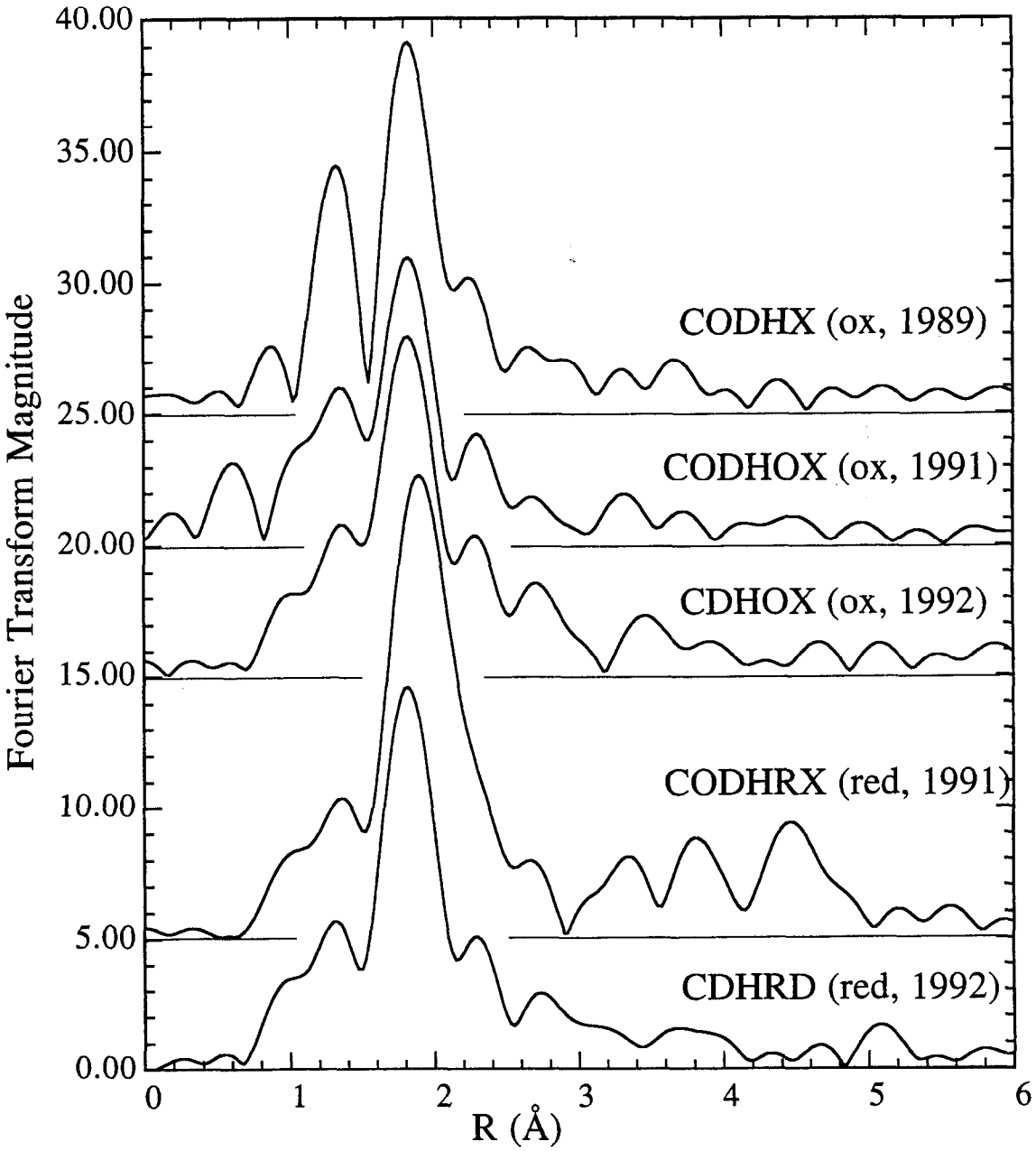

Figure 7.11. Fourier transformed Ni CODH protein data, using a Fourier window of k = 3.0–12.0 (0.1) $Å^{-1}$. Top to bottom : CODHX (oxidized, June 1989), CODHOX (oxidized, July 1991), CDHOX (oxidized, July 1992), CODHRX (reduced, July 1991), CDHRD (reduced, July 1992).

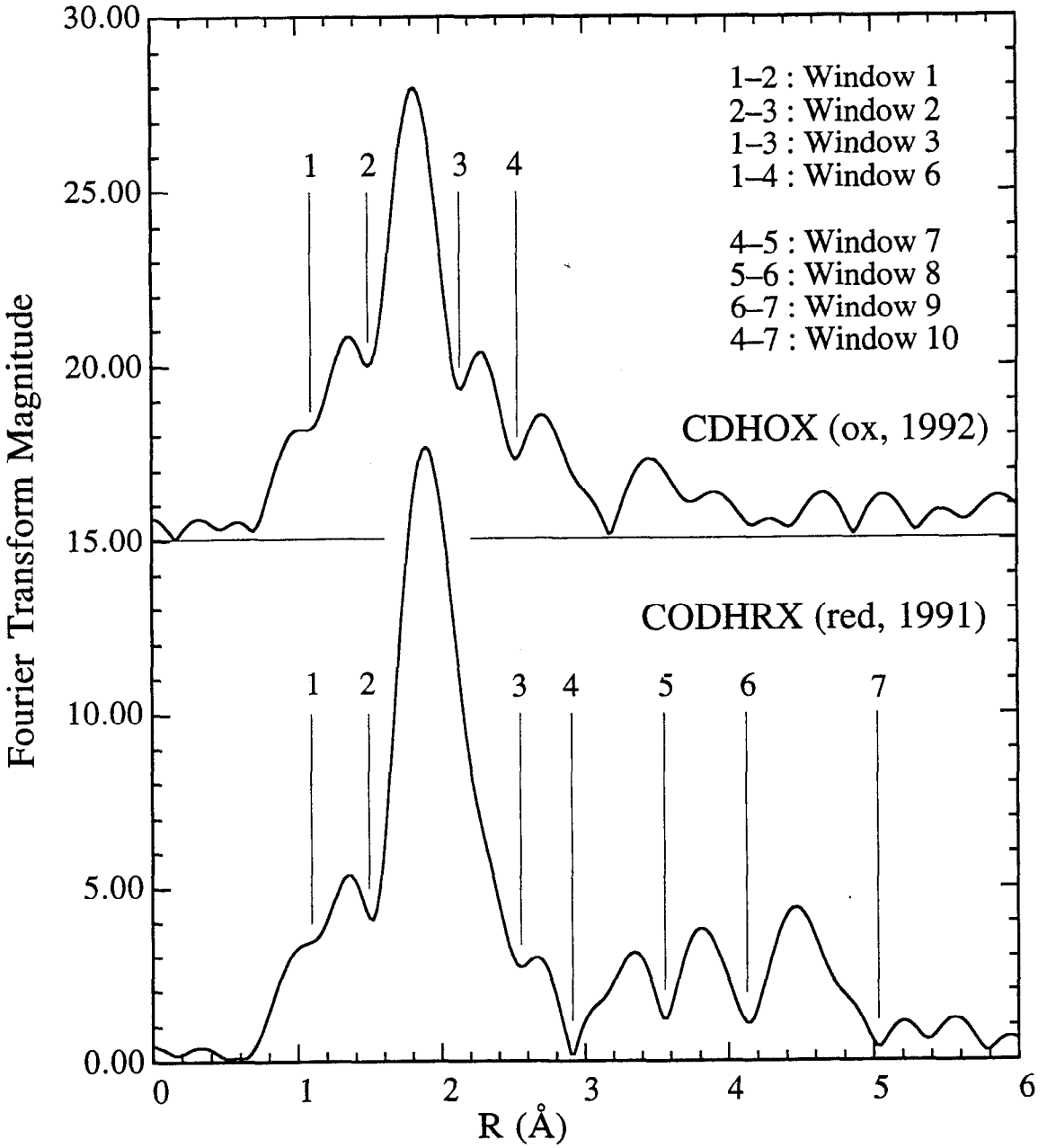

Figure 7.12. Fourier transforms over k = 3.0–12.0 (0.1) Å^{-1} of CDHOX (oxidized, July 1992) and CODHRX (reduced, July 1991), showing the Fourier windows used to generate filtered EXAFS data for curve-fitting. Windows 7–10 were only used for CODHRX. Note : While the peak at R' ~2.8 Å looks significant in CDHOX, in most of the data sets it is barely above the noise (see Figure 7.11).

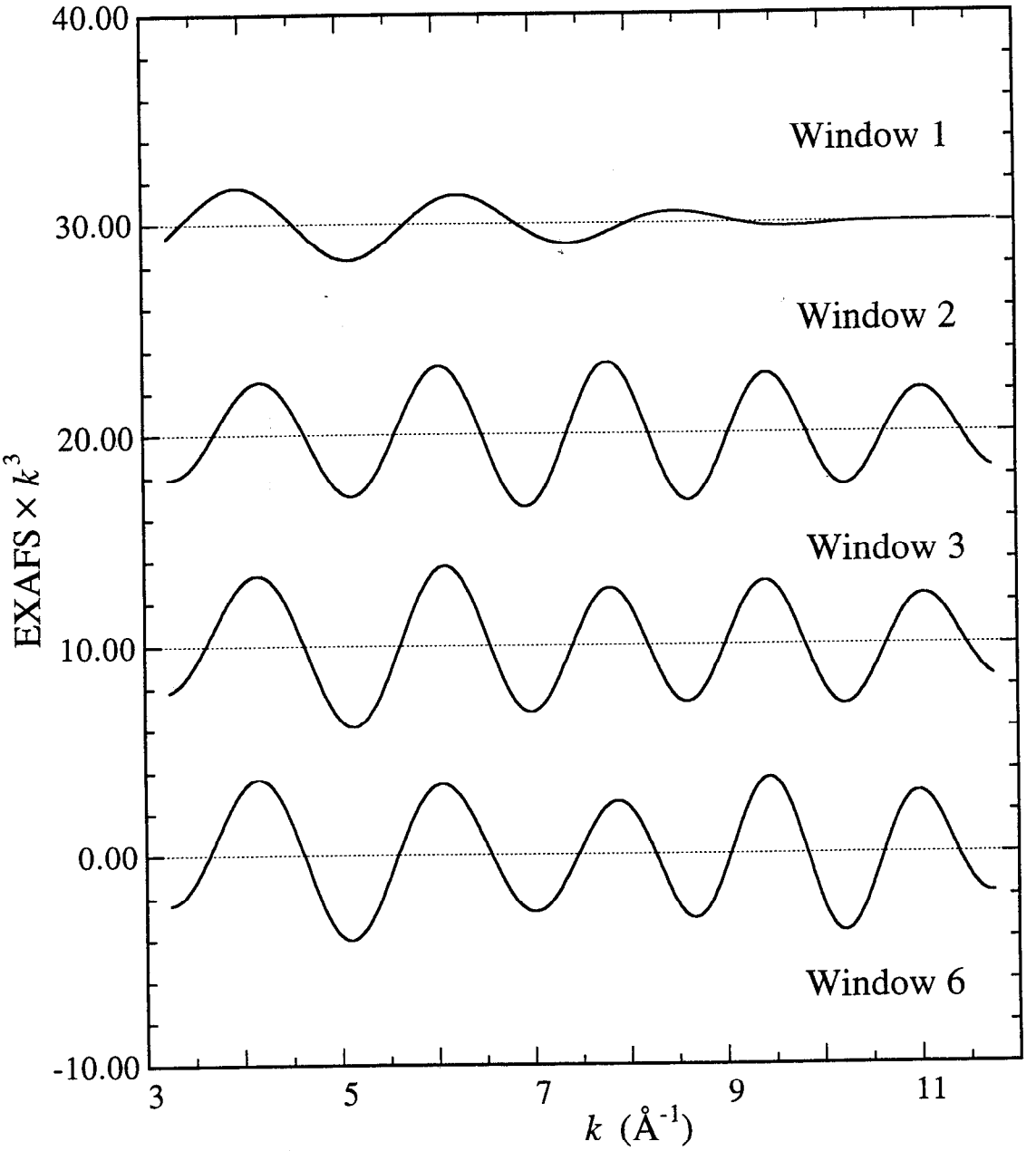

Figure 7.13. Examples of reverse Fourier transformed data ("filtered" data), to which various fits were made : Windows 1, 2, 3 and 6 from CDHOX (oxidized, July 1992).

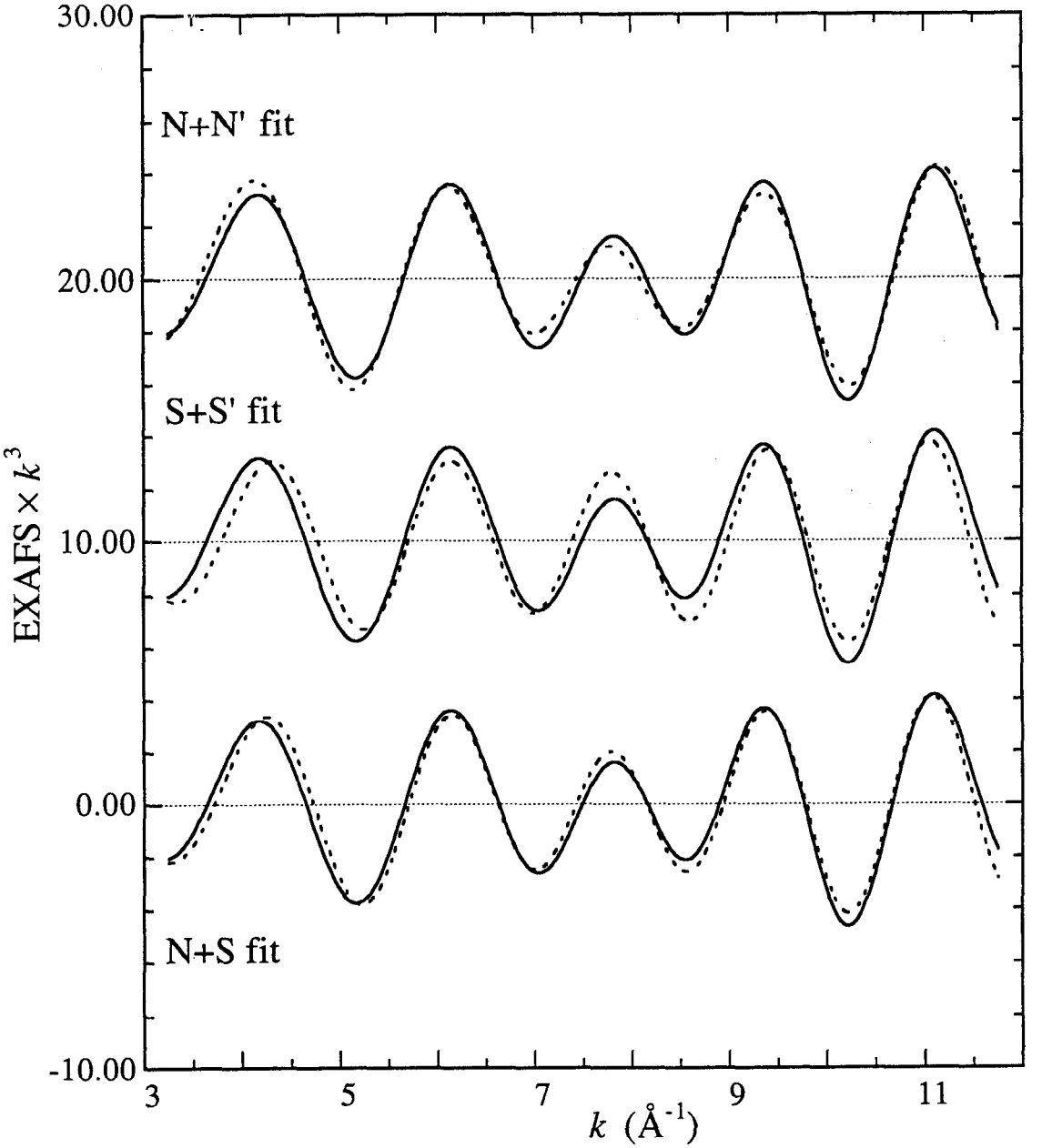

Figure 7.14. Type 2 fits (varying R and CN) (----) made to Window 3 of CODHX (oxidized, June 1989) (—). Top to bottom : N+N', S+S' and N+S.

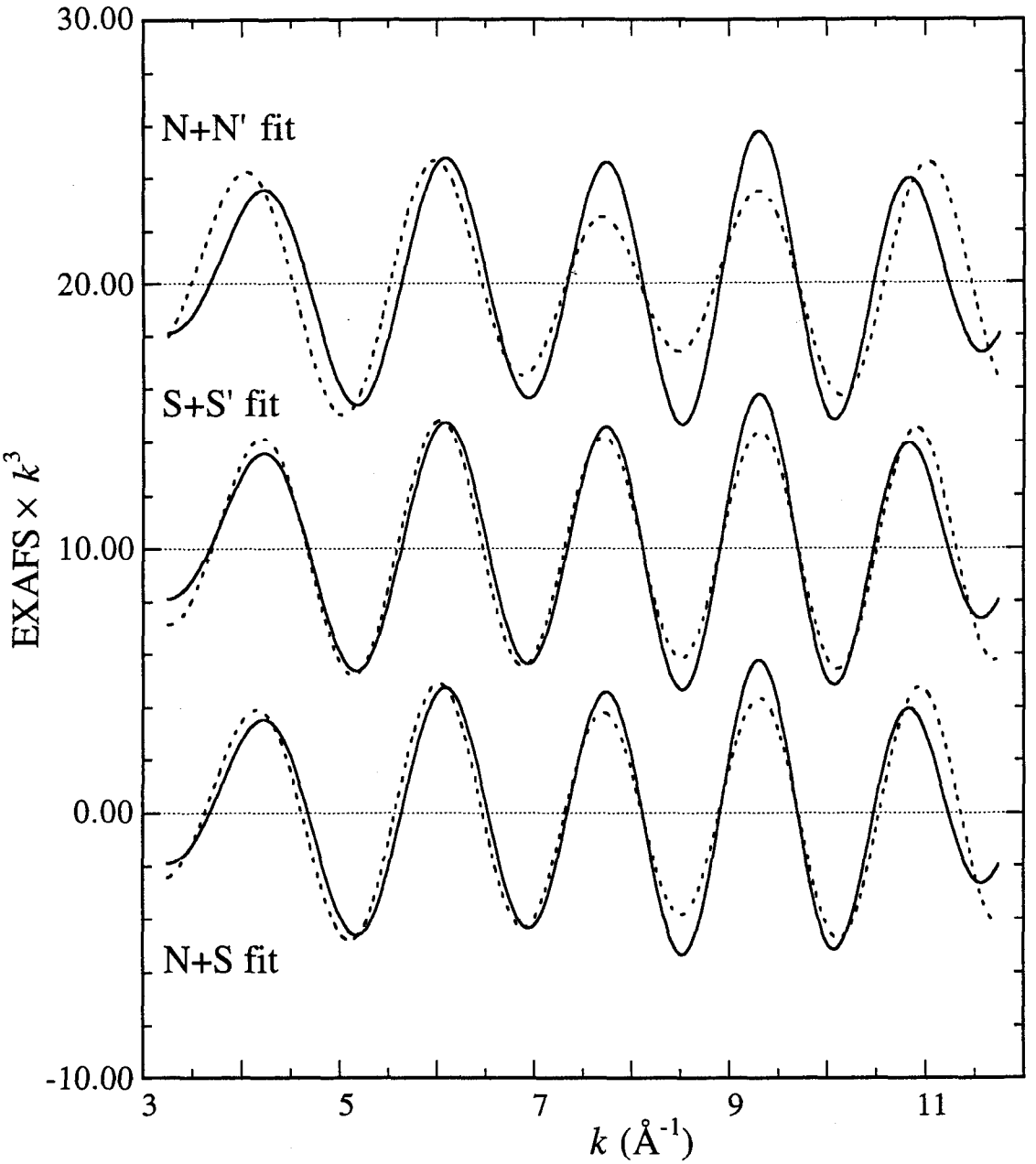

Figure 7.15. Type 2 fits (varying R and CN) (----) made to Window 3 of CODHRX (reduced, July 1991) (——). Top to bottom: N+N', S+S' and N+S.

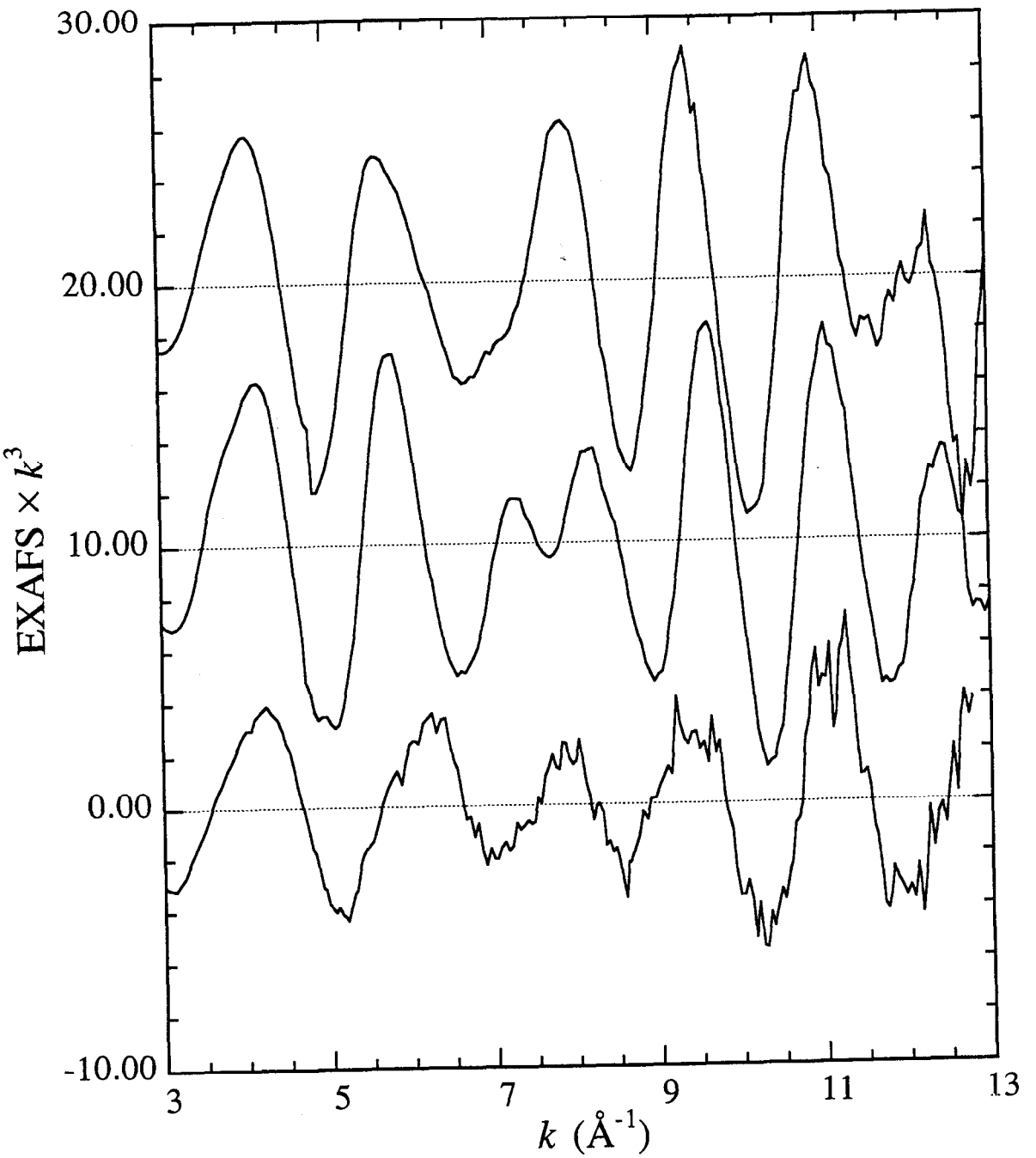

Figure 7.16. EXAFS spectra of the cubanes $(Et_4N)_3[NiFe_3S_4(SEt)_4]$ (**11**) (top) and $(Et_4N)_2[NiFe_3S_4(PPh_3)(SEt)_3]$ (**10**) (middle), and CODHX (oxidized CODH, June 1989) (bottom)

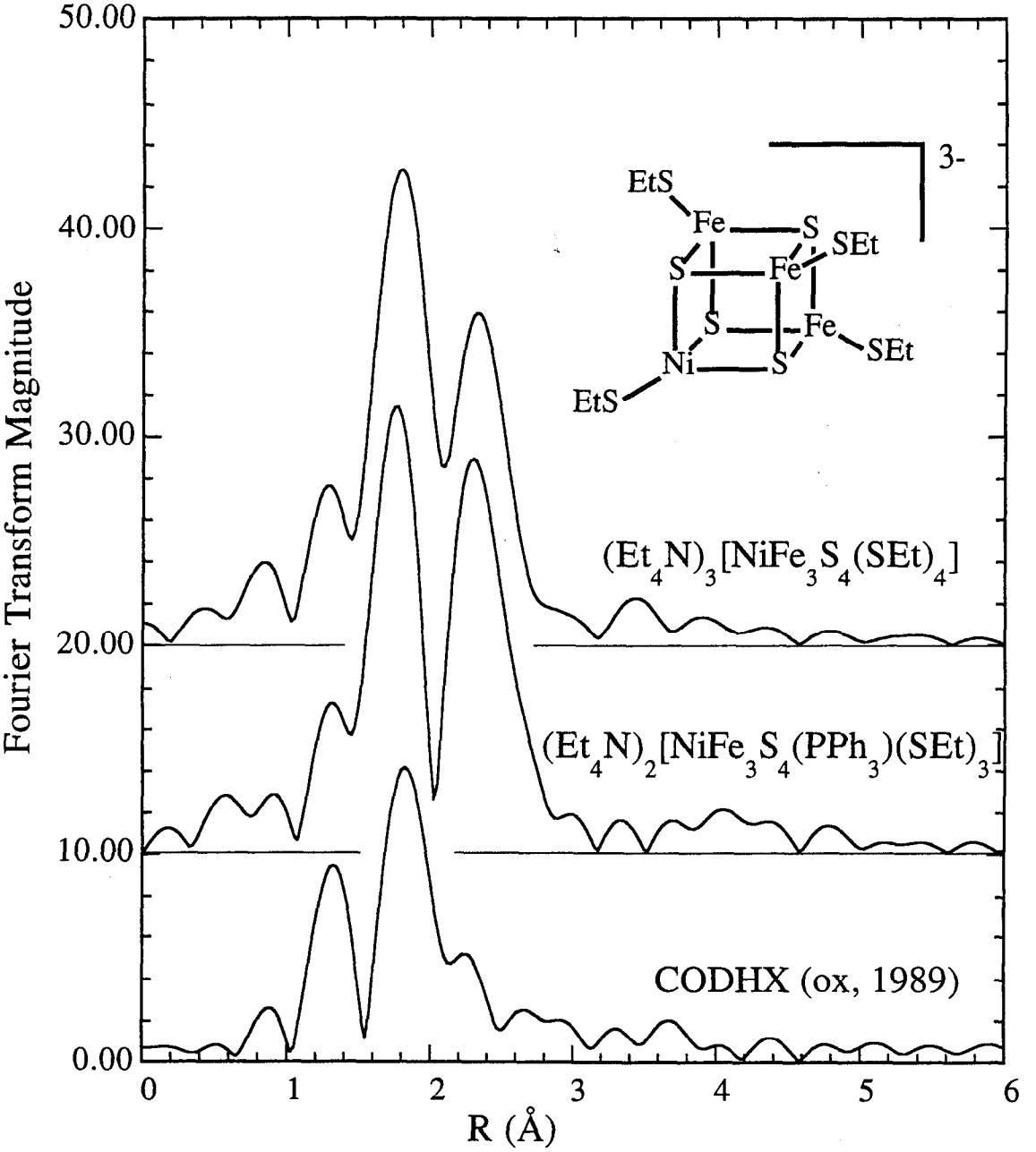

Figure 7.17. Fourier-transformed spectra of the cubanes $(Et_4N)_3[NiFe_3S_4(SEt)_4]$ (**11**) (top) and $(Et_4N)_2[NiFe_3S_4(PPh_3)(SEt)_3]$ (**10**) (middle), and CODHX (oxidized CODH, June 1989) (bottom). Fourier transform range : k = 3.0–12.0 (0.1) $Å^{-1}$

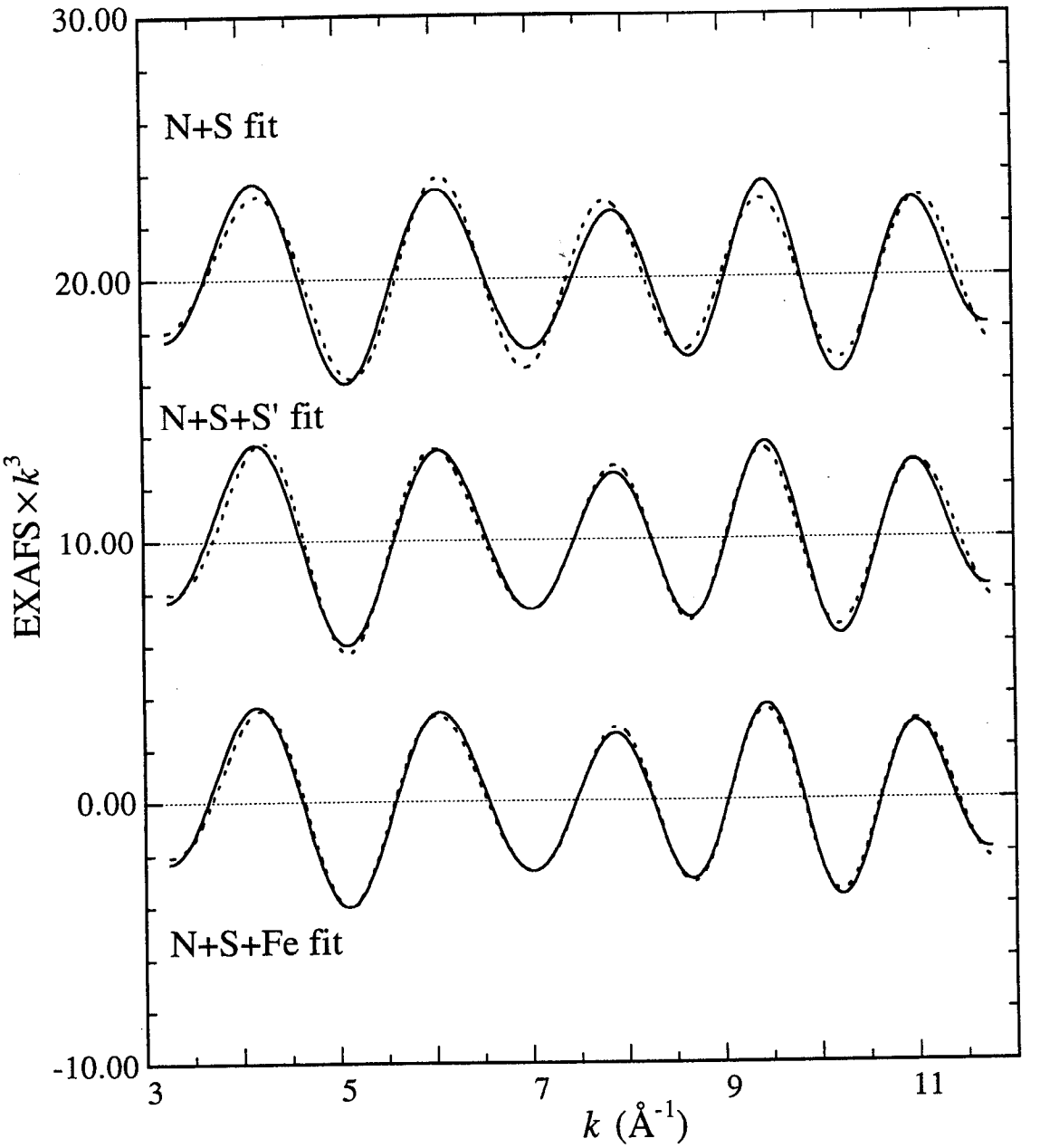

Figure 7.18. Filtered EXAFS data from CDHOX (Window 6) (——), with two- and three-wave Type 3 fits (varying R and c_2) (----). Top to bottom : 2N+2S, 2N+2S+1S' (S' at 2.90 Å) and 2N+2S+1Fe (Fe at 2.74 Å).

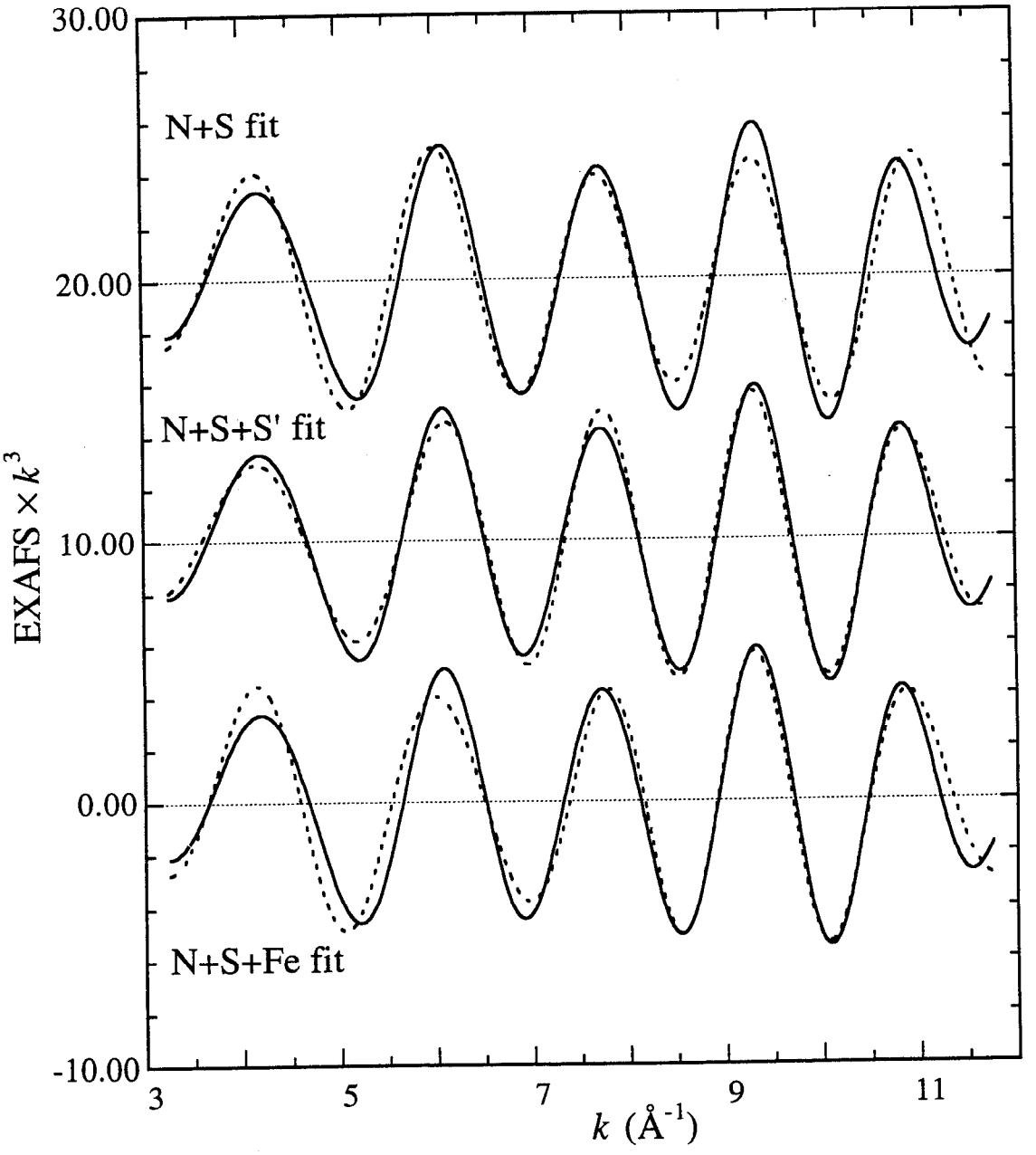

Figure 7.19. Filtered EXAFS data from CODHRX (Window 6) (——), with two- and three-wave Type 3 fits (varying R and c_2) (----). Top to bottom : 2N+3S, 2N+3S+1S' (S' at 2.61 Å) and 2N+3S+1Fe (Fe at 2.80 Å).

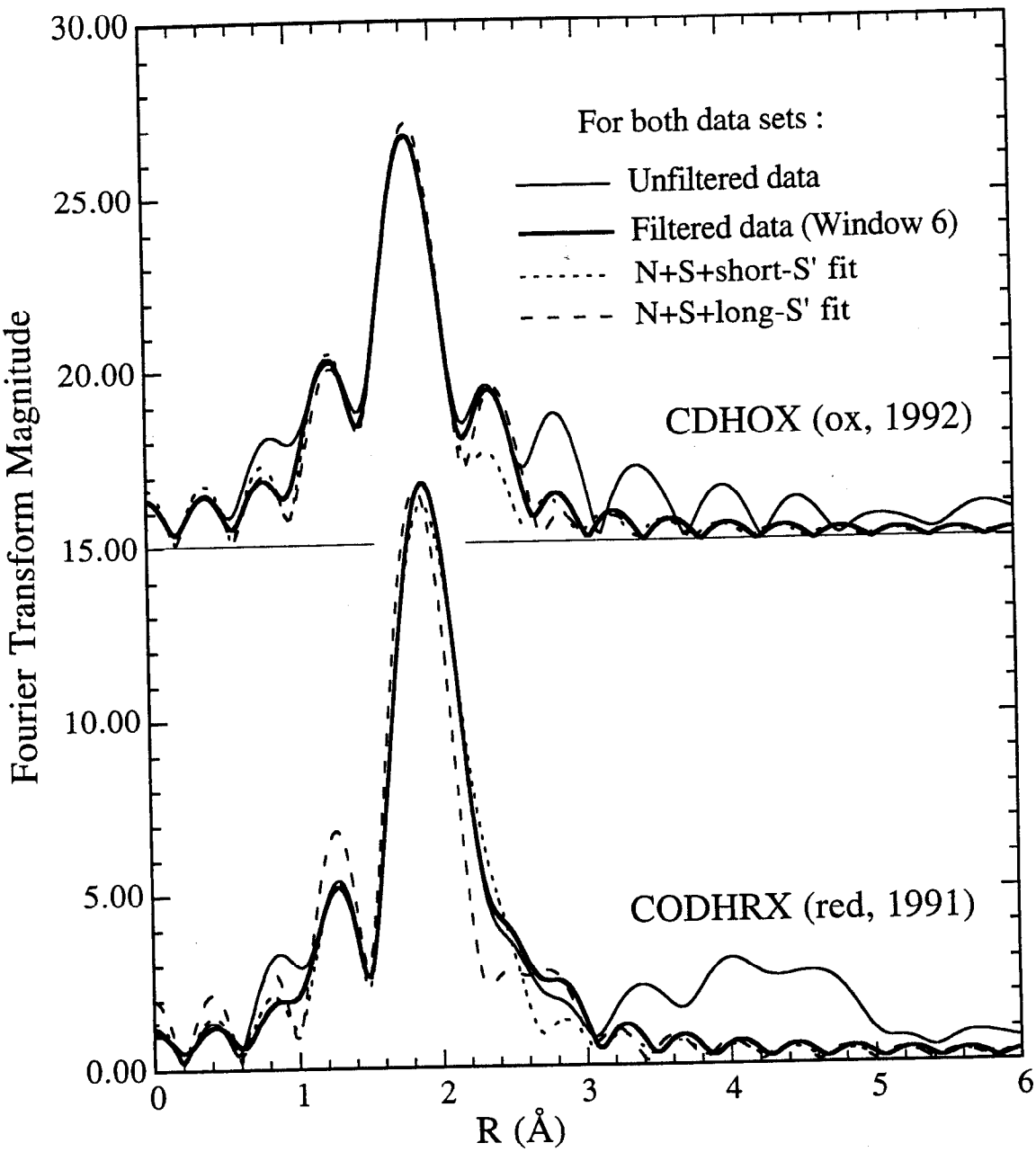

Figure 7.20. Fourier transforms of filtered (Window 6) and unfiltered protein data and some Type 3 N+S+S' fits to the filtered data. Fourier transform range : k = 3.5–11.5 (0.1) Å^{-1}. Top : CDHOX data and two 2N+2S+1S' fits to it. S' is found at 2.40 Å or 2.90 Å. Bottom : CODHRX data and two 2N+3S+1S' fits to it. S' is found at 2.61 Å or 3.23 Å.

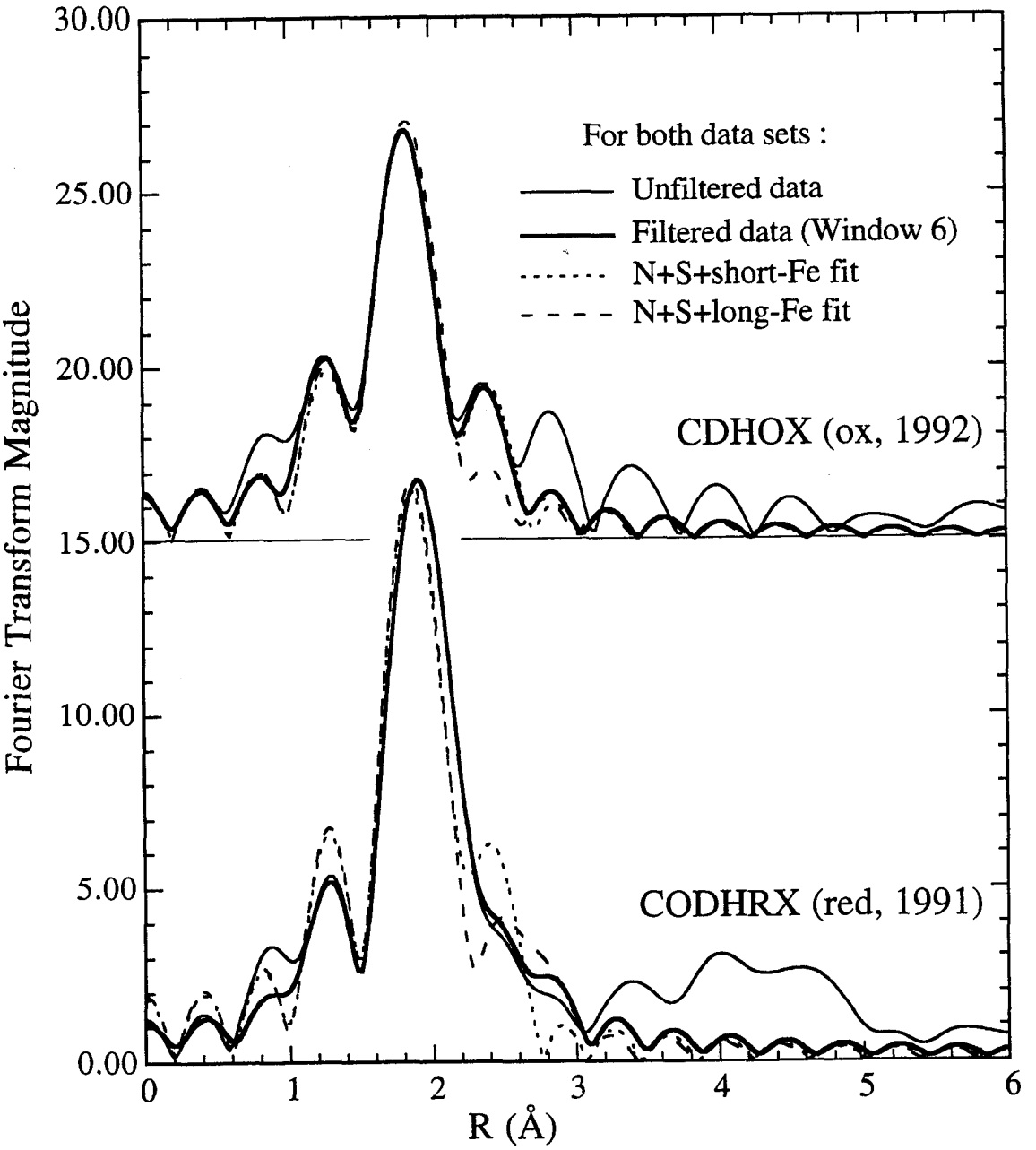

Figure 7.21. Fourier transforms of filtered (Window 6) and unfiltered protein data and some Type 3 N+S+Fe fits to the filtered data. Fourier transform range : k = 3.5–11.5 (0.1) Å^{-1}. Top : CDHOX data and two 2N+2S+1Fe fits to it. Fe is found at 2.74 Å or 3.56 Å. Bottom : CODHRX data and two 2N+3S+1Fe fits to it. Fe is found at 2.80 Å or 3.09 Å.

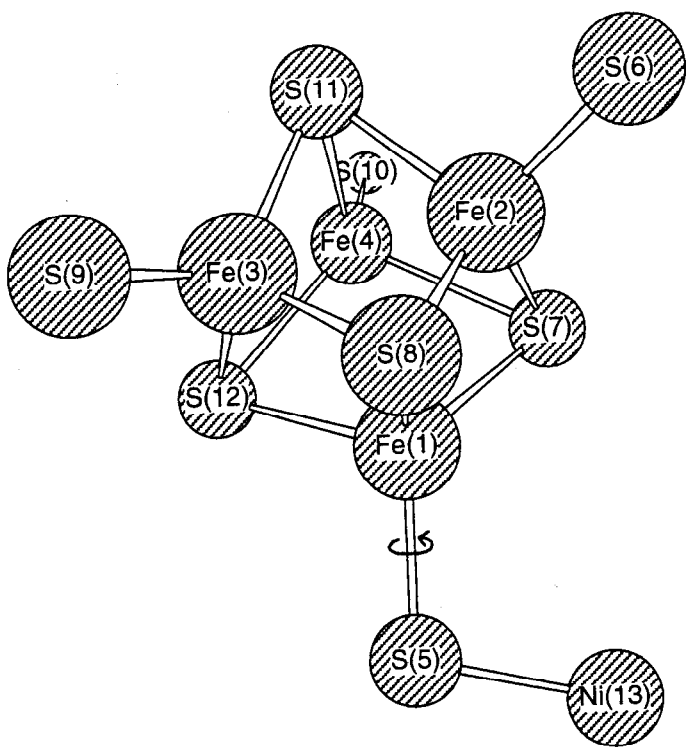

Figure 7.22. The core of $[Fe_4S_4(SPh)_4]^{3-}$, with Ni attached to one of the S(Ph) atoms.

Appendices

Appendix I. Complete Tables of Fits to EXAFS Spectra of Reduced Poplar Plastocyanin at pH 7.2 and 4.8 and a Cu(I)-N,S Model Compound

The following tables list the distances (R), coordination numbers (CN), c_2 values and fit indices (F) for the fits made for the EXAFS curve-fitting results discussed in Chapter 5. In the parameterized EXAFS equation employed by our analysis package (see Chapter 2), c_2 values vary in the same way as the squared term σ^2_{as} in the Debye-Waller factor, such that $\Delta c_2 = -2\Delta\sigma^2_{as}$. Thus, though the sign is reversed, the magnitude of c_2 is proportional to σ^2_{as}.

When using the fit index F to evaluate the goodness of a fit to the data, we have to bear in mind that F is not adjusted for the size of the signal. Thus, for equally good fits (as judged by viewing the match of phase and amplitude), we would expect the fit indices for fits to a larger EXAFS signal to be larger than those for fits to smaller EXAFS signals. So the fit index F should only be used to compare different fits made on the same data.

The windows used on the data sets are denoted by their data file names. Thus, fits to PCHI.FIL2 correspond to fits on Window 2 of PCHI, PCHI.FIL3 contains data filtered using Window 3, etc.

The tables also show what initial R, CN and c_2 values were used for beginning each fit. Unless otherwise stated, a fit result shown had as its initial values the results of the fit shown in the line immediately above. Thus, in a given table (e.g., N+S fits on PCHI.FIL2), the values listed as initial values were first used in a fit varying R's only. Then the results of this fit were in turn used in a fit varying R and CN (referred to as Type 2 fits in the text), whose results are listed below it. The results of this Type 2 fit were in turn used as initial values for the Type 1 fit (varying R's, CN's and c_2's) whose results are listed immediately below. An exception to this is that Type 3 fits (varying R's and c_2's), listed below Type 1 fits, generally used the results of fits varying R only as initial values. Bracketed CN or c_2 values were held fixed at the values shown.

List of Tables :

Results of fitting a Cu^{I}-N_2S_2 model with N & S

Grace Tan 14/12/90

(Numbers checked and corrected 17/4/93)

These fits are discussed in Chapter 5, Section (C.1).

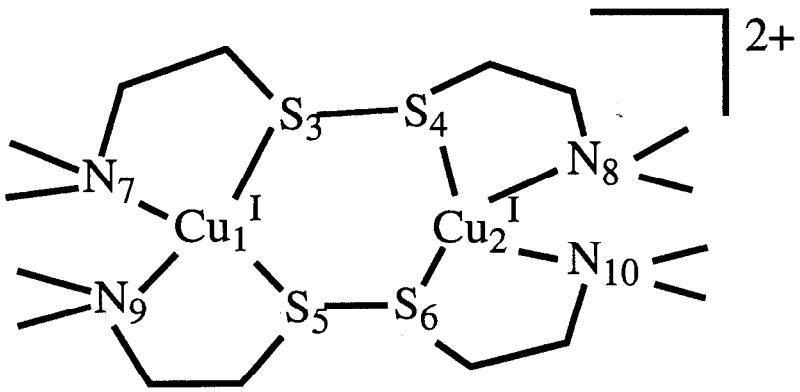

Cu_1-S_3	= 2.288 Å
Cu_1-S_5	= 2.302 Å
Cu_2-S_4	= 2.283 Å
Cu_2-S_6	= 2.326 Å
Cu_1-N_7	= 2.143 Å
Cu_1-N_9	= 2.184 Å
Cu_2-N_8	= 2.105 Å
Cu_2-N_{10}	= 2.089 Å

$Cu^{I}_2((CH_3)_2NCH_2CH_2SSCH_2CH_2N(CH_3)_2)_2(BF_4)_2$

Data to k = 17 Å^{-1}, but has some interesting problems :

(1) 9 scans collected, but Scans 3 & 4 were ruined by small earthquakes!
(2) A node in the EXAFS occurs at k = 13. EXAFS in this region underwent a change between Scans 5 & 6, when detuning changed from counterclockwise (the usual) to clockwise (required for this particular run on BL 4-2).
(3) Chose to use scans collected before the change occurred in the EXAFS.
(4) Spline to k = 17 Å^{-1} looks different from spline to k = 13 Å^{-1} because of the node at k = 13 Å^{-1}.
(5) Decided to use spline to k = 13 Å^{-1} because the glitch at k = 13.25 Å^{-1} *may* be due to Zn.
Pre-edge : 9043–9640 (-2)
Spline : 9025 (2) 9138 (3) 9343 (3) 9640

Forward FT : k = 3.5–12.5 (0.1) Å^{-1}

Reverse FT (to k = 4.0–12.0 Å^{-1}) :

CUNS2.FIL0 : R' = 1.35–2.35 (0.1) Å — main peak only

CUNS2.FIL2 : R' = 1.35–3.00 (0.1) Å — main peak + 1 higher-R peak

Parameters used in fits :

Cu^{I}-N : $Cu^{I}(N\text{-meim})_4ClO_4$,	10 K,	k = 4.0–12.0 Å^{-1}	(data to k = 17 Å^{-1})
Cu^{I}-S : $[Cu^{I}(detu)_3]_2SO_4$,	10 K,	k = 4.0–12.0 Å^{-1}	(data to k = 17 Å^{-1})

Fits of CUNS2.FIL0 :

N only :	R	CN	c_2	F
Initial	2.0	4	-0.02528	----
	2.1269	5.1923	"	0.847597
	2.1285	4.5318	-0.02291	0.833506

S only :				
Initial	2.2	3	-0.02161	----
	2.2755	1.9126	"	0.354235
	2.2760	2.3186	-0.02454	0.284316

N + S :

	R_N	CN_N	c_{2N}	R_S	CN_S	c_{2S}	F
Initial	2.0	2	-0.02528	2.2	2	-0.02161	-----
##	2.0643	"	"	2.2922	"	"	0.676022
	2.1145	1.5789	"	2.2795	1.4440	"	0.133608
	2.1070	0.5572	-0.01348	2.2830	1.8822	-0.02399	0.0716634
	2.0882	(1)	-0.01288	2.2955	(1)	-0.01586	0.245786
	2.1025	(2)	-0.02257	2.2890	(1)	-0.01803	0.180088
	2.1127	(3)	-0.03032	2.2803	(1)	-0.01851	0.229882
	2.1377	(1)	-0.01950	2.2741	(2)	-0.02625	0.105672
	2.1731	(2)	-0.02782	2.2615	(2)	-0.02545	0.173140
	2.1819	(3)	-0.05073	2.2693	(2)	-0.02336	0.233801
Initial	2.2	4	-0.02528	2.6	1	-0.02161	-----
	2.1283	"	"	2.6543	"	"	0.922859
	2.1284	5.2084	"	2.6466	0.5793	"	0.665233
	2.1308	5.0578	-0.02454	2.6921	2.1575	-0.04688	0.652876
Initial	2.6	1	-0.02528	2.2	3	-0.02161	-----
	2.6788	"	"	2.2775	"	"	1.35061
	2.6350	0.6904	"	2.2741	1.9086	"	0.300635
	2.6343	0.0303	+0.01088	2.2766	2.1750	-0.02306	0.215093

-- these R values used as starting values in each of the fixed-CN fits.

N + N' :

	R_N	CN_N	c_{2N}	$R_{N'}$	$CN_{N'}$	$c_{2N'}$	F
Initial	2.0	2	-0.02528	2.2	2	-0.02528	-----
	2.1262	"	"	2.1260	"	"	0.988750
	2.1269	2.4006	"	2.1270	2.7915	"	0.847597
	(Made a few attempts to vary c_2's, but program crashed each time.)						
Initial	2.2	4	-0.02528	2.6	1	-0.02528	-----
	2.1274	"	"	2.5123	"	"	0.756658
	2.1306	4.8439	"	2.5082	2.4561	"	0.432334
	2.1285	4.7205	-0.02505	2.5068	1.7462	-0.01980	0.426004

S + S' :

	R_S	CN_S	c_{2S}	$R_{S'}$	$CN_{S'}$	$c_{2S'}$	F
Initial	2.0	1	-0.02161	2.2	2	-0.02161	-----
	1.9950	"	"	2.2506	"	"	1.48276
	2.0528	-0.3031	"	2.2806	1.6904	"	0.171698
	2.0680	-0.1227	-0.01126	2.2805	2.1372	-0.02494	0.0559465
Initial	2.2	2	-0.02161	2.6	1	-0.02161	-----
	2.2746	"	"	2.7711	"	"	0.768813
	2.2752	1.9060	"	2.7604	0.1780	"	0.321687
	2.2767	2.2599	-0.02395	2.7425	0.0029	+0.01876	0.240476

N + N' + S : (these fits are exploratory)

Fixed c_2's

c_{2N} = -0.02528 $c_{2N'}$ = -0.02528 c_{2S} = -0.02161

	R_N	CN_N	$R_{N'}$	$CN_{N'}$	R_S	CN_S	F
Initial	2.1	1	2.2	1	2.3	2	-----
	2.0893	"	2.3154	"	2.2794	"	0.234863
	2.1314	2.3885	2.3014	-1.8216	2.2877	0.7262	0.0350366
Initial	2.0970*	1	2.1635*	1	2.2998*	2	-----
	2.0893	"	2.3155	"	2.2794	"	0.234863
	2.1144	1.1570	2.1145	0.4215	2.2795	1.4443	0.133608

Fixed CN's

CN_N = 1 $CN_{N'}$ = 1 CN_S = 2

	R_N	c_{2N}	$R_{N'}$	$c_{2N'}$	R_S	c_{2S}	F
Initial	2.0970*	-0.02528	2.1635*	-0.02528	2.2998*	-0.02161	-----
	4.3544	-0.33503	-0.0505	-0.49496	2.2754	-0.02266	0.318068

* --- averages of the crystallographic values

Results of fitting Reduced Pc with N & S

Grace Tan includes fits done 2/2/91 & 14/4/93

(numbers checked and corrected 17/4/93)

The following fits are discussed in Chapter 5, Sections (C.2.a) – (C.2.c). All fits made to the data set PCHI are first listed, followed by fits to PCLO.

Reduced Pc at pH 7.2 : PCHI — 21 acceptable scans
Reduced Pc at pH 4.8 : PCLO — 29 acceptable scans

Data to $k = 13$ Å^{-1}

Final pre-edge and spline for both (to $k = 13$ Å^{-1}) :
Pre-edge : 9045–9640 (2)
Spline : 9030 (2) 9146 (3) 9350 (3) 9640

Forward FT : $k = 3.5$–12.5 (0.1) Å^{-1} (but note large glitches removed at $k = 10.9$ Å^{-1})

Reverse FT (to $k = 4.0$–12.0 Å^{-1}) :

PCHI.FIL0 : R = 1.20–2.12 (0.1) Å — main peak only
PCLO.FIL0 : R = 1.25–2.12 (0.1) Å

PCHI.FIL1 : R = 1.20–2.45 (0.1) Å — main peak + 1 higher-R bump
PCLO.FIL1 : R = 1.25–2.40 (0.1) Å

PCHI.FIL2 : R = 1.20–2.85 (0.1) Å — main peak + 2 higher-R bumps
PCLO.FIL2 : R = 1.25–3.05 (0.1) Å

[PCHI.FIL3 : R = 0.85–2.45 (0.1) Å — main peak + low-R shoulder + 1 higher-R bump
PCLO.FIL3 : R = 0.85–2.40 (0.1) Å] *

* Of questionable reliability, because of spline dependence of low-R shoulder. However, fits show that the low-R shoulder probably really does contain some Cu-scatterer signal.

Parameters used in fits :

Cu^{I}-N : $Cu^{I}(N\text{-meim})_4ClO_4$, 10 K, $k = 4.0$–12.0 Å^{-1} (data to $k = 17$ Å^{-1})
Cu^{I}-S : $[Cu^{I}(detu)_3]_2SO_4$, 10 K, $k = 4.0$–12.0 Å^{-1} (data to $k = 17$ Å^{-1})

Fits of PCHI :

N only :	R	CN	c_2	F
Initial	1.9, 2.0	3	-0.02528	----
PCHI.FIL0	2.0396	3.0794	(-0.02528)	0.319982
	2.0387	3.4195	-0.02715	0.311351
PCHI.FIL1	2.0401	3.0926	(-0.02528)	0.358759
	2.0393	3.3990	-0.02697	0.352564
PCHI.FIL2	2.0402	3.1012	(-0.02528)	0.369850
	2.0395	3.4078	-0.02697	0.363911

S only :	R	CN	c_2	F
Initial	2.0, 2.2	3, 3, 2	-0.02161	----
PCHI.FIL0 :	2.1883	1.0524	(-0.02161)	0.449532
	2.1917	1.6187	-0.02842	0.358746
PCHI.FIL1 :	2.1880	1.0637	(-0.02161)	0.448154
	2.1905	1.4886	-0.02688	0.394862
PCHI.FIL2 :	2.1879	1.0642	(-0.02161)	0.466378
	2.1904	1.4754	-0.02673	0.419230

N + S :

	R_N	CN_N	c_{2N}	R_S	CN_S	c_{2S}	F
PCHI.FIL0 :							
Initial	2.0	2	-0.02528	2.2	2	-0.02161	-----
	1.9245	"	"	2.2137	"	"	1.47935
	2.0283	1.9372	"	2.2042	0.4824	"	0.0981685
	2.0704	2.4140	-0.03140	2.1643	0.9035	-0.02695	0.0390049
PCHI.FIL1 :							
Initial	2.0	2	-0.02528	2.2	1	-0.02161	-----
	1.9930	"	"	2.2213	"	"	0.575079
	2.0316	1.8568	"	2.1987	0.5050	"	0.166545
	2.1536	3.6166	-0.04308	2.1695	1.6997	-0.02709	0.0722466
	2.0815	(2)	-0.03219	2.1685	(1)	-0.02537	0.140060
	2.0907	(3)	-0.04227	2.1701	(1)	-0.02379	0.0882840
	2.2784	(1)	-0.01301	2.2061	(2)	-0.02505	0.151783
	2.2324	(2)	-0.01342	2.1883	(2)	-0.01956	0.0759371
PCHI.FIL2 :							
Initial	2.0	2	-0.02528	2.2	1	-0.02161	-----
	1.9934	"	"	2.2211	"	"	0.592753
	2.0331	1.8853	"	2.1972	0.4931	"	0.201165
	2.1667	3.9492	-0.04234	2.1698	1.8823	-0.02754	0.101359
	2.0401	(1)	-0.02071	2.1930	(1)	-0.02821	0.244280
	2.0840	(2)	-0.03219	2.1679	(1)	-0.02509	0.175027
	2.0926	(3)	-0.04197	2.1695	(1)	-0.02365	0.124069
	2.2793	(1)	-0.01288	2.2073	(2)	-0.02516	0.184585
	2.2336	(2)	-0.01362	2.1889	(2)	-0.01967	0.121799

	R_N	CN_N	c_{2N}	R_S	CN_S	c_{2S}	F
PCHI.FIL3 :							
Initial	2.0	2	-0.02528	2.2	1	-0.02161	-----
	1.9915	"	"	2.2199	"	"	0.632023
	2.0291	1.8725	"	2.1992	0.5297	"	0.374580
	2.0840	8.9573	-0.07794	2.1774	1.0164	-0.02270	0.218851
	2.0742	(2)	-0.03328	2.1712	(1)	-0.02531	0.331454

N + N' :

	R_N	CN_N	c_{2N}	$R_{N'}$	$CN_{N'}$	$c_{2N'}$	F
PCHI.FIL0 :							
Initial	2.0	2	-0.02528	2.2	2	-0.02528	-----
	1.9969	"	"	2.0831	"	"	0.335411
	1.8670	0.7403	"	2.0454	3.6946	"	0.156056
	1.9758	2.0898	-0.02579	2.0846	1.3695	-0.01512	0.0745650
PCHI.FIL1 :							
Initial	2.0	2	-0.02528	2.2	2	-0.02528	-----
	1.9978	"	"	2.0831	"	"	0.375270
	1.8678	0.7541	"	2.0460	3.7184	"	0.218781
	1.9879	2.2975	-0.02461	2.0942	0.9503	-0.01176	0.124775
Initial	2.2	2	-0.02528	2.8	2	-0.02528	-----
	2.0371	"	"	2.7321	"	"	0.727990
	2.0398	3.0930	"	2.7322	0.4783	"	0.336372
	2.0378	3.3018	-0.02642	2.6971	0.0293	+0.01086	0.280630
PCHI.FIL2 :							
Initial	2.0	2	-0.02528	2.2	2	-0.02528	-----
	1.9982	"	"	2.0830	"	"	0.385517
	1.8680	0.7564	"	2.0462	3.7288	"	0.235564
	1.9972	2.5680	-0.02601	2.0961	0.7106	-0.01020	0.148635
Initial	2.2	2	-0.02528	2.8	2	-0.02528	-----
	2.0375	"	"	2.7491	"	"	0.756576
	2.0401	3.1037	"	2.7471	0.3720	"	0.357205
	2.0377	3.3230	-0.02650	2.6824	0.0061	+0.02307	0.293565

S + S' :

	R_S	CN_S	c_{2S}	$R_{S'}$	$CN_{S'}$	$c_{2S'}$	F
PCHI.FIL0 :							
Initial	2.0	1	-0.02161	2.2	1	-0.02161	-----
	2.1390	"	"	2.2628	"	"	0.387970
	2.1755	1.3453	"	2.3315	0.5753	"	0.144278
	2.1630	0.9474	-0.02073	2.2805	1.1740	-0.03412	0.129104
PCHI.FIL1 :							
Initial	2.0	1	-0.02161	2.2	1	-0.02161	-----
	2.1388	"	"	2.2606	"	"	0.456676
	2.1808	1.3698	"	2.3471	0.5210	"	0.220856
	2.1794	1.5809	-0.02616	2.3475	2.0418	-0.05590	0.0996645
Initial	2.2	1	-0.02161	2.8	1	-0.02161	-----
	2.1873	"	"	2.9121	"	"	0.767793
	2.1878	1.0660	"	2.8937	0.1720	"	0.428490
	2.1889	1.3842	-0.02580	2.9302	2.9945	-0.08332	0.331988

	R_S	CN_S	c_{2S}	$R_{S'}$	$CN_{S'}$	$c_{2S'}$	F
PCHI.FIL2 :							
Initial	2.0	1	-0.02161	2.2	1	-0.02161	-----
	2.1389	"	"	2.2606	"	"	0.481035
	2.1816	1.3862	"	2.3507	0.5349	"	0.239043
	2.1792	1.5288	-0.02599	2.3440	2.5588	-0.06276	0.124938
Initial	2.2	1	-0.02161	2.8	1	-0.02161	-----
	2.1887	"	"	2.9884	"	"	0.770744
	2.1880	1.0670	"	2.9620	0.1455	"	0.454291
	2.1886	1.3874	-0.02578	2.9773	7.2110	-0.10937	0.322347

N + S + S' :

PCHI.FIL1 :

Fixed c_2's

c_{2N} = -0.02528 c_{2S} = -0.02161 $c_{2S'}$ = -0.02161

	R_N	CN_N	R_S	CN_S	$R_{S'}$	$CN_{S'}$	F
Initial	2.0	2	2.2	1	2.5	1	-----
	2.0064	"	2.2390	"	2.4507	"	0.532334
	2.0145	1.5767	2.2106	0.7994	2.4181	0.2607	0.107835
Initial	2.0	1	2.2	1	2.8	1	-----
	1.9999	"	2.2009	"	2.9296	"	0.736591
	2.0320	1.8321	2.1977	0.5106	2.8660	0.1253	0.135402
	2.0309	1.6898	2.1966	0.5504	2.9080	1.2912*	0.0939606
					[*c_2 = -0.06838]		

Fixed CN's

CN_N = 2 CN_S = 1 $CN_{S'}$ = 1

	R_N	c_{2N}	R_S	c_{2S}	$R_{S'}$	$c_{2S'}$	F
Initial	2.0	-0.02528	2.2	-0.02161	2.5	-0.02161	-----
	2.0592	-0.03735	2.1760	-0.02430	2.3658	-0.06231	0.0659733
Initial	2.0	-0.02528	2.2	-0.02161	2.8	-0.02161	-----
	2.0820	-0.03286	2.1689	-0.02510	2.9186	-0.06612	0.0821691

PCHI.FIL2 :

Fixed c_2's

c_{2N} = -0.02528 c_{2S} = -0.02161 $c_{2S'}$ = -0.02161

	R_N	CN_N	R_S	CN_S	$R_{S'}$	$CN_{S'}$	F
Initial	2.0	2	2.2	1	2.5	1	-----
	2.0069	"	2.2376	"	2.4481	"	0.536572
	2.0133	1.4933	2.2088	0.8491	2.4118	0.2935	0.147050
Initial	2.0	2	2.2	1	2.8	1	-----
	1.9920	"	2.2227	"	3.0214	"	0.818127
	2.0322	1.8873	2.1984	0.4951	3.0181	0.1267	0.180653
	2.0320	1.6423	2.1946	0.5609	2.9669	5.0354*	0.0879317
					[*c_2 = -0.10999]		

Fixed CN's

CN_N = 2 CN_S = 1 $CN_{S'}$ = 1

	R_N	c_{2N}	R_S	c_{2S}	$R_{S'}$	$c_{2S'}$	F
Initial	2.0	-0.02528	2.2	-0.02161	2.5	-0.02161	-----
	2.0605	-0.03729	2.1756	-0.02417	2.3677	-0.06143	0.101716
Initial	2.0	-0.02528	2.2	-0.02161	2.8	-0.02161	-----
	2.0807	-0.03187	2.1680	-0.02544	2.9822	-0.06090	0.0884258

PCHI.FIL3 :

Fixed c_2's

$c_{2N} = -0.02528$ $c_{2S} = -0.02161$ $c_{2S'} = -0.02161$

	R_N	CN_N	R_S	CN_S	$R_{S'}$	$CN_{S'}$	F
Initial	2.0	2	2.2	1	2.5	1	-----
	2.0056	"	2.2356	"	2.4457	"	0.623402
	1.9858	0.9573	2.2007	1.2182	2.3874	0.4824	0.317458
Initial	2.0	2	2.2	1	2.8	1	-----
	1.9906	"	2.2196	"	2.9593	"	0.896392
	2.0297	1.8404	2.1979	0.5375	2.8764	0.1342	0.360093

Fixed CN's

$CN_N = 2$ $CN_S = 1$ $CN_{S'} = 1$

	R_N	c_{2N}	R_S	c_{2S}	$R_{S'}$	$c_{2S'}$	F
Initial	2.0	-0.02528	2.2	-0.02161	2.5	-0.02161	-----
	2.0271	-0.04380	2.1797	-0.02246	2.3470	-0.04755	0.257595
Initial	2.0	-0.02528	2.2	-0.02161	2.8	-0.02161	-----
	2.0732	-0.03432	2.1722	-0.02502	2.9225	-0.06240	0.302079

N + S + N' :

PCHI.FIL1 :

Fixed c_2's

$c_{2N} = -0.02528$ $c_{2S} = -0.02161$ $c_{2N'} = -0.02528$

	R_N	CN_N	R_S	CN_S	$R_{N'}$	$CN_{N'}$	F
Initial	2.0	2	2.2	1	2.8	1	-----
	1.9921	"	2.2228	"	2.6798	"	0.538301
	2.0288	1.8401	2.2016	0.5189	2.7060	0.5028	0.101347
	2.0297	"	2.1997	"	2.7165	1.5021*	0.0838297
					[*c_2 = -0.04865]		

Fixed CN's

$CN_N = 2$ $CN_S = 1$ $CN_{N'} = 1$

	R_N	c_{2N}	R_S	c_{2S}	$R_{N'}$	$c_{2N'}$	F
Initial	2.0	-0.02528	2.2	-0.02161	2.8	-0.02528	-----
	2.0759	-0.03141	2.1690	-0.02610	2.7271	-0.04075	0.0592036

PCHI.FIL2 :

Fixed c_2's

$c_{2N} = -0.02528$ $c_{2S} = -0.02161$ $c_{2N'} = -0.02528$

	R_N	CN_N	R_S	CN_S	$R_{N'}$	$CN_{N'}$	F
Initial	2.0	2	2.2	1	2.8	1	-----
	1.9934	"	2.2211	"	2.8764	"	0.605381
	2.0316	1.8863	2.1990	0.4964	2.7198	0.3538	0.178645
	2.0318	"	2.1969	"	2.7639	7.6189*	0.103527
					[*c_2 = -0.10007]		

Fixed CN's

$CN_N = 2$ $CN_S = 1$ $CN_{N'} = 1$

	R_N	c_{2N}	R_S	c_{2S}	$R_{N'}$	$c_{2N'}$	F
Initial	2.0	-0.02528	2.2	-0.02161	2.8	-0.02528	-----
	2.0792	-0.03132	2.1678	-0.02577	2.7755	-0.04667	0.114648

N + N' + S :

PCHI.FIL3 :

Vary R's only

	c_{2N} = -0.02528		$c_{2N'}$ = -0.02528		c_{2S} = -0.02161		
	R_N	CN_N	$R_{N'}$	$CN_{N'}$	R_S	CN_S	F
Initial	2.15	1	2.40	1	2.15	1	-----
	2.1081	(1)	2.6267	(1)	2.1709	(1)	0.477251

Fixed c_2's

	c_{2N} = -0.02528		$c_{2N'}$ = -0.02528		c_{2S} = -0.02161		
	R_N	CN_N	$R_{N'}$	$CN_{N'}$	R_S	CN_S	F
Initial	2.15	1	2.40	1	2.15	1	-----
	2.0695	8.4489	2.3378	2.3380	2.0275	1.4595	0.214600

Fixed CN's

	CN_N = 1		$CN_{N'}$ = 1		CN_S = 1		
	R_N	c_{2N}	$R_{N'}$	$c_{2N'}$	R_S	c_{2S}	F
Initial	2.15	-0.02528	2.4	-0.02528	2.15	-0.02161	-----
	2.1062	-0.02673	2.0390	-0.03260	2.1674	-0.02552	0.330759

N + N' + S + S' :

PCHI.FIL3 :

Vary R's only

	c_{2N}=-0.02528		$c_{2N'}$=-0.02528		c_{2S}=-0.02161		$c_{2S'}$=-0.02161		
	R_N	CN_N	$R_{N'}$	$CN_{N'}$	R_S	CN_S	$R_{S'}$	$CN_{S'}$	F
Initial	2.15	1	2.40	0.6	2.15	1	2.9	0.13	-----
	2.1094	(1)	2.5926	(0.6)	2.1699	(1)	2.9116	(0.13)	0.419486

Fixed c_2's

	c_{2N}=-0.02528		$c_{2N'}$=-0.02528		c_{2S}=-0.02161		$c_{2S'}$=-0.02161		
	R_N	CN_N	$R_{N'}$	$CN_{N'}$	R_S	CN_S	$R_{S'}$	$CN_{S'}$	F
Initial	2.15	1	2.40	0.6	2.15	1	2.9	0.13	-----
	2.0916	(1)	2.3732	-0.9257	2.1661	(1)	2.9020	0.1727	0.346906

Fixed CN's

	CN_N = 1		$CN_{N'}$ = 0.6		CN_S = 1		$CN_{S'}$ = 0.13		
	R_N	c_{2N}	$R_{N'}$	$c_{2N'}$	R_S	c_{2S}	$R_{S'}$	$c_{2S'}$	F
Initial	2.15	-0.02528	2.4	-0.02528	2.15	-0.02161	2.9	-0.02161	-----
	2.1084	(-0.02528)	2.5925	-0.02420	2.1702	(-0.02161)	2.9034	-0.01323	0.411057

Fixed CN's

	CN_N = 1		$CN_{N'}$ = 1		CN_S = 1		$CN_{S'}$ = 1		
	R_N	c_{2N}	$R_{N'}$	$c_{2N'}$	R_S	c_{2S}	$R_{S'}$	$c_{2S'}$	F
Initial	2.15	-0.02528	2.4	-0.02528	2.15	-0.02161	2.9	-0.02161	-----
	2.1109	(-0.02528)	2.5862	-0.03395	2.1685	(-0.02161)	2.9514	-0.04971	0.397720

Fits of PCLO :

N only :	R	CN	c_2	F
Initial	1.9, 2.0	3	-0.02528	----
PCLO.FIL0 :	2.0185	2.5357	(-0.02528)	0.399961
	2.0210	1.9444	-0.02074	0.366448
PCLO.FIL1 :	2.0187	2.5608	(-0.02528)	0.442943
	2.0216	1.9001	-0.02021	0.405129
PCLO.FIL2 :	2.0189	2.5732	(-0.02528)	0.467742
	2.0218	1.9000	-0.02013	0.431117

S only :	R	CN	c_2	F
Initial	2.0, 2.2	3	-0.02161	----
PCLO.FIL0 :	2.1625	0.9153	(-0.02161)	0.250405
	2.1626	0.9214	-0.02171	0.250375
PCLO.FIL1 :	2.1616	0.9256	(-0.02161)	0.297636
	2.1611	0.8330	-0.02004	0.291756
PCLO.FIL2 :	2.1614	0.9271	(-0.02161)	0.345433
	2.1608	0.8154	-0.01970	0.338042

N + S :

	R_N	CN_N	c_{2N}	R_S	CN_S	c_{2S}	F
PCLO.FIL0 :							
Initial	2.0	2	-0.02528	2.2	2	-0.02161	-----
	1.8214	"	"	2.1673	"	"	1.58810
	1.8471	-0.3484	"	2.1601	0.8616	"	0.173218
	1.8735	-0.2489	-0.01424	2.1590	1.1207	-0.02623	0.145435
PCLO.FIL1 :							
Initial	2.0	2	-0.02528	2.2	1	-0.02161	-----
	1.9644	"	"	2.1972	"	"	0.884473
	2.1615	1.9275	"	2.1447	1.3502	"	0.0936219
	2.1471	1.7627	-0.02449	2.1403	1.1668	-0.02040	0.0756268
	2.1372	(1)	-0.02379	2.1453	(1)	-0.02042	0.138895
	2.1290	(2)	-0.03591	2.1453	(1)	-0.02112	0.0946570
	2.1285	(3)	-0.05201	2.1509	(1)	-0.02171	0.133749
	2.3059	(1)	-0.01230	2.2005	(2)	-0.03125	0.0819654
	2.2652	(2)	-0.01816	2.1893	(2)	-0.02495	0.139340
Initial	2.0	1	-0.02528	2.2	2	-0.02161	-----
	1.8085	"	"	2.1647	"	"	1.41993
	1.8559	-0.3635	"	2.1584	0.8765	"	0.232731
	1.8620	-0.3410	-0.02317	2.1581	0.9109	-0.02223	0.232553
	1.5304	(1)	-0.09279	2.1612	(1)	-0.02237	0.295742
	2.1290	(2)	-0.03591	2.1453	(1)	-0.02112	0.0946571
	2.1285	(3)	-0.05200	2.1509	(1)	-0.02170	0.133749
	1.6686	(1)	-0.04401	2.1622	(2)	-0.03308	0.482981
	1.6465	(2)	-0.06356	2.1622	(2)	-0.03284	0.479582

	R_N	CN_N	c_{2N}	R_S	CN_S	c_{2S}	F
PCLO.FIL2 :							
Initial	2.0	1	-0.02528	2.2	1	-0.02161	-----
	1.9702	"	"	2.1765	"	"	0.583442
	2.1724	2.1481	"	2.1474	1.4496	"	0.162931
	2.1553	1.8842	-0.02204	2.1400	1.2364	-0.01957	0.150964
	2.1425	(1)	-0.02241	2.1449	(1)	-0.01986	0.204154
	2.1301	(2)	-0.03395	2.1437	(1)	-0.02080	0.164210
	2.1297	(3)	-0.05019	2.1500	(1)	-0.02152	0.185921
	2.3063	(1)	-0.01194	2.2015	(2)	-0.03122	0.152135
	2.2662	(2)	-0.01772	2.1903	(2)	-0.02481	0.191943
Initial	2.0	1	-0.02528	2.2	2	-0.02161	-----
	1.8078	"	"	2.1645	"	"	1.42996
	1.8573	-0.3732	"	2.1581	0.8780	"	0.288522
PCLO.FIL3 :							
Initial	2.0	2	-0.02528	2.2	1	-0.02161	-----
	1.9587	"	"	2.1948	"	"	0.908152
	2.1582	2.3640	"	2.1407	1.4811	"	0.336404
	2.1053	2.5088	-0.01352	2.0905	1.2693	-0.01700	0.289273
Initial	2.2	1	-0.02528	2.2	1	-0.02161	-----
	2.1144	"	"	2.1432	"	"	0.387362
	2.1150	(1)	-0.01718	2.1311	(1)	-0.02042	0.377158

<u>N + N' :</u>

	R_N	CN_N	c_{2N}	$R_{N'}$	$CN_{N'}$	$c_{2N'}$	F
PCLO.FIL0 :							
Initial	2.0	2	-0.02528	2.2	2	-0.02528	-----
	1.9691	"	"	2.0696	"	"	0.575192
	2.0186	0.6003	"	2.0185	1.9354	"	0.399961
	2.0621	0.8075	-0.00931	1.9512	1.3789	-0.02159	0.119313
PCLO.FIL1 :							
Initial	2.0	2	-0.02528	2.2	2	-0.02528	-----
	2.0305	"	"	2.3685	"	"	0.544147
	2.0255	2.5835	"	2.3534	0.9337	"	0.324132
	2.0168	2.4271	-0.02614	2.3560	0.1359	+0.00142	0.203679
Initial	2.2	2	-0.02528	2.6	2	-0.02528	-----
	2.0165	"	"	2.6841	"	"	0.653670
	2.0185	2.5554	"	2.6821	0.4364	"	0.426829
	2.0187	1.8495	-0.01985	2.6609	0.0287	+0.01245	0.308331
PCLO.FIL2 :							
Initial	2.0	2	-0.02528	2.2	2	-0.02528	-----
	2.0309	"	"	2.3669	"	"	0.569470
	2.0260	2.6100	"	2.3506	0.9423	"	0.356093
	2.0166	2.5137	-0.02680	2.3530	0.1158	+0.00335	0.235593
Initial	2.2	2	-0.02528	2.6	2	-0.02528	-----
	2.0166	"	"	2.6790	"	"	0.711757
	2.0187	2.5692	"	2.6760	0.2552	"	0.462544
	2.0183	1.8886	-0.02018	2.6516	0.0160	+0.01775	0.326867

S + S' :

	R_S	CN_S	c_{2S}	$R_{S'}$	$CN_{S'}$	$c_{2S'}$	F
PCLO.FIL0 :							
Initial	2.0	1	-0.02161	2.2	1	-0.02161	-----
	2.1126	"	"	2.2413	"	"	0.584524
	2.1624	1.1098	"	2.3479	0.3051	"	0.0961859
	2.1432	0.6282	-0.01680	2.2528	0.6050	-0.02925	0.0686127
PCLO.FIL1 :							
Initial	2.0	1	-0.02161	2.2	1	-0.02161	-----
	2.1121	"	"	2.2391	"	"	0.651926
	2.1661	1.1643	"	2.3695	0.3890	"	0.0764028
	2.1548	0.9637	-0.02016	2.3231	0.8132	-0.03902	0.0533031
Initial	2.2	1	-0.02161	2.6	1	-0.02161	-----
	2.1598	"	"	2.8123	"	"	0.757800
	2.1614	0.9221	"	2.7756	0.1463	"	0.271934
	2.1601	0.7649	-0.01900	2.8546	2.0684	-0.07725	0.230939
PCLO.FIL2 :							
Initial	2.0	1	-0.02161	2.2	1	-0.02161	-----
	2.1123	"	"	2.2391	"	"	0.680619
	2.1664	1.1829	"	2.3705	0.4185	"	0.153913
	2.1544	0.9564	-0.01989	2.3229	0.8485	-0.03867	0.147856
Initial	2.2	1	-0.02161	2.6	1	-0.02161	-----
	2.1619	"	"	2.7510	"	"	0.807994
	2.1615	0.9245	"	2.7405	0.1365	"	0.325527
	2.1622	0.8630	-0.02056	2.7111	0.0438	-0.00591	0.311699

N + S + S' :

PCLO.FIL1 :

Fixed c_2's

$c_{2N} = -0.02528$ $c_{2S} = -0.02161$ $c_{2S'} = -0.02161$

	R_N	CN_N	R_S	CN_S	$R_{S'}$	$CN_{S'}$	F
Initial	2.2	1	2.2	1	2.5	1	-----
	1.9838	"	2.1972	"	2.4170	"	0.543114
	2.0247	0.4289	2.1662	0.9663	2.3806	0.3007	0.0604921
Initial	2.2	1	2.2	1	2.6	1	-----
	2.2998	"	2.1756	"	2.7382	"	0.750976
Initial	2.0	1	2.2	1	2.6	1	-----
	2.1158	"	2.1417	"	2.8242	"	0.724957
	2.1044	1.4764	2.1340	0.9445	2.8011	0.1017	0.0592774
	2.1044	"	2.1339	"	2.7991	0.0893*	0.0591259
					[*$c_{2S'} = -0.01971$]		

Fixed CN's

$CN_N = 1$ $CN_S = 1$ $CN_{S'} = 1$

	R_N	c_{2N}	R_S	c_{2S}	$R_{S'}$	$c_{2S'}$	F
Initial	2.2	-0.02528	2.2	-0.02161	2.5	-0.02161	-----
	1.7500	-0.09796	2.1544	-0.02057	2.3222	-0.04199	0.0394407
Initial	2.0	-0.02528	2.2	-0.02161	2.6	-0.02161	-----
	2.1470	-0.02443	2.1473	-0.02011	2.8353	-0.06972	0.0961449

	$CN_N = 2$		$CN_S = 1$		$CN_{S'} = 1$		
	R_N	c_{2N}	R_S	c_{2S}	$R_{S'}$	$c_{2S'}$	F
Initial	2.0	-0.02528	2.2	-0.02161	2.5	-0.02161	-----
	1.9820	"	2.2162	"	2.4265	"	0.535456
	1.7545	-0.12775	2.1547	-0.02057	2.3239	-0.04190	0.0395483
Initial	2.0	-0.02528	2.2	-0.02161	2.6	-0.02161	-----
	1.9629	"	2.1976	"	2.7850	"	1.15020
	2.1429	-0.03901	2.1491	-0.02092	2.7847	-0.07436	0.0438933

PCLO.FIL2 :

Fixed c_2's

	$c_{2N} = -0.02528$		$c_{2S} = -0.02161$		$c_{2S'} = -0.02161$		
	R_N	CN_N	R_S	CN_S	$R_{S'}$	$CN_{S'}$	F
Initial	2.1	1	2.1	1	2.5	1	-----
	1.9850	"	2.1961	"	2.4151	"	0.549125
	2.0237	0.3432	2.1666	1.0247	2.3783	0.3483	0.149209
	2.0433	"	2.1614	"	2.3685	0.4314*	0.148365
					[*$c_{2S'} = -0.02635$]		
Initial	2.2	1	2.2	1	2.6	1	-----
	2.2999	"	2.1754	"	2.7220	"	0.747763
	2.1945	2.2600	2.1556	1.5355	2.6955	0.0965	0.149291
	2.1936	"	2.1554	"	2.6974	0.0709#	0.148648
					[#$c_{2S'} = -0.01729$]		

Fixed CN's

	$CN_N = 1$		$CN_S = 1$		$CN_{S'} = 1$		
	R_N	c_{2N}	R_S	c_{2S}	$R_{S'}$	$c_{2S'}$	F
Initial	2.1	-0.02528	2.1	-0.02161	2.5	-0.02161	-----
	1.8028	-0.10862	2.1549	-0.02034	2.3277	-0.04069	0.146289
Initial	2.2	-0.02528	2.2	-0.02161	2.6	-0.02161	-----
	2.1973	-0.00614	2.1574	-0.01187	2.9765	-0.08189	0.162084
	$CN_N = 2$		$CN_S = 1$		$CN_{S'} = 1$		
	R_N	c_{2N}	R_S	c_{2S}	$R_{S'}$	$c_{2S'}$	F
Initial	2.1	-0.02528	2.1	-0.02161	2.5	-0.02161	-----
	2.0851	-0.01872	2.0993	-0.02245	2.4104	-0.08165	0.174820
Initial	2.1	-0.02528	2.1	-0.02161	2.6	-0.02161	-----
	1.8288	-0.14572	2.1551	-0.02039	2.3296	-0.04104	0.146606

PCLO.FIL3 :

Fixed c_2's

	$c_{2N} = -0.02528$		$c_{2S} = -0.02161$		$c_{2S'} = -0.02161$		
	R_N	CN_N	R_S	CN_S	$R_{S'}$	$CN_{S'}$	F
Initial	2.0	1	2.2	1	2.5	1	-----
	1.9799	"	2.1951	"	2.4148	"	0.660304
	1.8533	0.4149	2.1683	1.4006	2.3670	0.6005	0.301035
Initial	2.0	1	2.2	1	2.6	1	-----
	1.9563	"	2.1750	"	2.8029	"	0.951849
	2.1548	2.2829	2.1397	1.4438	2.8117	0.0537	0.333885

Fixed CN's

	$CN_N = 1$		$CN_S = 1$		$CN_{S'} = 1$		
	R_N	c_{2N}	R_S	c_{2S}	$R_{S'}$	$c_{2S'}$	F
Initial	2.2	-0.02528	2.2	-0.02161	2.5	-0.02161	-----
	1.8953	-0.03594	2.1611	-0.01854	2.3373	-0.03278	0.291028
Initial	2.2	-0.02528	2.2	-0.02161	2.6	-0.02161	-----
	2.3027	"	2.1744	"	2.7349	"	0.849961
	2.1109	-0.01647	2.1283	-0.02065	2.8622	-0.06505	0.354557

N + S + N' :

PCLO.FIL1

Fixed c_2's

	c_{2N} = -0.02528		c_{2S} = -0.02161		$c_{2N'}$ = -0.02528		
	R_N	CN_N	R_S	CN_S	$R_{N'}$	$CN_{N'}$	F
Initial	2.0	1	2.2	1	2.5	1	-----
	1.9633	"	2.1787	"	2.6341	"	0.510012
	2.0900	1.2523	2.1375	0.8462	2.6560	0.3982	0.0256428
Initial	2.0	1	2.2	1	2.35	1	-----
	2.0657	"	2.1479	"	2.2063	"	0.107831
	2.1247	1.4735	2.1413	1.1693	2.2256	0.4279	0.0790783
	2.1342	"	2.1460	"	2.2611	0.2155*	0.0768155
					[*$c_{2N'}$ = -0.01411]		

Fixed CN's

	CN_N = 1		CN_S = 1		$CN_{N'}$ = 1		
	R_N	c_{2N}	R_S	c_{2S}	$R_{N'}$	$c_{2N'}$	F
Initial	2.0	-0.02528	2.2	-0.02161	2.5	-0.02528	-----
	2.1391	-0.02630	2.1477	-0.02064	2.6388	-0.04286	0.0701327
Initial	2.0	-0.02528	2.2	-0.02161	2.35	-0.02528	-----
	2.1108	-0.04604	2.1350	-0.01980	2.1305	-0.01953	0.0823582

PCLO.FIL2

Fixed c_2's

	c_{2N} = -0.02528		c_{2S} = -0.02161		$c_{2N'}$ = -0.02528		
	R_N	CN_N	R_S	CN_S	$R_{N'}$	$CN_{N'}$	F
Initial	2.0	1	2.2	1	2.8	1	-----
	1.9690	"	2.1771	"	2.9136	"	0.586307
	2.1735	2.2397	2.1475	1.4776	2.9230	0.4552	0.126604
	2.1737	"	2.1476	"	2.9270	0.3261*	0.124790
					[*$c_{2N'}$ = -0.01952]		
Initial	2.0	2	2.2	1	2.5	1	-----
	1.9650	"	2.1782	"	2.6265	"	0.554268
	2.2061	2.2805	2.1596	1.5588	2.5452	0.3492	0.155786
	2.2040	"	2.1594	"	2.5531	0.1824†	0.153544
					[†$c_{2N'}$ = -0.01589]		
Initial	2.0	2	2.2	1	2.35	1	-----
	2.0659	"	2.1481	"	2.2077	"	0.172550
	2.1337	1.7369	2.1409	1.2420	2.2434	0.4025	0.154740
	2.1484	"	2.1455	"	2.2875	0.1040‡	0.152302
					[‡$c_{2N'}$ = -0.00844]		

Fixed CN's

	CN_N = 1		CN_S = 1		$CN_{N'}$ = 1		
	R_N	c_{2N}	R_S	c_{2S}	$R_{N'}$	$c_{2N'}$	F
Initial	2.0	-0.02528	2.2	-0.02161	2.8	-0.02528	-----
	2.1393	-0.02279	2.1446	-0.02006	2.7283	-0.06890	0.183819
Initial	2.0	-0.02528	2.2	-0.02161	2.5	-0.02528	-----
	2.1393	-0.02276	2.1445	-0.02006	2.7276	-0.06892	0.183819
Initial	2.0	-0.02528	2.2	-0.02161	2.35	-0.02528	-----
	2.1027	-0.04155	2.1334	-0.01824	2.1414	-0.01636	0.153919

Appendix II. Error Analysis for Laccase Difference Edge Analysis

The following error analysis was originally carried out for the paper published in 1990. (Cole, J. L.; Tan, G. O.; Yang, E. K.; Hodgson, K. O.; Solomon, E. I. *J. Am. Chem. Soc.* **1990**, *112*, 2243-2249.) As such, errors were only calculated for samples that were measured in 1987 and 1989, i.e. T2D1, T2D2 and T2D3 (and also T2DS and T26A, old data sets) for T2D laccase and 1ML01, 2ML01, MLRD and MLOX for T1Hg laccase (see Tables 6.1 and 6.2 in Chapter 6). Some inconsistencies in the original error analysis have been remedied, so that errors are now a little higher than originally reported.

Errors may be related either by addition or by multiplication. The propagation of errors was treated according to the following equations (from *Data Reduction and Error Analysis for the Physical Sciences* by Philip R. Bevington, McGraw-Hill, New York, pp. 56–65) :

Where x is the weighted sum of u and v, i.e., $x = au \pm bv$, then

$\sigma_x^2 = a^2\sigma_u^2 + b^2\sigma_v^2$, where u and v are independent

.....(II.1)

Where x is the weighted product of u and v, i.e. $x = \pm auv$, then

$\sigma_x^2 = a^2v^2\sigma_u^2 + a^2u^2\sigma_v^2$, or $\frac{\sigma_x^2}{x^2} = \frac{\sigma_u^2}{u^2} + \frac{\sigma_v^2}{v^2}$,

where u and v are independent .....(II.2)

Where x is obtained by division, i.e. $x = \pm\frac{au}{v}$,

$\frac{\sigma_x^2}{x^2} = \frac{\sigma_u^2}{u^2} + \frac{\sigma_v^2}{v^2}$, where u and v are independent .....(II.3)

Sources of error :

(1) Error from the noise of the data, based on measuring the half-height of typical noise. At most (in 1989), it is ±1% of the normalized amplitude. More usually, it is ±0.5%.

(2) Spline or normalization error. A conservative estimate is ±5% of the normalized amplitude (from the notes of James E. Penner-Hahn).

(3) Error in estimating content of native laccase in T2D and T1Hg samples, as measured by optical or EPR spectroscopy. Error is proportional to the amount of native present, and it is usually ~5% of all laccase present. However, this error can be neglected in most cases because the native edge used to correct the T2D or T1Hg edge is rather similar to the latter (i.e., a reduced edge is used to correct reduced samples, and an oxidized edge for oxidized samples), and so applying the correction makes very little difference to the shape of the edge, or its amplitude, as measured at 8984 eV. The only cases where this is not true is in the corrections applied to T2D2 and T2D3 (and T2DS) (see Table 6.2), where a largely oxidized edge is used to correct largely reduced edges. In this case, native is $10 \pm 2\%$ (6-7% for T2DS) of all laccase.

(4) Error in determining the redox state of "standard" samples. This is measured by optical or EPR spectroscopy, and is proportional to the signal measured. This error is:

Considered 0% error for fully oxidized (H_2O_2-treated) samples.

For reduced T2D (T2D1) : 0% (because no laccase was oxidized).

For reduced T1Hg (MLRD) : $10 \pm 2\%$ of T2 was oxidized, ~10% of T3 was oxidized. So, in terms of total Cu : $\sigma(T2) = \left(\frac{1}{3}\right) \times 0.02$, $\sigma(T3) = \left(\frac{2}{3}\right) \times 0.1$.

Errors not accounted for in this analysis :

(5) Systematic error in estimation of fully oxidized edges = 8% of all Cu present (from Kau, L.-S.; Spira-Solomon, D. J.; Penner-Hahn, J. E.; Hodgson, K. O.; Solomon, E. I. *J. Am. Chem. Soc.* **1987**, *109*, 6433-6442). This is the error involved in judging a laccase sample (e.g. T1Hg + 60× H_2O_2) to be fully oxidized when the edge is the only spectroscopic criterion used.

(6) Systematic error in estimation of fully reduced edges due to the range in amplitude of Cu(I) models at ~8984 eV(*ibid.*). This is the error involved in judging a laccase sample (e.g., fully reduced native laccase) to be fully reduced when the edge is the only spectroscopic criterion used.

(7) Systematic error due to range in heights (at 8984 eV) of various resting T2D samples (including T2DS), and various fully oxidized native laccase samples, run in the past (unpublished data).

(8) Error in measuring the edge amplitudes at 8984 eV. This was done by hand, using a pencil and a ruler marked in mm. The error in an individual measurement was about 0.5 mm. The impact this had on the amplitude calculated depended on the scale over which the graph was plotted, heights measured were usually about 50 mm when plotted.

Propagation of errors :

Errors in 100% oxidized edges (T26A and 2ML01) **:**

Only the spline and the noise contribute errors. So :

Normalized signal $E_N = SE_R$, where S = spline scaling factor, E_R = raw signal

.....(II.4)

Amplitude of oxidized edges at 8984 eV is ~0.1 normalized units, so the spline error is scaled down by this amount, while the noise error is not reduced.

So, using Equation II.2,

Error in totally oxidized laccase edge $\frac{\sigma_{E_N}}{E_N} = \sqrt{\left(\frac{\sigma_{E_R}}{E_R}\right)^2 + \left(\frac{\sigma_S}{S}\right)^2}$

$$= \sqrt{\left(\frac{0.005}{0.1}\right)^2 + (0.05)^2} = 0.071 \equiv 7\% \text{ (of normalized amplitude)}$$

Errors in 100% reduced edges :

Amplitude of reduced edges (both T2D and T1Hg) at 8984 eV is ~0.6 units, so the spline error is scaled down by this amount, while the noise error is not reduced. Amplitude of T2DS at 8984 eV is ~0.5 units.

(a) For fully reduced T2D (T2D1) :

Only the spline and the noise contribute errors. So, using Equations II.2 and II.4,

Error in T2D1 = $\frac{\sigma_{E_N}}{E_N} = \sqrt{\left(\frac{\sigma_{E_R}}{E_R}\right)^2 + \left(\frac{\sigma_S}{S}\right)^2}$

$$= \sqrt{\left(\frac{0.005}{0.6}\right)^2 + 0.05^2} = 0.051 \equiv 5\% \text{ (of amplitude at 8984 eV)}$$

(b) For fully reduced T1Hg (MLRD) :

Errors are from the spline, the noise and the redox state. So

Normalized signal $E_N = SRE_R$, where S = spline scaling factor, E_R = raw signal and R = proportion of reduced Cu.

.....(II.5)

Using Equation II.1,

Error in redox state of MLRD = $\sigma_R = \sqrt{a^2\sigma_{R_1}^2 + b^2\sigma_{R_2}^2}$

$$= \sqrt{\left(\frac{1}{3}\right)^2 0.02^2 + \left(\frac{2}{3}\right)^2 0.1^2} = 0.067 \equiv 7\% \text{ (of total Cu)}$$

Using Equation II.2,

$$\text{Error in MLRD} = \frac{\sigma_{E_N}}{E_N} = \sqrt{\left(\frac{\sigma_S}{S}\right)^2 + \left(\frac{\sigma_R}{R}\right)^2 + \left(\frac{\sigma_{E_R}}{E_R}\right)^2}$$

$$= \sqrt{0.05^2 + 0.067^2 + \left(\frac{0.01}{0.6}\right)^2} = 0.085 \equiv 9\% \text{ (of amplitude at 8984 eV)}$$

(c) For resting T2D laccase (≡ "fully reduced T3 Cu") :

The native correction cannot be neglected in this case. So

Corrected T2DS = 1.111[T2DS] – 0.111[NTVL] (Equation 6.2 in Chapter 6)

$$\text{The combined spline and noise error in NTVL} = \frac{\sigma_{E_N}}{E_N} = \sqrt{\left(\frac{\sigma_{E_R}}{E_R}\right)^2 + \left(\frac{\sigma_S}{S}\right)^2}$$

$$= \sqrt{\left(\frac{0.005}{0.2}\right)^2 + 0.05^2} = 0.056 \equiv 6\%$$

The combined spline and noise error in T2DS is approximated by the error found for T2D1 above (= 0.051).

Error in corrected T2DS

$$= \sqrt{1.111^2(0.051)^2 + 0.111^2(0.056)^2} = 0.057 \equiv 6\% \text{ (of normalized amp.)}$$

Errors in 100% reduced difference edge standards :

100% reduced difference edge $\Delta E_{100} = E_{red} - E_{ox}$, where E_{red} is the reduced edge and E_{ox} is the oxidized edge.

So $\sigma_{\Delta E_{100}} = \sqrt{(\sigma_{E_{red}})^2 + (\sigma_{E_{ox}})^2}$ (from Equation II.1)

(a) 100% reduced ΔT2D laccase :

Error in (T2D1 – T26A) = $\sqrt{(0.051)^2 + (0.071)^2} = 0.087 \equiv 9\%$ (of amp. at 8984 eV)

(b) 100% reduced ΔT1Hg laccase :

Error in (MLRD – 2ML01) = $\sqrt{(0.085)^2 + (0.071)^2} = 0.111 \equiv 11\%$ (amp. at 8984 eV)

(c) 100% reduced ΔT3 Cu :

Error in 1.5(T2DS – T26A) = $\sqrt{1.5^2[(0.057)^2 + (0.071)^2]} = 0.136 \equiv 14\%$
(of amplitude at 8984 eV)

Errors in difference edges of reoxidized samples (T2D2-T2D3 series or MLOX) :

Difference edge $\Delta E_D = E_N - E_S$, where E_N = edge with redox state to be determined
E_S = standard (100% oxidized) edge

(a) Samples close to totally reduced (T2D2 and T2D3):

Correction for native must be first taken into account (*vide supra*). 10 ± 2% of native were subtracted and the edge renormalized in the following equation :

Corrected T2D2 or T2D3 = 1.1481[T2D(2,3)] – 0.1481[NTVL]
(Equation 6.2 in Chapter 6)

The combined spline and noise error in T2D2, T2D3 is approximated by the error found above for T2D1 (0.051 units).

So, using Equation II.1, error due to native correction in E_N (T2D2 and T2D3)
$= \sqrt{1.1481^2(0.051)^2 + 0.1481^2(0.056)^2} = 0.059 \equiv 6\%$ (of normalized amp.)

Then, error in $\Delta E_D = \sigma_{E_D} = \sqrt{\sigma_{E_N}^2 + \sigma_{E_S}^2}$

$= \sqrt{0.059^2 + 0.071^2} = 0.092 \equiv 9\%$ (of normalized amplitude at 8984 eV)

(b) Samples close to totally oxidized (MLOX):

Amplitudes of both E_N and E_S are ~0.1 at 8984 eV. Spline error σ_S is scaled down to 0.5%, while the noise error σ_R remains at 0.5%.

For spline and noise error (Equation II.3),

$$\frac{\sigma_{E_S}}{E_S} = \sqrt{\left(\frac{\sigma_S}{S}\right)^2 + \left(\frac{\sigma_{E_R}}{E_R}\right)^2}.$$

$$= \sqrt{(0.05)^2 + \left(\frac{0.005}{0.1}\right)^2} = 0.071 \equiv 7\% \text{ (of normalized amplitude at 8984 eV)}$$

$$\frac{\sigma_{E_N}}{E_N} = \sqrt{\left(\frac{\sigma_S}{S}\right)^2 + \left(\frac{\sigma_{E_R}}{E_R}\right)^2}$$

$$= \sqrt{(0.05)^2 + \left(\frac{0.01}{0.1}\right)^2} = 0.112 \equiv 11\% \text{ (of normalized amplitude at 8984 eV)}$$

So, error in (MLOX - 2ML01) difference edge

$$\sigma_{\Delta E_D} = \sqrt{\sigma_{E_N}^2 + \sigma_{E_S}^2}$$

$$= \sqrt{(0.071)^2 + (0.112)^2}$$

$$= 0.132 \equiv 13.2\% \text{ (of normalized amplitude at 8984 eV)}$$

Errors in quantitating proportion of reduced Cu :

Proportion of Cu(I) determined, "Cu" $= \dfrac{\Delta E_D}{\Delta E_{100}}$

So, using Equation II.3, $\dfrac{\sigma_{\text{"Cu"}}^2}{\text{"Cu"}^2} = \dfrac{\sigma_{\Delta E_D}^2}{\Delta E_D{}^2} + \dfrac{\sigma_{\Delta E_{100}}^2}{\Delta E_{100}{}^2}$

Since the errors for E_D and E_{100} already take into account the amplitudes of the component edges at 8984 eV, the errors are divided by $\Delta E_D / E_N$ and $\Delta E_{100} / E_{red}$ rather than just ΔE_D or ΔE_{100}.

(a) For the T2D series (T2D2 and T2D3) :

Error in proportion of Cu determined in T2D3 (T2D2 is taken to be similar)

$$= \frac{\sigma_{\text{"Cu"}}}{\text{"Cu"}} = \sqrt{\left(\frac{0.092}{0.4/0.5}\right)^2 + \left(\frac{0.087}{0.5/0.6}\right)^2} = 0.155 \equiv 16\% \text{ (of Cu(I) determined)}$$

This works out to a Cu(I) content of 76 ± 12% in T2D laccase exposed for 63 hours (T2D3).

Error in proportion of T3 Cu determined in T2D3

$$= \frac{\sigma_{\text{"T3 Cu"}}}{2/3\text{"T3 Cu"}} = \sqrt{\left(\frac{0.092}{0.4/0.5}\right)^2 + \left(\frac{2/3 \times 0.136}{0.4/0.5}\right)^2} = 0.161 \equiv 16\% \text{ (of Cu(I) determined)}$$

This works out to a Cu(I) content of 88 ± 14% of T3 Cu in T2D laccase exposed for 63 hours (T2D3).

(b) For T1Hg reoxidized (MLOX) :

Error in proportion of Cu determined

$$= \frac{\sigma_{\text{"Cu"}}}{\text{"Cu"}} = \sqrt{\left(\frac{0.132}{0.01/0.1}\right)^2 + \left(\frac{0.111}{0.5/0.6}\right)^2} = 1.329 \equiv 133\% \text{ (of Cu(I) determined)}$$

This works out to a Cu(I) content of 2 ± 3% in reoxidized T1Hg laccase (MLOX).

Appendix III. Complete Tables of Fits to EXAFS Spectra of Oxidized and Reduced *Rhodospirillum rubrum* Ni CODH and Associated Model Compounds

The following tables list the distances (R), coordination numbers (CN), c_2 values and fit indices (F) for the fits made for the EXAFS curve-fitting results discussed in Chapter 7. In the parameterized EXAFS equation employed by our analysis package (see Chapter 2), c_2 values vary in the same way as the squared term σ^2_{as} in the Debye-Waller factor, such that $\Delta c_2 = -2\Delta\sigma^2_{as}$. Thus, though the sign is reversed, the magnitude of c_2 is proportional to σ^2_{as}.

When using the fit index F to evaluate the goodness of a fit to the data, we have to bear in mind that F is not adjusted for the size of the signal. Thus, for equally good fits (as judged by viewing the match of phase and amplitude), we would expect the fit indices for fits to a larger EXAFS signal to be larger than those for fits to smaller EXAFS signals. So the fit index F should only be used to compare different fits made on the same data.

The windows used on the data sets are denoted by their data file names. Thus, fits to CODHX.FIL2 correspond to fits on Window 2 of CODHX, CODHX.FIL3 contains data filtered using Window 3, etc.

The tables also show what initial R, CN and c_2 values were used for beginning each fit. Unless otherwise stated, a fit result shown had as its initial values the results of the fit shown in the line immediately above. Thus, in a given table (e.g., N+S fits on CODHX.FIL2), the values listed as initial values were first used in a fit varying R's only. Then the results of this fit were in turn used in a fit varying R and CN (referred to as Type 2 fits in the text), whose results are listed below it. The results of this Type 2 fit were in turn used as initial values for the Type 1 fit (varying R's, CN's and c_2's) whose results are listed immediately below. An exception to this is that Type 3 fits (varying R's and c_2's), listed below Type 1 fits, generally used the results of fits varying R only as initial values. Bracketed CN or c_2 values were held fixed at the values shown.

List of Tables :

One-shell N or S fits of Ni models

Grace Tan 2nd Feb 1993

(fits checked and correct on 3rd Feb 1993)

These fits are discussed in Chapter 7, Section (E.1.a).

Parameters used in fits :

Ni^{II}-N : $[Ni^{II}(dimethylglyoxime)_2]$, 10 K, k = 3.25-11.75 Å^{-1} (data to k = 15 Å^{-1})
Ni^{II}-S : $Ni^{II}(S_2CN(CH_2CH_3)_2)_2$, 10 K, k = 3.25-11.75 Å^{-1} (data to k = 15 Å^{-1})

Ni-N compounds :

		R(cryst)	Coord.
NBC004	[Ni(isobacteriochlorin)]	1.915–1.934, av. 1.921	sq pl
NPC004	[Ni(phthalocyanine)]	-------	sq pl
NTP004	[Ni(tetraphenylporphyrin)]	-------	sq pl
NTM004	[Ni(tetramethylcyclam)]$(ClO_4)_2$	-------	sq pl
NC4004	[Ni(cyclops)](ClO_4)	-------	sq pl
NC5004	[Ni(cyclops)(py)](ClO_4)	1.859–1.897, av. 1.874*	sq py
N33004	[Ni(tropocoronand-3,3)]	1.854–1.868, av. 1.861	dist. sq pl
N66004	[Ni(tropocoronand-6,6)]	1.944–1.950, av. 1.947	dist. T_d
N6C004	[Ni(corphin)NCS]$_2$	-------	O_h
NEN004	$[Ni(ethylenediamine)_3]^{2+}$	2.124	O_h
NPH004	$[Ni(phen)_3]Cl_2.7H_2O$	2.078–2.106, av. 2.090	O_h
NTA004	$[Ni([9]aneN_3)_2](ClO_4)_2$	2.093–2.116, av. 2.1052	O_h
N4C004#	[Ni(octaethylpyrrocorphin)]	1.899–1.914, av. 1.909	sq pl

* — for equatorial N, from crystal structure of [Ni(cyclops)I](ClO_4)
# — data extremely noisy, no fits done

Ni-S compounds :

		R(cryst)	Coord.
N2M004	$[(n\text{-}Bu)_4N]_2[Ni(mnt)_2]$	2.173–2.176, av. 2.175	sq pl
N3M004	$[(n\text{-}Bu)_4N][Ni(mnt)_2]$	2.147–2.151, av. 2.149	sq pl
NI2S	$[Ni(SC_2H_4SC_2H_4S)]_2$	2.14–2.22, av. 2.18	sq pl*
NS4004	$[Ni(S\text{-}Ph)_4]^{2-}$	2.272–2.303, av. 2.288	T_d
NTT004	$[Ni([9]aneS_3)_2]^{2+}$	2.377–2.400, av. 2.386	O_h

* — 2 square planar coordinated Ni hinged together with folding angle of 111.3°

N only :

	R	CN	c_2	F
NBC004	1.9	4	-0.02297	------
	1.9107	3.3206	"	0.467720
	1.9119	5.0781	-0.02987	0.206093
	1.9111	(4)	-0.02652	0.302562
NPC004	1.9	4	-0.02297	------
	1.8764	4.0022	"	0.250106
	1.8768	4.6482	-0.02534	0.171814
	1.8764	(4)	-0.02338	0.238654
NTM004	1.9	4	-0.02297	------
	1.9607	3.3551	"	0.409008
	1.9608	3.8249	-0.02506	0.389323
	1.9609	(4)	-0.02566	0.391376
NTP004	1.9	4	-0.02297	------
	1.9111	4.4215	"	0.344177
	1.9114	5.4100	-0.02617	0.220816
	1.9108	(4)	-0.02232	0.415830
NC4004	1.9	4	-0.02297	------
	1.8595	4.1748	"	0.331356
	1.8594	4.0824	-0.02262	0.330108
	1.8594	(4)	-0.02236	0.330946
NC5004	1.9	5	-0.02297	------
	1.8560	3.6654	"	0.298606
	1.8557	3.1738	-0.02074	0.248012
	1.8567	(5)	-0.02690	0.554885
N33004	1.9	4	-0.02297	------
	1.8469	4.2980	"	0.180921
	1.8469	4.3164	-0.02304	0.180831
	1.8467	(4)	-0.02206	0.202419
N66004	2.0	4	-0.02297	------
	1.9314	3.7921	"	0.282243
	1.9315	4.6106	-0.02608	0.181014
	1.9313	(4)	-0.02421	0.231207
N6C004	1.9	6	-0.02297	------
	2.0705	5.2572	"	0.529425
	2.0706	7.5424	-0.02886	0.257256
	2.0703	(6)	-0.02565	0.375924
NEN004	2.1	6	-0.02297	------
	2.1163	4.7950	"	0.786185
	2.1182	6.5761	-0.02812	0.706368
	2.1176	(6)	-0.02680	0.712755

	R	CN	c_2	F
NPH004	2.1	6	-0.02297	------
	2.0791	5.1554	"	0.632345
	2.0793	5.8675	-0.02502	0.609498
	2.0793	(6)	-0.02532	0.610100
NTA004	2.1	6	-0.02297	------
	2.1054	4.3436	"	0.671186
	2.1067	5.4507	-0.02663	0.631083
	2.1073	(6)	-0.02803	0.637859

S only :

	R	CN	c_2	F
N2M004	2.2	4	-0.02044	------
	2.1750	4.1131	"	0.464713
	2.1750	4.0588	-0.02023	0.463380
	2.1750	(4)	-0.02005	0.464650
N3M004	2.2	4	-0.02044	------
	2.1425	4.3384	"	0.571261
	2.1425	4.1975	-0.01993	0.563203
	2.1425	(4)	-0.01934	0.576458
NI2S*	2.2	4	-0.02044	------
	2.1698	3.7044	"	0.704884
	2.1698	3.7293	-0.02054	0.704696
	2.1697	(4)	-0.02143	0.721648
NS4004	2.3	4	-0.02044	------
	2.2869	3.9708	"	0.390313
	2.2869	4.2157	-0.02137	0.365219
	2.2868	(4)	-0.02071	0.381030
NTT004	2.4	6	-0.02044	------
	2.3801	5.6034	"	0.519830
	2.3803	6.3948	-0.02254	0.344368
	2.3802	(6)	-0.02171	0.384669

* — bad fits may be due to some contribution from the Ni-Ni signal, which was not completely separable from the Ni-S signal over this data range.

Results of fitting Ni-N,S models with N & S

Grace Tan 9th February, 1993

(checked and corrected 9th February, 1993)

These fits are discussed in Chapter 7, Section (E.1.b).

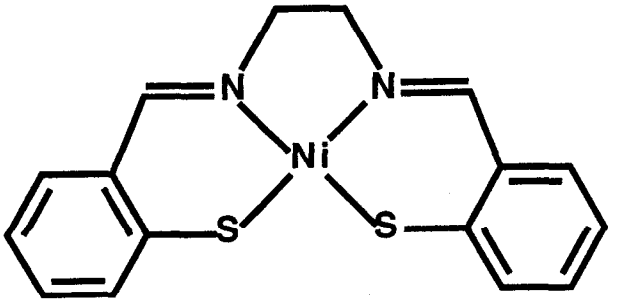

Models used :

Ni(tsalen) or Ni (S-salen) **(SSALEN)**

Ni-N = 1.85, 1.86, av. 1.86 Å
Ni-S = 2.174, 2.139, av. 2.157 Å

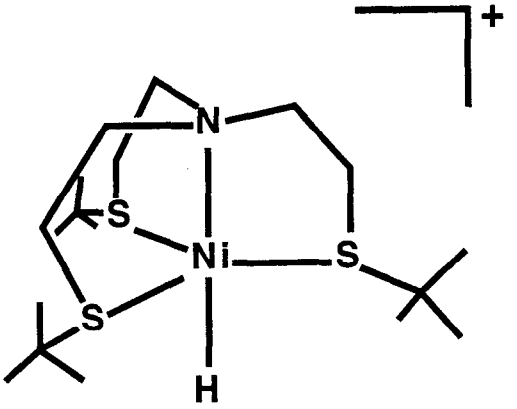

$[Ni(NS_3^{t\text{-}Bu})H][BPh_4]$ **(NS3BH)**

Ni-N = 2.02 Å
Ni-S = 2.234, 2.227, 2.218, av. 2.226 Å
Ni-H = 2.0 Å

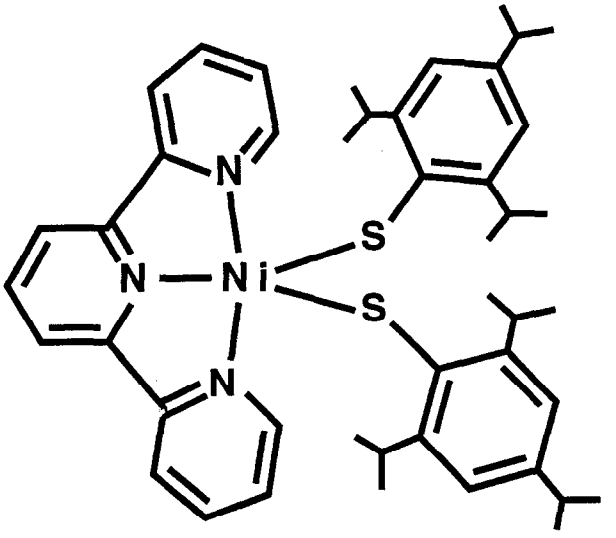

$[Ni(terpy)(S\text{-}2,4,6\text{-}(iPr)_3\text{-}C_6H_2)_2].1.5CH_3CN$ **(N3S2)**

Molecule 1:
Ni-N = 2.113 Å, 1.974 Å, 2.086 Å
Ni-S = 2.274 Å, 2.332 Å

Molecule 2 :
Ni-N = 2.075 Å, 1.968 Å, 2.125 Å
Ni-S = 2.298 Å, 2.302 Å

Average bond distances :
Ni-N = 2.057 Å
Ni-S = 2.302 Å

Ni(tsalen) or Ni (S-salen) **(SSALEN)**

Crystal structure : T. Yamamura, M. Tadokoro & R. Kuroda, *Chem. Lett.*, 1245-6 **(1989)**.
The compound was supplied by R. H. Holm. Data was collected at BL 7-3 in July 1992 to $k = 15$ Å^{-1}.
Pre-edge : 8360–9211 (2)
Spline : 8356 (2) 8515 (3) 8793 (3) 9211

[Ni(NS$_3$t-Bu)H][BPh$_4$] **(NS3BH)**

Crystal structure : P. Stavropoulos, M. C. Muetterties, M. Carrie, R. H. Holm, *J. Am. Chem. Soc.* **1991, 113**, 8485-92.
The compound was supplied by R. H. Holm. Data was collected at BL 7-3 in July 1991 to $k = 15$ Å^{-1}.
Pre-edge : 8380–9211 (-2)
Spline : 8383 (2) 8515 (3) 8765 (3) 9211

[Ni(terpy)(S-2,4,6-(iPr)$_3$-C$_6$H$_2$)$_2$].1.5CH$_3$CN **(N3S2)**

Crystal structure : Narayan Baidya, Marilyn Olmstead, Pradip K. Mascharak, *Inorg. Chem.* **1991, 30**, 929-37.
The compound was synthesized by Grace Tan. There is some doubt about the purity about the compound, since microanalysis gave 64.69 % C instead of the expected 69.93 %. Data was collected at BL 7-3 in June 1991 to $k = 15$ Å^{-1}.
Pre-edge : 8399–9219 (-2)
Spline : 8382 (2) 8557 (3) 8825 (3) 9219

Forward FT on all compound data : $k = 3.0$–12.0 (0.1) Å^{-1}

Reverse FT (to $k = 3.25$–11.75 Å^{-1}) :

SSALEN.FIL: R' = 0.95–2.35 (0.1) Å — main peak, including some smudged-in shoulders
NS3BH.FIL1: R' = 0.95–2.35 (0.1) Å — main peak, includes low-R shoulder
NS3BH.FIL2: R' = 1.25–2.35 (0.1) Å — main peak, excludes low-R shoulder
N3S2.FIL: R' = 1.00–2.30 (0.1) Å — main peak, including a smudged-in low-R shoulder

Parameters used in fits :

Ni^{II}-N : [Ni^{II}(dimethylglyoxime)$_2$],	10 K,	$k = 3.25$–11.75 Å^{-1}	(data to $k = 15$ Å^{-1})
Ni^{II}-S : Ni^{II}(S$_2$CN(CH$_2$CH$_3$)$_2$)$_2$,	10 K,	$k = 3.25$–11.75 Å^{-1}	(data to $k = 15$ Å^{-1})

Fits of SSALEN.FIL :

N only :	R	CN	c_2	F
Initial	2.0	4	-0.02297	------
	1.9671	3.8085	"	1.62750
	1.9486	10.4802	-0.04133	1.20930
	1.9564	(6)	-0.03190	1.35256

S only :	R	CN	c_2	F
Initial	2.2	3	-0.02044	------
	2.1384	1.9095	"	1.03187
	2.1358	3.7131	-0.03169	0.572879
	2.1362	(3)	-0.02838	0.634010

N + S :

	R_N	CN_N	c_{2N}	R_S	CN_S	c_{2S}	F
Initial	1.9	2	-0.02297	2.2	2	-0.02044	--------
##	1.8729	"	"	2.1599	"	"	0.328662
	1.8702	1.9292	"	2.1589	2.0396	"	0.323872
	1.8880	3.6795	-0.03209	2.1643	1.6257	-0.01956	0.293489
	1.8848	(1)	-0.01009	2.1644	(1)	-0.01030	0.824633
	1.8935	(2)	-0.01840	2.1707	(1)	-0.01161	0.614017
	1.8983	(3)	-0.02435	2.1728	(1)	-0.01287	0.469283
	1.8626	(1)	-0.01540	2.1533	(2)	-0.01960	0.426399
**	1.8719	(2)	-0.02418	2.1587	(2)	-0.02058	0.319308
	1.8784	(3)	-0.03092	2.1603	(2)	-0.02169	0.302882
	1.8438	(1)	-0.02095	2.1475	(3)	-0.02607	0.364792
	1.8555	(2)	-0.03123	2.1514	(3)	-0.02701	0.413729
	1.8670	(3)	-0.04078	2.1509	(3)	-0.02827	0.479455

— these R values used as starting values in each of the fixed-CN fits.

** — Of the fixed-CN fits, this has the best initial fit (F=0.328662). Next best initial fit has F=0.703896 (for Ni-N_1S_2).

N + N' :

	R_N	CN_N	c_{2N}	$R_{N'}$	$CN_{N'}$	$c_{2N'}$	F
Initial	1.9	2	-0.02297	2.2	4	-0.02297	--------
	1.9546	"	"	2.3823	"	"	1.50744
	1.9601	3.4254	"	2.3882	2.7790	"	1.22597
	1.9506	13.9697	-0.05127	2.3562	2.6270	-0.02074	0.453035
	1.9558	(3)	-0.02432	2.3827	(3)	-0.02144	1.23441

S + S' :

	R_S	CN_S	c_{2S}	$R_{S'}$	$CN_{S'}$	$c_{2S'}$	F
Initial	1.9	1	-0.02044	2.2	2	-0.02044	--------
##	2.0479	"	"	2.1721	"	"	0.505807
	2.0401	1.1897	"	2.1745	2.2855	"	0.437660
	1.9804	0.2472	-0.00796	2.1437	3.0153	-0.02380	0.410389
	2.0616	(1)	-0.00993	2.1985	(1)	-0.00726	0.649207
	2.0844	(2)	-0.02124	2.2099	(1)	-0.01279	0.438570
**	2.0359	(1)	-0.01485	2.1766	(2)	-0.01650	0.427572
	2.0661	(2)	-0.02707	2.1862	(2)	-0.02180	0.494142

— These R values used as starting values in each of the fixed-CN fits.

** — Of the fixed-CN fits, this has the best initial fit (F=0.505807). Next best initial fit has F=1.47535 (for Ni-S_2S_2).

Fits of NS3BH.FIL1 :

N only :

	R	CN	c_2	F
Initial	1.9	6	-0.02297	------
	2.0582	6.6969	"	1.71884
	2.0549	8.4918	-0.02683	1.67317
	2.0586	(6)	-0.02224	1.75080

S only :

	R	CN	c_2	F
Initial	2.2	4	-0.02044	------
	2.2209	3.2004	"	0.575304
	2.2208	3.7716	-0.02307	0.479932
	2.2209	(4)	-0.02387	0.491639
	2.2207	(3)	-0.02013	0.620913

N + S :

	R_N	CN_N	c_{2N}	R_S	CN_S	c_{2S}	F
Initial	1.9	1	-0.02297	2.2	3	-0.02044	--------
##	1.9909	"	"	2.2275	"	"	0.456864
	1.9863	1.0212	"	2.2277	3.0490	"	0.454281
	2.0002	1.8359	-0.03209	2.2265	2.9106	-0.02047	0.446785
	1.9862	(1)	-0.01179	2.2368	(2)	-0.01437	0.661055
	1.9966	(2)	-0.02088	2.2367	(2)	-0.01567	0.549644
	2.0040	(3)	-0.02784	2.2341	(2)	-0.01652	0.499962
	2.0093	(4)	-0.03377	2.2311	(2)	-0.01694	0.488908
**	1.9872	(1)	-0.02319	2.2274	(3)	-0.02028	0.455875
	2.0046	(2)	-0.03594	2.2251	(3)	-0.02091	0.449014
	2.0165	(3)	-0.04625	2.2229	(3)	-0.02101	0.466119
	2.3964	(1)	-0.03444	2.2227	(4)	-0.02414	0.435986
	2.3775	(2)	-0.04760	2.2231	(4)	-0.02389	0.416295

— these R values used as starting values in each of the fixed-CN fits.

** — Of the fixed-CN fits, this has the best initial fit (F=0.456864). Next best initial fit has F=0.713959 (for Ni-N_2S_3).

N + N' :

	R_N	CN_N	c_{2N}	$R_{N'}$	$CN_{N'}$	$c_{2N'}$	F
Initial	1.9	1	-0.02297	2.2	5	-0.02297	--------
**	2.0576	"	"	2.0577	"	"	1.75944
	1.8836	3.4180	"	2.0636	9.7620	"	0.929487
	1.9652	6.8178	-0.02974	2.0950	4.2223	-0.01463	0.811436
Initial	1.9	2	-0.02297	2.1	4	-0.02297	--------
	1.9393	(2)	-0.00920	2.0860	(4)	-0.00955	1.12285

** — The program crashed when this was used as an initial value for a fixed-CN fit.

S + S' :

	R_S	CN_S	c_{2S}	$R_{S'}$	$CN_{S'}$	$c_{2S'}$	F
Initial	1.9	1	-0.02044	2.2	3	-0.02044	--------
##	1.9644	"	"	2.2074	"	"	1.82054
	1.9391	-0.2684	"	2.2244	3.1562	"	0.440953
	1.9518	-0.7237	-0.04276	2.2225	3.2172	-0.02132	0.405034
	2.2180	(1)	-0.01554	2.2230	(1)	-0.01548	1.11624
	2.2191	(2)	-0.02016	2.2239	(1)	-0.02005	0.620909
	2.2171	(1)	-0.02018	2.2225	(2)	-0.02009	0.620910
**	2.2242	(1)	-0.02398	2.2197	(3)	-0.02383	0.491639
	2.3565	(2)	-0.12748	2.2203	(3)	-0.02015	0.605174

— These R values used as starting values in each of the fixed-CN fits.

** — Of the fixed-CN fits, this has the best initial fit (F=1.82054). Next best initial fit has F=2.67538 (for Ni-S_1S_2).

Fits of NS3BH.FIL2 :

N only :	R	CN	c_2	F
Initial	1.9	6	-0.02297	------
	2.0583	6.6288	"	1.65568
	2.0560	7.9550	-0.02591	1.62596
	2.0587	(6)	-0.02227	1.68174

S only :	R	CN	c_2	F
Initial	2.2	4	-0.02044	------
	2.2210	3.1635	"	0.461855
	2.2209	3.6537	-0.02274	0.367634
	2.2210	(4)	-0.02397	0.402886
	2.2208	(3)	-0.02023	0.501004

N + S :

	R_N	CN_N	c_{2N}	R_S	CN_S	c_{2S}	F
Initial	1.9	1	-0.02297	2.2	3	-0.02044	--------
##	1.9931	"	"	2.2277	"	"	0.339631
	1.9964	1.0067	"	2.2276	2.9620	"	0.338022
	1.9683	0.1267	-0.00088	2.2255	3.2370	-0.02034	0.301583
	1.9865	(1)	-0.01042	2.2388	(2)	-0.01416	0.466062
	1.9986	(2)	-0.01965	2.2388	(2)	-0.01575	0.412076
	2.0082	(3)	-0.02704	2.2350	(2)	-0.01686	0.430708
	2.0154	(4)	-0.03349	2.2307	(2)	-0.01734	0.476941
**	1.9947	(1)	-0.02124	2.2286	(3)	-0.02054	0.335679
	2.0240	(2)	-0.03644	2.2236	(3)	-0.02130	0.394777
	2.0347	(3)	-0.04999	2.2212	(3)	-0.02106	0.448007
	2.4049	(1)	-0.03156	2.2229	(4)	-0.02437	0.309284
	2.3910	(2)	-0.04287	2.2237	(4)	-0.02415	0.270586

— these R values used as starting values in each of the fixed-CN fits.
** — Of the fixed-CN fits, this has the best initial fit (F=0.339631). Next best initial fit has F=0.677349 (for Ni-N_2S_3).

N + N' :

	R_N	CN_N	c_{2N}	$R_{N'}$	$CN_{N'}$	$c_{2N'}$	F
Initial	1.9	2	-0.02297	2.2	4	-0.02297	--------
**	2.0579	"	"	2.0579	"	"	1.69004
	1.8851	2.9742	"	2.0637	9.2827	"	1.07902
	1.9845	5.9620	-0.02472	2.1062	2.9362	-0.01104	0.924210
##	2.1194	(2)	-0.00529	1.9936	(4)	-0.01534	1.02939

** — The program crashed when this was used as an initial value for a fixed-CN fit.
— This fit started from scratch, with the initial values in the first line.

S + S' :

	R_S	CN_S	c_{2s}	$R_{S'}$	$CN_{S'}$	$c_{2s'}$	F
Initial	1.9	1	-0.02044	2.2	3	-0.02044	--------
##	1.9508	"	"	2.2065	"	"	1.72846
	1.9600	-0.2441	"	2.2244	3.0676	"	0.350825
	1.9505	-0.0282	+0.00357	2.2238	3.3162	-0.02088	0.305316
	1.7514	(1)	-0.03599	2.2217	(1)	-0.00870	1.70386
	1.6766	(2)	-0.07169	2.2207	(1)	-0.00890	1.76198
	2.2162	(1)	-0.02028	2.2231	(2)	-0.02018	0.500995
	2.2194	(2)	-0.02405	2.2226	(2)	-0.02388	0.402885
**	2.6621	(1)	-0.03425	2.2206	(3)	-0.02039	0.395206
	1.7137	(2)	-0.15933	2.2206	(3)	-0.02024	0.490190

— These R values used as starting values in each of the fixed-CN fits.
** — Of the fixed-CN fits, this has the best initial fit (F=1.72846). Next best initial fit has F=2.50533 (for Ni-S_1S_2).

Fits to N3S2.FIL :

N only :	R	CN	c_2	F
Initial	1.9	6	-0.02297	------
	2.1096	4.0888	"	1.25793
	2.0958	9.9822	-0.03902	0.921433
	2.1021	(6)	-0.03051	1.04192

S only :	R	CN	c_2	F
Initial	2.2	3	-0.02044	------
	2.2785	1.9258	"	0.879282
	2.2785	3.5311	-0.03055	0.567713
	2.2783	(3)	-0.02804	0.594806

N + S :

	R_N	CN_N	c_{2N}	R_S	CN_S	c_{2S}	F
Initial	2.0	3	-0.02297	2.3	2	-0.02044	--------
##	2.0335	"	"	2.3126	"	"	0.663878
	2.0255	1.8546	"	2.3001	1.9201	"	0.460677
	2.0639	7.0138	-0.04208	2.3008	0.9038	-0.01656	0.330640
	2.0333	(1)	-0.01158	2.3036	(1)	-0.01134	0.793849
	2.0431	(2)	-0.01982	2.3088	(1)	-0.01286	0.620257
	2.0490	(3)	-0.02577	2.3097	(1)	-0.01426	0.499180
	2.0534	(4)	-0.03074	2.3085	(1)	-0.01545	0.415118
	2.0160	(1)	-0.01815	2.2935	(2)	-0.02066	0.520464
**	2.0285	(2)	-0.02698	2.2973	(2)	-0.02196	0.437079
	2.0386	(3)	-0.03397	2.2969	(2)	-0.02327	0.403855
	2.0487	(4)	-0.04055	2.2937	(2)	-0.02437	0.397933
	2.0065	(1)	-0.02614	2.2882	(3)	-0.02729	0.488580
	2.0345	(2)	-0.03837	2.2879	(3)	-0.02893	0.490095
	2.0976	(3)	-0.05682	2.2772	(3)	-0.02958	0.490976

— these R values used as starting values in each of the fixed-CN fits.

** — Of the fixed-CN fits, this has the best initial fit (F=0.605521). Next best initial fit has F=0.663878 (for Ni-N_3S_2).

N + N' :

	R_N	CN_N	c_{2N}	$R_{N'}$	$CN_{N'}$	$c_{2N'}$	F
Initial	2.0	3	-0.02297	2.3	3	-0.02297	--------
	2.0489	"	"	2.1607	"	"	1.03334
	1.9653	3.1425	"	2.1303	6.4630	"	0.382125
	2.0215	6.2990	-0.03290	2.1586	3.4295	-0.01875	0.361463
	2.0108	(3)	-0.01856	2.1560	(3)	-0.01346	0.587170

S + S' :

	R_S	CN_S	c_{2s}	$R_{S'}$	$CN_{S'}$	$c_{2s'}$	F
Initial	2.0	2	-0.02044	2.3	2	-0.02044	--------
##	2.2198	"	"	2.3503	"	"	0.687830
	2.2129	1.3882	"	2.3297	1.8072	"	0.570914
	2.0925	0.0202	-0.00031	2.2780	3.4237	-0.02928	0.559072
	2.2129	(1)	-0.01096	2.3428	(1)	-0.00950	0.716779
	2.2400	(2)	-0.02232	2.3535	(1)	-0.01761	0.579599
	2.2758	(3)	-0.02807	2.4063	(1)	-0.07312	0.549273
	2.1988	(1)	-0.01805	2.3191	(2)	-0.02035	0.575700
**	2.2721	(2)	-0.02633	2.2972	(2)	-0.04346	0.571999
	2.2755	(3)	-0.02801	2.4293	(2)	-0.08963	0.523333
	2.2737	(1)	-0.02312	2.2830	(3)	-0.03812	0.576022
	2.2725	(2)	-0.02470	2.3098	(3)	-0.05969	0.592135
	2.2753	(3)	-0.02799	2.4392	(3)	-0.10131	0.505789

— These R values used as starting values in each of the fixed-CN fits.

** — Of the fixed-CN fits, this has the best initial fit (F=0.687830). Next best initial fit has F=1.18764 (for Ni-S_2S_1).

Fits to $(Et_4N)_3[NiFe_3S_4(SEt)_4]$

Grace Tan 30th Mar 1993

(checked and corrected 30th Mar 1993)

These fits are discussed in Chapter 7, Sections (E.1.a) and (E.1.c).

There is no crystal structure for $(Et_4N)_3[NiFe_3S_4(SEt)_4]$; however, there is a structure for the related compound $(Et_4N)_2[NiFe_3S_4(PPh_3)(SEt)_3]$, for which the average Ni-S distance (in the cubane) is 2.258 Å and the average Ni··Fe distance is 2.689 Å. Data were collected in July 1991 on SSRL BL 7-3 to k = 15 Å^{-1}. The Fourier transform shows two large peaks which are not well-separated. Although the second peak was fitted on its own as a test for Ni-Fe parameters, reliable results can really only be obtained by fitting both peaks together.

Pre-edge : 8380–9218 (2)
Spline : 8370 (2) 8512 (3) 8790 (3) 9218

Forward FT range :
2NFS.FT-K12 : k = 3.0–12.0 (0.1) Å^{-1}

Reverse FT ranges (to k = 3.25–11.75 (0.1) Å^{-1}):
2NFS.FIL-K12 : R' = 2.03–2.80 (0.1) Å (2nd peak only)
2NFS.FIL2 : R' = 1.37–2.85 (0.1) Å (1st and 2nd peaks)
2NFS.FIL3 : R' = 1.00–2.85 (0.1) Å (1st + 2nd peaks + left shoulder of 1st peak)

Parameters used in fits :

Parameters were extracted over the same ranges as the compound data they were used to fit.

Ni^{II}-N :	Ni^{II}(dimethylglyoxime)$_2$,	10 K,	data to k = 15 Å^{-1}
Ni^{II}-S :	$Ni^{II}(S_2CN(CH_2CH_3)_2)_2$,	10 K,	data to k = 15 Å^{-1}
Ni^{II}-Fe :	$[Et_4N]_2[NiFe_3S_4(PPh_3)(SEt)_3]$,	10 K,	data to k = 15 Å^{-1}

Fits to 2NFS.FIL-K12 :

Fe only :

	R_{Fe}	CN_{Fe}	c_{2Fe}	F
Initial	2.689	3	-0.01530	-----
	2.7551	"	"	0.753763
	2.7546	2.5759	"	0.649238
	2.7545	2.5133	-0.01500	0.648880
	2.7553	(3)	-0.01694	0.665921

Fits to 2NFS.FIL2 :

S + Fe :

				R_S	CN_S	c_{2s}	R_{Fe}	CN_{Fe}	c_{2Fe}	F
Initial	----	----	----	2.26	4	-0.02044	2.7	3	-0.01530	-----
	----	----	----	2.2540	"	"	2.7550	"	"	1.63204
	----	----	----	2.2534	2.9257	"	2.7525	2.3029	"	0.633902
	----	----	----	2.2548	2.6692	-0.01840	2.7545	4.4331	-0.02441	0.363886
	----	----	----	2.2555	(4)	-0.02444	2.7502	(3)	-0.01835	0.749545

S + S' + Fe :

	R_S	CN_S	c_{2s}	R_S	CN_S	c_{2s}	R_{Fe}	CN_{Fe}	c_{2Fe}	F
Initial	2.2	1	-0.02044	2.3	3	-0.02044	2.7	3	-0.01530	-----
	2.1754	"	"	2.2767	"	"	2.7488	"	"	1.08318
	2.2533	0.6550	"	2.2534	2.2706	"	2.7525	2.3029	"	0.633902
	2.2418	(1)	-0.00998	2.2878	(3)	-0.03844	2.7622	(3)	-0.01842	0.226081
Initial	2.2	3	-0.02044	2.3	1	-0.02044	2.7	3	-0.01530	-----
	2.2384	"	"	2.3664	"	"	2.7528	"	"	0.805266
	2.2569	3.5247	"	2.4709	0.9967	"	2.7628	2.1791	"	0.298169
	2.2522	(3)	-0.01867	2.4410	(1)	-0.02831	2.7599	(3)	-0.01938	0.221558

N + S + Fe :

	R_N	CN_N	c_{2N}	R_S	CN_S	c_{2s}	R_{Fe}	CN_{Fe}	c_{2Fe}	F
Initial	1.9	2	-0.02297	2.25	3	-0.02044	2.7	1	-0.01530	-----
	2.0309	"	"	2.2697	"	"	2.7490	"	"	1.17169
	2.1643	3.6611	"	2.2219	2.6681	"	2.7562	2.3764	"	0.399007
	2.2612	(2)	-0.01395	2.2475	(3)	-0.01534	2.7581	(3)	-0.01900	0.271620

Fits to 2NFS.FIL3 :

S + Fe :

				R_S	CN_S	c_{2s}	R_{Fe}	CN_{Fe}	c_{2Fe}	F
Initial	----	----	----	2.26	4	-0.02044	2.7	3	-0.01530	-----
	----	----	----	2.2538	"	"	2.7543	"	"	1.71837
	----	----	----	2.2533	2.9996	"	2.7519	2.2838	"	0.947706
	----	----	----	2.2548	2.8675	-0.01914	2.7537	4.4251	-0.02431	0.794062
	----	----	----	2.2552	(4)	-0.02426	2.7498	(3)	-0.01845	0.961986

S + S' + Fe :

	R_S	CN_S	c_{2s}	R_S	CN_S	c_{2s}	R_{Fe}	CN_{Fe}	c_{2Fe}	F
Initial	2.2	1	-0.02044	2.3	3	-0.02044	2.7	3	-0.01530	-----
	2.1756	"	"	2.2762	"	"	2.7483	"	"	1.23391
	2.2572	3.6993	"	2.4706	1.1614	"	2.7641	2.1443	"	0.686624
	2.2440	(1)	-0.00976	2.2821	(3)	-0.03911	2.7618	(3)	-0.01879	0.650552
Initial	2.2	3	-0.02044	2.3	1	-0.02044	2.7	3	-0.01530	-----
	2.2376	"	"	2.3610	"	"	2.7520	"	"	1.04255
	2.2572	3.6993	"	2.4707	1.1618	"	2.7641	2.1439	"	0.686624
	2.2514	(3)	-0.01850	2.4343	(1)	-0.02826	2.7595	(3)	-0.01940	0.694287

N + S + Fe :

	R_N	CN_N	c_{2N}	R_S	CN_S	c_{2s}	R_{Fe}	CN_{Fe}	c_{2Fe}	F
Initial	1.9	2	-0.02297	2.25	3	-0.02044	2.7	1	-0.01530	-----
	2.0232	"	"	2.2694	"	"	2.7480	"	"	1.30169
	2.1884	4.3548	"	2.2216	3.3538	"	2.7552	2.3748	"	0.780023
	2.2328	(2)	-0.01835	2.2415	(3)	-0.01712	2.7567	(3)	-0.01929	0.743525

Results of fitting Ni CODH with N & S

Grace Tan 30th Mar 1993

(Numbers checked and corrected : 30th Mar 1993)

These fits are discussed in Chapter 7, Sections (E.2.a) – (E.2.e). The fits are listed by data set in the following order : CODHX, CODHOX, CDHOX, CODHRX and CDHRD. However, the three-wave fits to Window 6 (discussed in Section (E.2.d)) of all five data sets are listed separately in landscape mode, after all the other fits.

Several data sets being curve-fitted over :
k = 3.25–11.75 Å^{-1} (Forward FT : k = 3.0–12.0 (0.1) Å^{-1})

Parameters used in fits :

Parameters were extracted over the same ranges as the protein data they were used to fit.

Ni^{II}-N :	Ni^{II}(dimethylglyoxime)$_2$,	10 K,	data to k = 15 Å^{-1}
Ni^{II}-S :	$Ni^{II}(S_2CN(CH_2CH_3)_2)_2$,	10 K,	data to k = 15 Å^{-1}
Ni^{II}-Fe :	$[Et_4N]_2[NiFe_3S_4(PPh_3)(SEt)_3]$,	10 K,	data to k = 15 Å^{-1}

(1) CODHX (oxidized CODH) :

Data were collected at NSLS Beam Line X19A in June 1989 using 13-element germanium detector. 16 EXAFS scans collected, with 11 good detectors. Problem with energy calibration due to bug in software, so calibration may be slightly off, but calibration accuracy is quite acceptable for EXAFS. Data to k = 15 Å^{-1}, but, owing to huge monochromator glitch at k = 12.8 Å^{-1}, only useable up to k = 12.0 Å^{-1}. This data set was initially fit over k = 4–11 Å^{-1}, but now it is being fit over the maximum range that the glitch will allow, k = 3.25–11.75 Å^{-1}. (The data were resplined for this purpose.) This data set is the only one that shows a large peak at very low R in the Fourier transform.

Final pre-edge : 8390.2–8970.8 (2)
Final spline : 8384.5 (2) 8518.9 (3) 8716.3 (3) 8970.8

Forward FT over k = 3.0–12.0 (0.1) Å^{-1}
Reverse FT (to k = 3.25–11.75 Å^{-1}) :

CODHX.FIL1 : R' = 1.00–1.58 (0.1) Å — 1st large peak only
CODHX.FIL2 : R' = 1.50–2.25 (0.1) Å — 2nd large peak only
CODHX.FIL3 : R' = 1.00–2.25 (0.1) Å — 2 main peaks included
CODHX.FIL6 : R' = 1.00–2.55 (0.1) Å — 2 main peaks + right shoulder of 2nd peak

(2) CODHOX (oxidized CODH):

Data were collected in July 1991 at SSRL on BL 7-3, using the 13-element Ge detector. 29 good scans and 9 detectors were averaged together. This data set is noisier than CODHX, but on the other hand there is no glitch to cut the data short and it is good up

to k = 14.5 Å^{-1} or so. However, it was not considered worthwhile to attempt fits to the limit of the data, because of the noise.

Final pre-edge : 8365-9213 (2)
Final spline : 8381 (2) 8554 (3) 8774 (3) 9213

Forward FT over k = 3.0–12.0 (0.1) Å^{-1}
Reverse FT (to k = 3.25–11.75 Å^{-1}) :

CODHOX.FIL1 : R' = 0.80–1.60 (0.1) Å — 1eft shoulder of main peak only
CODHOX.FIL2 : R' = 1.45–2.20 (0.1) Å — main peak only
CODHOX.FIL3 : R' = 0.80–2.20 (0.1) Å — main peak + left shoulder
CODHOX.FIL4 : R' = 2.07–2.60 (0.1) Å — peak or right shoulder on 2nd peak
CODHOX.FIL5 : R' = 1.45–2.60 (0.1) Å — main peak + right shoulder
CODHOX.FIL6 : R' = 0.80–2.60 (0.1) Å — main peak + both shoulders
(Note: CODHOX.FIL4 and CODHOX.FIL5 were not used in curvefitting.)

(3) CDHOX (oxidized CODH) :

This sample was prepared at very short notice by Jeff Fox of Paul Ludden's group, who does not usually work on Ni CODH. Data were collected in July 1992 at SSRL on BL 7-3, using the 13-element Ge detector. 31 good scans and all 13 detectors were averaged together. This data set is less noisy than CODHOX, and it does not have a huge step glitch like CODHX. Unfortunately, it still does have enough of a glitch at k = 12.9 Å^{-1} to make it unwise to curvefit the data beyond k = 12 Å^{-1}.

Final pre-edge : 8392.7-8962.4 (2)
Final spline : 8386.9 (2) 8506.1 (3) 8695.0 (3) 8962.4

Forward FT over k = 3.0–12.0 (0.1) Å^{-1}
Reverse FT (to k = 3.25–11.75 Å^{-1}) :

CDHOX.FIL1 : R' = 1.05–1.60 (0.1) Å — left shoulder of main peak only
CDHOX.FIL2 : R' = 1.40–2.25 (0.1) Å — main peak only
CDHOX.FIL3 : R' = 1.05–2.25 (0.1) Å — main peak + left shoulder
CDHOX.FIL4 : R' = 2.07–2.60 (0.1) Å — right shoulder of main peak
CDHOX.FIL5 : R' = 1.40–2.60 (0.1) Å — main peak + right shoulder
CDHOX.FIL6 : R' = 1.05–2.60 (0.1) Å — main peak + both shoulders
(Note: CDHOX.FIL4 and CDHOX.FIL5 were not used in curvefitting.)

(4) CODHRX (reduced CODH):

Data were collected in July 1991 at SSRL on BL 7-3, using the 13-element Ge detector, at the same time as CODHOX. 34 good scans and all 13 detectors were averaged together. This data set is low in noise, but the same glitch that cut short CODHX also affects this data set, so it can only be curve-fit to around k = 12 Å^{-1}. Of all the data sets analyzed, only CODHRX shows 3 Fourier peaks at higher R. These peaks are analyzed separately.

Final pre-edge : 8365-8970 (2)
Final spline : 8387.1 (2) 8520.8 (3) 8738.9 (3) 8970

Forward FT over k = 3.0–12.0 (0.1) Å^{-1}
Reverse FT (to k = 3.25–11.75 Å^{-1}) :

CODHRX.FIL1 : R' = 1.00–1.60 (0.1) Å — left shoulder of main peak only
CODHRX.FIL2 : R' = 1.45–2.60 (0.1) Å — main peak only
CODHRX.FIL3 : R' = 1.00–2.60 (0.1) Å — main peak + left shoulder
CODHRX.FIL4 : R' = 2.45–2.95 (0.1) Å — right shoulder of main peak
CODHRX.FIL5 : R' = 1.45–2.95 (0.1) Å — main peak + right shoulder
CODHRX.FIL6 : R' = 1.00–2.95 (0.1) Å — main peak + both shoulders
CODHRX.FIL7 : R' = 2.85–3.60 (0.1) Å — first high-R peak
CODHRX.FIL8 : R' = 3.52–4.20 (0.1) Å — second high-R peak
CODHRX.FIL9 : R' = 4.10–5.07 (0.1) Å — third high-R peak
CODHRX.FIL10 : R' = 2.85–5.07 (0.1) Å — all three high-R peaks
(Note: CODHRX.FIL4 and CODHRX.FIL5 were not used in curvefitting.)

(4) CDHRD (reduced CODH) :

This sample was prepared at very short notice by Jeff Fox of Paul Ludden's group, who does not usually work on Ni CODH. Data were collected in July 1992 at SSRL on BL 7-3, using the 13-element Ge detector, at the same time as CDHOX. 30 good scans and 13 detectors were averaged together. This data set is noisier than CODHRX, but it does not have a huge step glitch. Unfortunately, it still does have enough of a glitch at k = 12.9 Å^{-1} to make it unwise to curvefit the data beyond k = 12 Å^{-1}. Another problem is that it looks more like the EXAFS of the oxidized spectra than it does like CODHRX. In particular, it looks extremely similar to CDHOX.

Final pre-edge : 8417.5-8960.6 (2)
Final spline : 8362.0 (2) 8519.7 (3) 8721.2 (3) 8960.6

Forward FT over k = 3.0–12.0 (0.1) Å^{-1}
Reverse FT (to k = 3.25–11.75 Å^{-1}) :

CDHRD.FIL1 : R' = 1.00–1.57 (0.1) Å — left shoulder of main peak only
CDHRD.FIL2 : R' = 1.40–2.25 (0.1) Å — main peak only
CDHRD.FIL3 : R' = 1.00–2.25 (0.1) Å — main peak + left shoulder
CDHRD.FIL4 : R' = 2.07–2.60 (0.1) Å — right shoulder of main peak
CDHRD.FIL5 : R' = 1.40–2.60 (0.1) Å — main peak + right shoulder
CDHRD.FIL6 : R' = 1.00–2.60 (0.1) Å — main peak + both shoulders
(Note: CDHRD.FIL4 and CDHRD.FIL5 were not used in curvefitting.)

Fits of CODHX.FIL1 :

N only :	R	CN	c_2	F
Initial	1.8	2	-0.02297	----
	1.8701	1.2232	"	0.836605
	1.8954	2.6490	-0.03643	0.815026

S only :	R	CN	c_2	F
Initial	1.8	1	-0.02044	----
	1.6437	0.4447	"	0.556344
	1.6445	0.4068	-0.01905	0.554704

Fits of CODHX.FIL2 :

N only :	R	CN	c_2	F
Initial	2.2	3	-0.02297	----
	2.0791	3.1020	"	1.13913
	2.0880	1.6474	-0.01356	1.04482

S only :	R	CN	c_2	F
Initial	2.2	2	-0.02044	----
	2.2342	1.5821	"	0.481026
	2.2350	1.1153	-0.01515	0.363842
	2.2341	(2)	-0.02275	0.611829

N + S :

	R_N	CN_N	c_{2N}	R_S	CN_S	c_{2S}	F
Initial	2.1	2	-0.02297	2.2	2	-0.02044	-----
##	2.1915	"	"	2.2130	"	"	0.697786
	2.2439	-2.1515	"	2.2503	0.9185	"	0.344041
	2.1136	1.8605	-0.01288	2.1503	2.0125	-0.03314	0.279135
	2.1136	(2)	-0.01333	2.1466	(2)	-0.03264	0.279658
Initial	1.9	2	-0.02297	2.2	2	-0.02044	-----
##	1.8390	"	"	2.2253	"	"	0.866683
	1.8235	0.6429	"	2.2306	1.6824	"	0.261428
	1.8504	4.3139	-0.08322	2.2368	1.1533	-0.01532	0.141425
	1.8774	(1)	-0.04505	2.2360	(1)	-0.01358	0.250479
	1.8770	(2)	-0.06024	2.2367	(1)	-0.01365	0.205969
**	1.8180	(1)	-0.02767	2.2307	(2)	-0.02226	0.334292
	1.8122	(2)	-0.04170	2.2330	(2)	-0.02190	0.341081
	1.8041	(1)	-0.02247	2.2274	(3)	-0.02910	0.633917
	1.7967	(2)	-0.03447	2.2297	(3)	-0.02830	0.643040

— these R values used as starting values in the fixed-CN fits following them.

** — Of the fixed-CN fits with short Ni-N, this one has the best initial fit (F = 0.481030). Next best initial fit is F = 0.866683 (for Ni-N_2S_2).

N + N' :

	R_N	CN_N	c_{2N}	$R_{N'}$	$CN_{N'}$	$c_{2N'}$	F
Initial	2.0	2	-0.02297	2.2	2	-0.02297	-----
##	2.0485	"	"	2.1087	"	"	1.20713
	2.0791	1.4209	"	2.0709	1.6805	"	1.13913
	1.9403	(2)	-0.02383	2.0980	(2)	-0.01129	0.614664
	1.9415	4.2253	-0.04126	2.0985	1.9373	-0.01288	0.579619

— these R values used as starting values in the fixed-CN fit.

S + S' :

	R_S	CN_S	c_{2S}	$R_{S'}$	$CN_{S'}$	$c_{2S'}$	F
Initial	2.0	2	-0.02044	2.2	2	-0.02044	-----
##	1.9725	"	"	2.1958	"	"	2.08342
	1.9869	0.4128	"	2.2253	1.8304	"	0.143003
++	2.0316	0.8998	-0.04393	2.2361	1.4597	-0.01730	0.100094
††	2.0708	1.5587	-0.06854	2.2380	1.1833	-0.01551	0.100935
	2.1025	(1)	-0.05626	2.2385	(1)	-0.01370	0.158999
	2.1031	(2)	-0.07897	2.2379	(1)	-0.01385	0.114662
**	2.0001	(1)	-0.03615	2.2314	(2)	-0.02082	0.185063
	2.0059	(2)	-0.05747	2.2360	(2)	-0.02123	0.292066
	1.9701	(1)	-0.02765	2.2215	(3)	-0.02699	0.405871
	1.9804	(2)	-0.04456	2.2302	(3)	-0.02632	0.496987

— these R values used as starting values in all the fixed-CN fits.
++ — Initial values from fixed-c_2 fit.
†† — Initial values from fixed-CN fit (CN_S=2,2).
** — Of the fixed-CN fits, this one has the best initial fit (F = 0.978747). Next best initial fit is F = 1.59468 (for Ni-S_1S_3).

Fits of CODHX.FIL3 :

N + S :

	R_N	CN_N	c_{2N}	R_S	CN_S	c_{2S}	F
Initial	1.9	2	-0.02297	2.2	2	-0.02044	-----
##	1.8527	"	"	2.2257	"	"	0.447884
	1.8534	2.1108	"	2.2257	2.0834	"	0.437524
	1.8328	0.8571	-0.01029	2.2140	2.7689	-0.02723	0.297795
	1.8613	(1)	-0.01594	2.2235	(1)	-0.01238	0.765617
	1.8781	(2)	-0.02555	2.2309	(1)	-0.01151	0.693149
	1.8889	(3)	-0.03224	2.2356	(1)	-0.01142	0.661207
	1.8421	(1)	-0.01284	2.2172	(2)	-0.02158	0.390134
**	1.8532	(2)	-0.02158	2.2244	(2)	-0.01993	0.427638
	1.8614	(3)	-0.02783	2.2301	(2)	-0.01934	0.521801
	1.8323	(1)	-0.01178	2.2145	(3)	-0.02817	0.316082
	1.8403	(2)	-0.02011	2.2211	(3)	-0.02612	0.478031
	1.8468	(3)	-0.02605	2.2268	(3)	-0.02521	0.637938

— these R values used as starting values in each of the fixed-CN fits.
** — of the fixed-CN fits, this one has the best initial fit (F = 0.447884). Next best initial fit is F = 0.777492 (for Ni-N_3S_2).

N + N' :

	R_N	CN_N	c_{2N}	$R_{N'}$	$CN_{N'}$	$c_{2N'}$	F
Initial	1.9	2	-0.02297	2.2	2	-0.02297	-----
##	1.8463	"	"	2.0615	"	"	1.65487
	1.8647	4.2687	"	2.0659	6.5082	"	0.380288
	1.8975	(2)	-0.01642	2.0817	(2)	-0.00906	0.833410
	1.8967	5.6339	-0.02913	2.0880	3.9911	-0.01636	0.295387

— these R values used as starting values in the fixed-CN fit.

S + S' :

	R_S	CN_S	c_{2S}	$R_{S'}$	$CN_{S'}$	$c_{2S'}$	F
Initial	1.9	2	-0.02044	2.2	2	-0.02044	-----
##	1.9948	"	"	2.2056	"	"	1.99164
	2.0126	1.0278	"	2.2215	2.4526	"	0.781242
	1.9526	0.1889	-0.00015	2.1971	3.9120	-0.03676	0.495614
	2.0790	(1)	-0.02753	2.2414	(1)	-0.01081	0.962526
	2.1062	(2)	-0.04126	2.2469	(1)	-0.01220	0.921942
	2.1201	(3)	-0.05188	2.2471	(1)	-0.01306	0.930681
**	2.0227	(1)	-0.02019	2.2243	(2)	-0.01750	0.807401
	2.0552	(2)	-0.03326	2.2407	(2)	-0.01787	0.909897
	2.0721	(3)	-0.04387	2.2472	(2)	-0.01919	1.02340
	1.9966	(1)	-0.01786	2.2131	(3)	-0.02364	0.753216
	2.0273	(2)	-0.02948	2.2319	(3)	-0.02235	0.945813
	2.0451	(3)	-0.03921	2.2423	(3)	-0.02321	1.10665

— these R values used as starting values in each of the fixed-CN fits.

** — of the fixed-CN fits, this one has the best initial fit (F = 1.03979). Next best initial fit is F = 1.40465 (for Ni-S_2S_3).

Fits of CODHX.FIL6 :

N + S :

	R_N	CN_N	c_{2N}	R_S	CN_S	c_{2S}	F
Initial	1.9	2	-0.02297	2.2	2	-0.02044	-----
##	1.8519	"	"	2.2253	"	"	0.552835
	1.8531	2.1949	"	2.2252	2.1440	"	0.527269
	1.8390	0.9872	-0.01149	2.2149	2.4268	-0.02389	0.434658
	1.8638	(1)	-0.01508	2.2230	(1)	-0.01158	0.748252
	1.8785	(2)	-0.02446	2.2300	(1)	-0.01076	0.669697
	1.8880	(3)	-0.03101	2.2346	(1)	-0.01066	0.642017
	1.8441	(1)	-0.01215	2.2164	(2)	-0.02082	0.460528
**	1.8542	(2)	-0.02077	2.2234	(2)	-0.01924	0.492443
	1.8616	(3)	-0.02691	2.2290	(2)	-0.01866	0.583967
	1.8340	(1)	-0.01119	2.2137	(3)	-0.02748	0.472033
	1.8413	(2)	-0.01943	2.2202	(3)	-0.02548	0.598408
	1.8472	(3)	-0.02529	2.2257	(3)	-0.02458	0.740544

— these R values used as starting values in each of the fixed-CN fits.

** — of the fixed-CN fits, this one has the best initial fit (F = 0.553835). Next best initial fit is F = 0.825130 (for Ni-N_3S_2).

Fits of CODHOX.FIL1 :

N only :	R	CN	c_2	F
Initial	1.8	2	-0.02297	----
	1.9234	0.8445	"	0.734775
	1.9704	7.6276	-0.06843	0.514273

S only :	R	CN	c_2	F
Initial	1.8	1	-0.02044	----
	1.6259	0.2584	"	0.669872
	1.6086	1.2005	-0.04969	0.436320

Fits of CODHOX.FIL2 :

N only :	R	CN	c_2	F
Initial	2.2	3	-0.02297	----
	2.0813	2.4597	"	0.917343
	2.0768	3.0740	-0.02666	0.909784

S only :	R	CN	c_2	F
Initial	2.2	2	-0.02044	----
	2.2431	1.2726	"	0.359707
	2.2416	(2)	-0.02762	0.330690
	2.2421	1.6663	-0.02483	0.305961

N + S :

	R_N	CN_N	c_{2N}	R_S	CN_S	c_{2S}	F
Initial	2.1	2	-0.02297	2.2	2	-0.02044	-----
##	2.2391	"	"	2.2304	"	"	0.544938
	2.3147	-1.6805	"	2.2198	0.8705	"	0.220784
	2.1352	(2)	-0.01809	2.1714	(2)	-0.03193	0.197806
	2.1270	1.6866	-0.01771	2.1775	2.4321	-0.03886	0.171607
Initial	1.9	2	-0.02297	2.2	2	-0.02044	-----
##	1.9181	"	"	2.2509	"	"	0.962368
	1.9093	0.4489	"	2.2444	1.3751	"	0.256763
	1.8752	5.8284	-0.10235	2.2461	1.5305	-0.02343	0.120416
**	1.9612	(1)	-0.03552	2.2500	(1)	-0.01763	0.306386
	1.9584	(2)	-0.05022	2.2498	(1)	-0.01803	0.262811
	1.8417	(1)	-0.03934	2.2424	(2)	-0.02654	0.169631
	1.8363	(2)	-0.05798	2.2443	(2)	-0.02663	0.160718
	1.8038	(1)	-0.03314	2.2383	(3)	-0.03369	0.345112
	1.7912	(2)	-0.04963	2.2404	(3)	-0.03338	0.343644

— these R values used as starting values in the fixed-CN fits following them.

** — of the fixed-CN fits, this one has the best <u>initial</u> fit (F = 0.722955). Next best initial fit is F = 0.739005 (for Ni-N_1S_2).

N + N' :

	R_N	CN_N	c_{2N}	$R_{N'}$	$CN_{N'}$	$c_{2N'}$	F
Initial	2.0	2	-0.02297	2.2	2	-0.02297	-----
##	2.0201	"	"	2.1303	"	"	0.935261
	1.8938	1.7802	"	2.0823	4.0884	"	0.528860
	1.9536	(2)	-0.02427	2.1079	(2)	-0.01442	0.531512
	1.9445	5.4822	-0.04956	2.1039	2.4353	-0.01979	0.456391

— these R values used as starting values in the fixed-CN fit.

S + S' :

	R_S	CN_S	c_{2S}	$R_{S'}$	$CN_{S'}$	$c_{2S'}$	F
Initial	2.0	2	-0.02044	2.2	2	-0.02044	-----
##	2.1780	"	"	2.3257	"	"	1.17627
	2.0832	0.3138	"	2.2488	1.5191	"	0.202850
	2.1331	2.2509	-0.08405	2.2482	1.3623	-0.02214	0.0677134
**	2.1731	(1)	-0.04251	2.2550	(1)	-0.01898	0.168878
	2.2471	(2)	-0.02594	2.0492	(1)	-0.05515	0.102657
	2.0492	(1)	-0.05154	2.2471	(2)	-0.02594	0.102657
	2.0536	(2)	-0.08130	2.2473	(2)	-0.02680	0.145034
	1.9890	(1)	-0.04044	2.2383	(3)	-0.03166	0.225618
	1.9946	(2)	-0.06463	2.2439	(3)	-0.03222	0.288993

— these R values used as starting values in the fixed-CN fit.

** — of the fixed-CN fits, this one has the best initial fit (F = 0.795829). Next best initial fit is F = 1.17627 (for Ni-S_2S_2).

Fits of CODHOX.FIL3 :

N + S :

	R_N	CN_N	c_{2N}	R_S	CN_S	c_{2S}	F
Initial	1.9	2	-0.02297	2.2	2	-0.02044	-----
##	1.8898	"	"	2.2405	"	"	0.724252
	1.8881	1.3284	"	2.2400	1.6277	"	0.557644
	1.8520	1.3382	-0.02417	2.2352	2.9839	-0.03133	0.355326
	1.9110	(1)	-0.02509	2.2444	(1)	-0.01622	0.743935
	1.9252	(2)	-0.03393	2.2504	(1)	-0.01625	0.627362
	1.9329	(3)	-0.04009	2.2537	(1)	-0.01655	0.541367
	1.8675	(1)	-0.02194	2.2363	(2)	-0.02520	0.469848
**	1.8826	(2)	-0.03136	2.2439	(2)	-0.02449	0.401736
	1.8925	(3)	-0.03810	2.2491	(2)	-0.02451	0.379323
	1.8473	(1)	-0.02049	2.2325	(3)	-0.03201	0.361065
	1.8592	(2)	-0.02989	2.2398	(3)	-0.03079	0.370358
	1.8684	(3)	-0.03677	2.2455	(3)	-0.03052	0.418617

— these R values used as starting values in each of the fixed-CN fits.

** — of the fixed-CN fits, this one has the best initial fit (F = 0.724253). Next best initial fit is F = 0.891128 (for Ni-N_1S_1).

N + N' :

	R_N	CN_N	c_{2N}	$R_{N'}$	$CN_{N'}$	$c_{2N'}$	F
Initial	1.9	2	-0.02297	2.2	2	-0.02297	-----
##	1.8839	"	"	2.0741	"	"	1.30700
	1.8852	3.1127	"	2.0767	5.1437	"	0.473235
	1.9249	(2)	-0.02126	2.0969	(2)	-0.01323	0.828709
	1.9296	8.5826	-0.04645	2.1088	3.4690	-0.02164	0.238650

— these R values used as starting values in the fixed-CN fit.

S + S' :

	R_S	CN_S	c_{2S}	$R_{S'}$	$CN_{S'}$	$c_{2S'}$	F
Initial	1.9	2	-0.02044	2.2	2	-0.02044	-----
##	2.1674	"	"	2.3161	"	"	1.28882
	2.0666	0.7031	"	2.2462	1.9111	"	0.640577
	1.9694	0.1772	-0.00681	2.2177	4.1988	-0.04112	0.447074
**	2.1405	(1)	-0.02991	2.2657	(1)	-0.01660	0.715005
	2.1583	(2)	-0.04383	2.2654	(1)	-0.01864	0.611635
	2.2414	(3)	-0.02837	2.0386	(1)	-0.02778	0.557399
	2.0790	(1)	-0.02921	2.2527	(2)	-0.02287	0.594757
	2.1099	(2)	-0.04308	2.2631	(2)	-0.02500	0.599888
	2.1275	(3)	-0.05615	2.2631	(2)	-0.02719	0.645506
	2.0386	(1)	-0.02778	2.2414	(3)	-0.02837	0.557399
	2.0743	(2)	-0.04133	2.2574	(3)	-0.02942	0.637388
	2.0949	(3)	-0.05399	2.2628	(3)	-0.03187	0.725129

— these R values used as starting values in each of the fixed-CN fits.

** — of the fixed-CN fits, this one has the best initial fit (F = 1.10817). Next best initial fit is F = 1.28882 (for Ni-S_2S_2).

Fits of CODHOX.FIL6 :

N + S :

	R_N	CN_N	c_{2N}	R_S	CN_S	c_{2S}	F
Initial	1.9	2	-0.02297	2.2	2	-0.02044	-----
##	1.8854	"	"	2.2387	"	"	0.726064
	1.8838	1.4193	"	2.2385	1.7025	"	0.615818
	1.9804	15.8992	-0.07700	2.2534	0.3605	-0.00682	0.380030
	1.9066	(1)	-0.02254	2.2422	(1)	-0.01482	0.780674
	1.9193	(2)	-0.03180	2.2483	(1)	-0.01482	0.679282
	1.9268	(3)	-0.03829	2.2517	(1)	-0.01510	0.611608
	1.8677	(1)	-0.01998	2.2344	(2)	-0.02406	0.599412
**	1.8799	(2)	-0.02938	2.2417	(2)	-0.02331	0.560426
	1.8885	(3)	-0.03618	2.2468	(2)	-0.02329	0.559547
	1.8489	(1)	-0.01896	2.2310	(3)	-0.03106	0.574874
	1.8583	(2)	-0.02828	2.2380	(3)	-0.02982	0.593449
	1.8661	(3)	-0.03512	2.2435	(3)	-0.02951	0.637468

— these R values used as starting values in each of the fixed-CN fits.

** — of the fixed-CN fits, this one has the best initial fit (F = 0.726064). Next best initial fit is F = 0.820817 (for Ni-N_1S_2).

Fits of CDHOX.FIL1 :

N only :	R	CN	c_2	F
Initial	1.9	2	-0.02297	----
	1.9445	0.8477	"	0.600747
	1.9760	6.5532	-0.06415	0.342871
	1.9556	(2)	-0.03875	0.459719

S only :	R	CN	c_2	F
Initial	1.9	1	-0.02044	----
	2.1375	0.2860	"	0.688747
	2.2066	3.0869	-0.07163	0.536515
	2.1702	(1)	-0.04305	0.583757
Initial	1.8	1	-0.02044	----
	1.6538	0.2179	"	0.618596
	1.6233	0.9682	-0.05034	0.499593
	1.6226	(1)	-0.05120	0.499676

Fits of CDHOX.FIL2 :

N only :	R	CN	c_2	F
Initial	2.2	3	-0.02297	----
	2.0692	3.0407	"	1.20585
	2.0622	4.1465	-0.02816	1.18758
	2.0683	(3)	-0.02351	1.20466

S only :	R	CN	c_2	F
Initial	2.2	2	-0.02044	----
	2.2318	1.6076	"	0.448623
	2.2305	1.9988	-0.02397	0.403157
	2.2305	(2)	-0.02398	0.403157

N + S :

	R_N	CN_N	c_{2N}	R_S	CN_S	c_{2S}	F
Initial	2.1	2	-0.02297	2.2	2	-0.02044	-----
##	2.1925	"	"	2.2096	"	"	0.619535
	2.1055	-2.0064	"	2.2429	2.3162	"	0.145000
	2.0788	-2.2232	-0.02710	2.2347	2.7240	-0.02330	0.116052
	2.1539	(2)	-0.01269	2.1714	(2)	-0.02076	0.275736
	2.1433	0.8533	-0.01067	2.1934	2.3879	-0.02844	0.199087
Initial	1.9	2	-0.02297	2.2	2	-0.02044	-----
##	1.9299	"	"	2.2442	"	"	0.762130
	1.9050	0.6785	"	2.2341	1.7583	"	0.236180
	1.9022	1.6042	-0.04108	2.2363	1.7982	-0.02147	0.219064
	1.9650	(1)	-0.02226	2.2441	(1)	-0.01380	0.394268
	1.9685	(2)	-0.03425	2.2443	(1)	-0.01472	0.335090
	1.9679	(3)	-0.04347	2.2431	(1)	-0.01520	0.314259
**	1.8857	(1)	-0.03198	2.2337	(2)	-0.02265	0.224250
	1.8815	(2)	-0.04898	2.2352	(2)	-0.02306	0.230234
	1.8264	(1)	-0.03180	2.2286	(3)	-0.02915	0.389999
	1.8111	(2)	-0.04913	2.2304	(3)	-0.02918	0.397881

— these R values used as starting values in the fixed-CN fits following them.
** — of the fixed-CN fits, this one has the best initial fit (F = 0.458946). Next best initial fit is F = 0.762130 (for Ni-N_2S_2).

N + N' :

	R_N	CN_N	c_{2N}	$R_{N'}$	$CN_{N'}$	$c_{2N'}$	F
Initial	2.0	2	-0.02297	2.2	4	-0.02297	-----
	1.8946	"	"	2.0745	"	"	0.845906
	1.8882	2.3220	"	2.0732	5.1551	"	0.701418
	1.9645	4.8807	-0.03550	2.1066	1.9580	-0.01374	0.607712
	1.9071	(2)	-0.01902	2.0806	(4)	-0.01842	0.674207

— these R values used as starting values in the fixed-CN fit.

S + S' :

	R_S	CN_S	c_{2S}	$R_{S'}$	$CN_{S'}$	$c_{2S'}$	F
Initial	2.0	2	-0.02044	2.2	2	-0.02044	-----
##	2.1670	"	"	2.3036	"	"	1.08142
	2.0668	0.4378	"	2.2368	1.9652	"	0.135596
	2.1279	1.1006	-0.03733	2.2462	1.5212	-0.01962	0.118222
**	2.1580	(1)	-0.02437	2.2620	(1)	-0.01501	0.181291
	2.1715	(2)	-0.04650	2.2460	(1)	-0.01655	0.143265
	2.0850	(1)	-0.03975	2.2406	(2)	-0.02231	0.141492
	2.0878	(2)	-0.06913	2.2375	(2)	-0.02349	0.214243
	2.0123	(1)	-0.03817	2.2311	(3)	-0.02751	0.285323
	2.0113	(2)	-0.06371	2.2338	(3)	-0.02855	0.356797

— these R values used as starting values in all the fixed-CN fits.
** — of the fixed-CN fits, this one has the best initial fit (F = 0.977790). Next best initial fit is F = 1.08142 (for Ni-S_2S_2).

Fits of CDHOX.FIL3 :

N + S :

	R_N	CN_N	c_{2N}	R_S	CN_S	c_{2S}	F
Initial	1.9	2	-0.02297	2.2	2	-0.02044	-----
##	1.8906	"	"	2.2325	"	"	0.521377
	1.8867	1.2987	"	2.2313	1.9554	"	0.298998
	1.8794	1.9001	-0.03028	2.2332	2.3246	-0.02348	0.178573
	1.9313	(1)	-0.02252	2.2379	(1)	-0.01330	0.669272
	1.9403	(2)	-0.03135	2.2420	(1)	-0.01365	0.523433
	1.9448	(3)	-0.03762	2.2439	(1)	-0.01404	0.413173
**	1.8788	(1)	-0.02180	2.2294	(2)	-0.02166	0.298819
	1.8916	(2)	-0.03143	2.2353	(2)	-0.02147	0.201606
	1.8992	(3)	-0.03847	2.2388	(2)	-0.02171	0.181675
	1.8513	(1)	-0.02052	2.2249	(3)	-0.02793	0.210301
	1.8615	(2)	-0.03045	2.2308	(3)	-0.02728	0.274092
	1.8685	(3)	-0.03793	2.2349	(3)	-0.02731	0.359848

— these R values used as starting values in each of the fixed-CN fits.

** — of the fixed-CN fits, this one has the best initial fit (F = 0.376892). Next best initial fit is F = 0.521377 (for Ni-N_2S_2).

N + N' :

	R_N	CN_N	c_{2N}	$R_{N'}$	$CN_{N'}$	$c_{2N'}$	F
Initial	1.9	2	-0.02297	2.2	4	-0.02297	-----
##	1.8806	"	"	2.0683	"	"	0.859557
	1.8815	3.3056	"	2.0699	5.9759	"	0.508232
	1.9421	8.2590	-0.04383	2.1027	2.6796	-0.01676	0.362955
	1.8924	(2)	-0.01691	2.0722	(4)	-0.01788	0.669458

— these R values used as starting values in the fixed-CN fit.

S + S' :

	R_S	CN_S	c_{2S}	$R_{S'}$	$CN_{S'}$	$c_{2S'}$	F
Initial	1.9	2	-0.02044	2.2	2	-0.02044	-----
##	2.1627	"	"	2.2997	"	"	1.13989
	2.0565	0.7045	"	2.2349	2.2471	"	0.388308
	1.9787	0.2140	-0.00813	2.2124	3.4706	-0.03137	0.287360
	2.1428	(1)	-0.02431	2.2590	(1)	-0.01377	0.554025
	2.1577	(2)	-0.03930	2.2538	(1)	-0.01591	0.400694
	2.2327	(3)	-0.02520	2.0388	(1)	-0.02697	0.379396
	2.0839	(1)	-0.02740	2.2438	(2)	-0.02012	0.387140
**	2.1085	(2)	-0.04238	2.2489	(2)	-0.02222	0.413168
	2.1222	(3)	-0.05771	2.2455	(2)	-0.02377	0.493842
	2.0388	(1)	-0.02697	2.2327	(3)	-0.02520	0.379396
	2.0676	(2)	-0.04152	2.2435	(3)	-0.02646	0.515051
	2.0812	(3)	-0.05712	2.2442	(3)	-0.02841	0.639731

— these R values used as starting values in each of the fixed-CN fits.

** — of the fixed-CN fits, this one has the best initial fit (F = 1.13989). Next best initial fit is F = 1.15599 (for Ni-S_1S_1).

Fits of CDHOX.FIL6 :

N + S :

	R_N	CN_N	c_{2N}	R_S	CN_S	c_{2S}	F
Initial	1.9	2	-0.02297	2.2	2	-0.02044	-----
##	1.8870	"	"	2.2320	"	"	0.623468
	1.8843	1.4143	"	2.2315	2.0452	"	0.474256
	1.9614	9.0689	-0.05927	2.2460	0.7367	-0.01104	0.379624
	1.9274	(1)	-0.01973	2.2381	(1)	-0.01191	0.715149
	1.9358	(2)	-0.02892	2.2425	(1)	-0.01227	0.589091
	1.9400	(3)	-0.03541	2.2445	(1)	-0.01267	0.504941
**	1.8806	(1)	-0.01926	2.2292	(2)	-0.02049	0.497701
	1.8906	(2)	-0.02879	2.2352	(2)	-0.02026	0.459532
	1.8968	(3)	-0.03578	2.2388	(2)	-0.02046	0.467319
	1.8556	(1)	-0.01855	2.2247	(3)	-0.02688	0.537332
	1.8631	(2)	-0.02821	2.2306	(3)	-0.02622	0.574973
	1.8684	(3)	-0.03545	2.2346	(3)	-0.02619	0.631741

— these R values used as starting values in each of the fixed-CN fits.

** — of the fixed-CN fits, this one has the best initial fit (F = 0.536094). Next best initial fit is F = 0.623468 (for Ni-N_2S_2).

Fits of CODHRX.FIL1 :

N only :	R	CN	c_2	F
Initial	1.8	2	-0.02297	----
	1.9367	0.6988	"	0.608393
	1.9775	7.4559	-0.07223	0.357312
	1.9520	(2)	-0.04196	0.468848

S only :	R	CN	c_2	F
Initial	1.8	1	-0.02044	----
	1.6309	0.2018	"	0.576076
	1.6068	1.0291	-0.05302	0.418188
	1.6074	(1)	-0.05224	0.418275

Fits of CODHRX.FIL2 :

N only :	R	CN	c_2	F
Initial	2.2	6	-0.02297	----
	2.0962	4.1545	"	2.17745
	2.1056	2.7231	-0.01652	2.14610
	2.0891	(6)	-0.02775	2.24697

S only :	R	CN	c_2	F
Initial	2.2	4	-0.02044	----
	2.2546	2.3448	"	1.18616
	2.2563	1.9716	-0.01777	1.16202
	2.2562	(2)	-0.01794	1.16215
	2.2502	(4)	-0.02795	1.49473

N + S :

	R_N	CN_N	c_{2N}	R_S	CN_S	c_{2S}	F
Initial	2.1	2	-0.02297	2.2	2	-0.02044	-----
	2.1643	"	"	2.2335	"	"	1.44535
	2.2916	-5.6858	"	2.4138	-0.6560	"	0.412677
	2.2765	-5.3165	-0.01918	2.4992	-0.0198	+0.01546	0.233357
Initial	2.0	2	-0.02297	2.2	2	-0.02044	-----
##	1.8871	"	"	2.2504	"	"	1.47229
	1.8932	1.1491	"	2.2532	2.6127	"	0.988918
	1.9144	3.4693	-0.04486	2.2606	1.9513	-0.01669	0.933126
	1.9964	(1)	-0.01133	2.2734	(1)	-0.00737	1.03944
	1.9956	(2)	-0.02284	2.2727	(1)	-0.00870	1.02904
	1.9913	(3)	-0.03132	2.2709	(1)	-0.00938	1.03122
	1.9295	(1)	-0.01985	2.2576	(2)	-0.01627	0.946596
	1.9232	(2)	-0.03181	2.2596	(2)	-0.01661	0.937056
	1.9151	(3)	-0.04116	2.2602	(2)	-0.01688	0.933812
**	1.8859	(1)	-0.01986	2.2511	(3)	-0.02195	1.03819
	1.8777	(2)	-0.03144	2.2538	(3)	-0.02189	1.03010
	1.8683	(3)	-0.04065	2.2550	(3)	-0.02199	1.02630

— these R values used as starting values in the fixed-CN fits.

** — of the fixed-CN fits, this one has the best initial fit (F = 1.13032). Next best initial fit is F = 1.13388 (for Ni-N_2S_3).

N + N' :

	R_N	CN_N	c_{2N}	$R_{N'}$	$CN_{N'}$	$c_{2N'}$	F
Initial	2.0	2	-0.02297	2.2	4	-0.02297	-----
	1.8911	"	"	2.0902	"	"	2.03341
	1.8986	3.3374	"	2.0929	7.1910	"	1.66695
	1.9965	4.8515	-0.02714	2.1366	1.8881	-0.00796	1.45968
	1.9408	(2)	-0.01281	2.1084	(4)	-0.01285	1.53757

— these R values used as starting values in the fixed-CN fit.

S + S' :

	R_S	CN_S	c_{2S}	$R_{S'}$	$CN_{S'}$	$c_{2S'}$	F
Initial	2.0	2	-0.02044	2.2	2	-0.02044	-----
	1.9972	"	"	2.2241	"	"	2.73166
	2.0505	0.8463	"	2.2509	3.0671	"	0.826914
	2.2090	1.4835	-0.01257	2.3263	0.3689	+0.00163	0.679031
Initial	2.2	2	-0.02044	2.3	2	-0.02044	-----
##	2.2013	"	"	2.3063	"	"	1.56607
	2.0505	0.8463	"	2.2509	3.0671	"	0.826914
	2.1686	(1)	-0.00922	2.3001	(1)	-0.00447	0.707893
	2.1785	(2)	-0.02681	2.2877	(1)	-0.00943	0.727397
	2.2542	(3)	-0.01954	2.0611	(1)	-0.02215	0.810885
	2.1151	(1)	-0.01950	2.2691	(2)	-0.01402	0.745128
**	2.1180	(2)	-0.03713	2.2685	(2)	-0.01601	0.742070
	2.2599	(3)	-0.02033	2.0687	(2)	-0.03714	0.815432
	2.0611	(1)	-0.02216	2.2542	(3)	-0.01954	0.810884
	2.0687	(2)	-0.03716	2.2599	(3)	-0.02033	0.815433
	2.0660	(3)	-0.04956	2.2608	(3)	-0.02103	0.846089

— these R values used as starting values in the fixed-CN fit.
** — of the fixed-CN fits, this one has the best initial fit (F = 1.56607). Next best initial fit is F = 1.64489 (for Ni-S_1S_2).

Fits of CODHRX.FIL3 :

N + S :

	R_N	CN_N	c_{2N}	R_S	CN_S	c_{2S}	F
Initial	1.9	2	-0.02297	2.2	2	-0.02044	-----
##	1.8805	"	"	2.2486	"	"	1.31657
	1.8879	1.9134	"	2.2507	2.8097	"	0.859414
	1.9135	5.7409	-0.04453	2.2622	2.0813	-0.01687	0.756178
	1.9733	(1)	-0.01634	2.2658	(1)	-0.00840	1.28502
	1.9687	(2)	-0.02645	2.2666	(1)	-0.00892	1.17295
	1.9660	(3)	-0.03279	2.2671	(1)	-0.00918	1.09040
	1.9083	(1)	-0.01791	2.2532	(2)	-0.01645	0.998284
	1.9120	(2)	-0.02663	2.2568	(2)	-0.01622	0.888951
	1.9141	(3)	-0.03269	2.2592	(2)	-0.01621	0.822320
	1.8802	(1)	-0.01598	2.2468	(3)	-0.02202	0.943755
**	1.8834	(2)	-0.02453	2.2508	(3)	-0.02140	0.858024
	1.8856	(3)	-0.03056	2.2536	(3)	-0.02116	0.823796

— these R values used as starting values in each of the fixed-CN fits.
** — of the fixed-CN fits, this one has the best initial fit (F = 0.900116). Next best initial fit is F = 1.08034 (for Ni-N_3S_3).

N + N' :

	R_N	CN_N	c_{2N}	$R_{N'}$	$CN_{N'}$	$c_{2N'}$	F
Initial	1.9	2	-0.02297	2.2	4	-0.02297	-----
##	1.8845	"	"	2.0879	"	"	2.05387
	1.8930	4.4335	"	2.0891	7.9991	"	1.52312
	1.9545	10.8089	-0.04436	2.1235	3.1923	-0.01418	1.31894
	1.9236	(2)	-0.01329	2.1003	(4)	-0.01360	1.63201

— these R values used as starting values in the fixed-CN fit.

S + S' :

	R_S	CN_S	c_{2S}	$R_{S'}$	$CN_{S'}$	$c_{2S'}$	F
Initial	1.9	2	-0.02044	2.2	2	-0.02044	-----
##	2.0101	"	"	2.2283	"	"	2.67054
	2.0517	1.1972	"	2.2495	3.3967	"	0.703665
	2.1158	2.5260	-0.03589	2.2707	2.1041	-0.01588	0.641231
	2.1622	(1)	-0.01187	2.2928	(1)	-0.00556	0.958742
	2.1688	(2)	-0.02740	2.2850	(1)	-0.00893	0.778885
	2.1684	(3)	-0.03724	2.2799	(1)	-0.00980	0.717124
	2.1036	(1)	-0.01846	2.2656	(2)	-0.01361	0.789916
	2.1173	(2)	-0.03088	2.2709	(2)	-0.01492	0.660279
	2.1216	(3)	-0.04004	2.2716	(2)	-0.01578	0.648337
**	2.0597	(1)	-0.01866	2.2514	(3)	-0.01879	0.715752
	2.0792	(2)	-0.02964	2.2615	(3)	-0.01892	0.667176
	2.0874	(3)	-0.03844	2.2655	(3)	-0.01962	0.716611

— these R values used as starting values in each of the fixed-CN fits.

** — of the fixed-CN fits, this one has the best initial fit (F = 1.23011). Next best initial fit is F = 1.69110 (for Ni-S_1S_2).

Fits of CODHRX.FIL6 :

N + S :

	R_N	CN_N	c_{2N}	R_S	CN_S	c_{2S}	F
Initial	1.9	2	-0.02297	2.2	2	-0.02044	-----
	1.8813	"	"	2.2491	"	"	1.35061
	1.8885	1.9373	"	2.2511	2.8263	"	0.896653
	1.9170	5.8737	-0.04476	2.2631	1.9980	-0.01629	0.790356
	1.9743	(1)	-0.01558	2.2665	(1)	-0.00813	1.28807
	1.9695	(2)	-0.02583	2.2672	(1)	-0.00871	1.17837
	1.9665	(3)	-0.03226	2.2677	(1)	-0.00899	1.09739
	1.9101	(1)	-0.01747	2.2536	(2)	-0.01627	1.02046
	1.9134	(2)	-0.02620	2.2572	(2)	-0.01605	0.914357
	1.9152	(3)	-0.03227	2.2596	(2)	-0.01605	0.850497
	1.8820	(1)	-0.01570	2.2472	(3)	-0.02185	0.981302
**	1.8848	(2)	-0.02424	2.2511	(3)	-0.02125	0.899519
	1.8868	(3)	-0.03026	2.2540	(3)	-0.02102	0.867523
	1.8674	(2)	-0.02286	2.2468	(4)	-0.02562	1.02764

— these R values used as starting values in each of the fixed-CN fits.

** — of the fixed-CN fits, this one has the best initial fit (F = 0.931386). Next best initial fit is F = 1.10296 (for Ni-N_3S_3).

Fits of CODHRX.FIL7 :

S only :	R	CN	c_2	F
Initial	3.5	1	-0.02044	----
	3.6809	"	"	0.198078
	3.6804	0.8295	"	0.182519
	3.6813	0.4925	-0.01265	0.152753
	3.6806	(1)	-0.02127	0.196553

Fe only :	R	CN	c_2	F
Initial	3.5	1	-0.01530	----
	3.5316	"	"	0.277812
	3.5301	0.6571	"	0.202757
	3.5308	0.5963	-0.01411	0.202273
	3.5275	(1)	-0.01991	0.215713

S + Fe :

	R_S	CN_S	c_{2S}	R_{Fe}	CN_{Fe}	c_{2Fe}	F
Initial	3.7	1	-0.02044	3.5	1	-0.01530	-----
	3.7589	"	"	3.4859	"	"	0.458880
	3.6446	0.5076	"	3.5597	0.4429	"	0.164241
	3.5427	1.0796	-0.04451	3.5378	0.8948	-0.01674	0.147789
	3.5358	(1)	-0.04091	3.5372	(1)	-0.01754	0.148316
Initial	3.5	1	-0.02044	3.5	1	-0.01530	-----
	3.5280	0.5703	"	3.5384	1.0963	"	0.155372

Fits of CODHRX.FIL8 :

S only :	R	CN	c_2	F
Initial	4.2	1	-0.02044	----
	4.1890	"	"	0.278934
	4.1896	1.4360	"	0.233608
	4.1895	1.4640	-0.02074	0.233562
	4.1918	(1)	-0.01624	0.246277
	4.1871	(2)	-0.02504	0.244550

Fe only :	R	CN	c_2	F
Initial	4.2	1	-0.01530	----
	4.0377	"	"	0.363886
	4.0377	0.9811	"	0.363797
	4.0289	1.8351	-0.02338	0.349329
	4.0363	(1)	-0.01644	0.361547

S + Fe :

	R_S	CN_S	c_{2S}	R_{Fe}	CN_{Fe}	c_{2Fe}	F
Initial	4.2	1	-0.02044	4.0	1	-0.01530	-----
	4.2361	"	"	3.9957	"	"	0.371268
	4.1766	2.0881	"	3.9983	-0.6701	"	0.202677
	4.1985	(1)	-0.01509	3.8881	(1)	-0.03640	0.207320
Initial	4.0	1	-0.02044	4.0	1	-0.01530	-----
	4.1255	"	"	4.0817	"	"	0.250436
	4.0825	1.7013	"	4.0769	1.9476	"	0.216222
	4.0873	2.7728	-0.04071	4.0615	1.6667	-0.01906	0.197129
	4.1149	(1)	-0.00696	4.1114	(1)	-0.00488	0.244849
	4.0775	(2)	-0.03081	4.0639	(2)	-0.01909	0.205390

Fits of CODHRX.FIL9 :

S only :

	R	CN	c_2	F
Initial	5.0	1	-0.02044	----
	5.0293	"	"	0.524656
	5.0300	2.3089	"	0.417930
	5.0208	1.0199	-0.00866	0.351502

Fe only :

	R	CN	c_2	F
Initial	5.0	1	-0.01530	----
	4.8714	"	"	0.423678
	4.8725	2.3228	"	0.177896
	4.8724	2.2378	-0.01485	0.177619
	4.8731	(3)	-0.01805	0.193257

S + Fe :

	R_S	CN_S	c_{2S}	R_{Fe}	CN_{Fe}	c_{2Fe}	F
Initial	4.8	1	-0.02044	4.9	2	-0.01530	-----
	4.6519	"	"	4.8790	"	"	0.149722
	4.6552	0.5958	"	4.8756	2.0401	"	0.106902
	4.6340	0.4021	-0.01181	4.8820	1.4982	-0.01117	0.0996890
	4.6526	(1)	-0.03082	4.8729	(2)	-0.01460	0.107332
Initial	5.0	1	-0.02044	4.9	2	-0.01530	-----
	4.9787	"	"	4.8890	"	"	0.280214
	4.8847	-1.3039	"	4.8521	1.5836	"	0.0730962
	5.2231	(1)	-0.04212	4.8714	(2)	-0.01339	0.143901

Fits of CODHRX.FIL10 :

S + Fe, 3 to 6 Waves :

	R_S	CN_S	c_{2S}	R_{Fe}	CN_{Fe}	c_{2Fe}	F
Peak 1	3.7638	(1)	(-0.02044)	3.4841	(1)	(-0.01530)	0.581478
Peak 2	4.1926	(1)	(-0.02044)	----	----	----	
Peak 3	----	----	----	4.8752	(2)	(-0.01530)	
Peak 1	3.8484	-0.4090	(-0.02044)	3.5268	0.4649	(-0.01530)	0.348254
Peak 2	4.1875	(1)	(-0.02044)	----	----	----	
Peak 3	----	----	----	4.8732	(2)	(-0.01530)	
Peak 1	3.8134	-0.6876	(-0.02044)	3.5566	0.5286	(-0.01530)	0.263842
Peak 2	4.1864	1.6581	(-0.02044)	----	----	----	
Peak 3	----	----	----	4.8711	2.3584	(-0.01530)	
Peak 1	----	----	----	3.5250	(1)	(-0.01530)	0.428777
Peak 2	4.1795	(1)	(-0.02044)	----	----	----	
Peak 3	----	----	----	4.8719	(2)	(-0.01530)	
Peak 1	----	----	----	3.5264	0.6217	(-0.01530)	0.336138
Peak 2	4.1838	1.4222	(-0.02044)	----	----	----	
Peak 3	----	----	----	4.8722	2.2728	(-0.01530)	

	R_S	CN_S	c_{2S}	R_{Fe}	CN_{Fe}	c_{2Fe}	F
Peak 1	3.6739	(1)	(-0.02044)	----	----	----	0.423233
Peak 2	4.1878	(2)	(-0.02044)	----	----	----	
Peak 3	----	----	----	4.8706	(2)	(-0.01530)	
Peak 1	3.6741	0.7426	(-0.02044)	----	----	----	0.343948
Peak 2	4.1879	1.4389	(-0.02044)	----	----	----	
Peak 3	----	----	----	4.8727	2.3210	(-0.01530)	
Peak 1	3.9185	(1)	(-0.02044)	3.5235	(1)	(-0.01530)	0.214485
Peak 2	4.1877	(2)	(-0.02044)	3.9187	(1)	(-0.01530)	
Peak 3	4.6511	(1)	(-0.02044)	4.8777	(2)	(-0.01530)	
Peak 1	3.7559	0.5039	(-0.02044)	3.5223	0.2110	(-0.01530)	0.0841238
Peak 2	4.1761	(2)	(-0.02044)	3.8289	(1)	(-0.01530)	
Peak 3	4.6558	(1)	(-0.02044)	4.8752	(2)	(-0.01530)	
Peak 1	----	----	----	3.5704	0.4897	(-0.01530)	0.133686
Peak 2	4.1743	2.0977	(-0.02044)	3.8271	(1)	(-0.01530)	
Peak 3	4.6614	(1)	(-0.02044)	4.8723	(2)	(-0.01530)	
Peak 1	----	----	----	3.5374	(0.4897)	(-0.01530)	0.0829290
Peak 2	4.1765	1.7783	(-0.02044)	3.8376	0.5638	(-0.01530)	
Peak 3	4.6489	(1)	(-0.02044)	4.8773	(2)	(-0.01530)	
Peak 1	----	----	----	3.5379	(0.4897)	(-0.01530)	0.0721235
Peak 2	4.1753	(1.7783)	(-0.02044)	3.8349	(0.5638)	(-0.01530)	
Peak 3	4.6522	1.0658	(-0.02044)	4.8769	1.8254	(-0.01530)	
Peak 1	3.7337	0.7867	(-0.02044)	----	----	----	0.0878662
Peak 2	4.1742	1.9878	(-0.02044)	3.8184	1.0766	(-0.01530)	
Peak 3	4.6563	(1)	(-0.02044)	4.8748	(2)	(-0.01530)	
Peak 1	3.7332	(0.7867)	(-0.02044)	----	----	----	0.0796796
Peak 2	4.1736	(1.9878)	(-0.02044)	3.8176	(1.0766)	(-0.01530)	
Peak 3	4.6587	1.0291	(-0.02044)	4.8742	1.8529	(-0.01530)	

Fits of CDHRD.FIL1 :

N only :	R	CN	c_2	F
Initial	1.8	2	-0.02297	----
	1.9201	0.6334	"	0.637959
	1.9740	7.4909	-0.07422	0.415094
	1.9435	(2)	-0.04329	0.506762

S only :	R	CN	c_2	F
Initial	1.8	1	-0.02044	----
	1.6224	0.2243	"	0.533847
	1.6059	0.9354	-0.04840	0.385836
	1.6048	(1)	-0.05016	0.386334

Fits of CDHRD.FIL2 :

N only :	R	CN	c_2	F
Initial	2.2	3	-0.02297	----
	2.0798	3.5449	"	1.24005
	2.0791	3.6788	-0.02357	1.23968
	2.0821	(3)	-0.02088	1.24820

S only :	R	CN	c_2	F
Initial	2.2	2	-0.02044	----
	2.2403	1.8164	"	0.379339
	2.2399	2.0361	-0.02226	0.360653
	2.2400	(2)	-0.02202	0.361055
	2.2389	(3)	-0.02807	0.531841

N + S :

	R_N	CN_N	c_{2N}	R_S	CN_S	c_{2S}	F
Initial	1.9	2	-0.02297	2.2	2	-0.02044	-----
##	1.9750	"	"	2.2599	"	"	0.858254
	1.8890	0.4937	"	2.2401	1.9343	"	0.253392
	1.8711	3.7475	-0.07541	2.2430	1.9986	-0.02167	0.153089
	1.9931	(1)	-0.02260	2.2523	(1)	-0.01314	0.482859
	1.9931	(2)	-0.03557	2.2503	(1)	-0.01385	0.429123
	1.9895	(3)	-0.04505	2.2487	(1)	-0.01407	0.404089
**	1.8777	(1)	-0.03842	2.2415	(2)	-0.02133	0.199267
	1.8763	(2)	-0.05466	2.2427	(2)	-0.02147	0.166762
	1.8732	(3)	-0.06728	2.2430	(2)	-0.02161	0.154976
	1.8229	(1)	-0.03090	2.2374	(3)	-0.02726	0.316474
	1.8147	(2)	-0.04621	2.2393	(3)	-0.02706	0.317938
	1.8074	(3)	-0.05859	2.2403	(3)	-0.02709	0.330015

— these R values used as starting values in the fixed-CN fit.

** — of the fixed-CN fits, this one has the best initial fit (F = 0.612090). Next best initial fit is F = 0.858254 (for Ni-N_2S_2).

N + N' :

	R_N	CN_N	c_{2N}	$R_{N'}$	$CN_{N'}$	$c_{2N'}$	F
Initial	2.0	2	-0.02297	2.2	4	-0.02297	-----
##	1.8870	"	"	2.0777	"	"	1.04605
	1.8879	2.3569	"	2.0791	5.7030	"	0.738293
	1.9528	5.8440	-0.04212	2.1044	2.8989	-0.01699	0.642506
	1.9168	(2)	-0.01953	2.0898	(4)	-0.01743	0.720253

— these R values used as starting values in the fixed-CN fit.

S + S' :

	R_S	CN_S	c_{2S}	$R_{S'}$	$CN_{S'}$	$c_{2S'}$	F
Initial	2.0	2	-0.02044	2.2	2	-0.02044	-----
##	2.1808	"	"	2.3094	"	"	1.03127
	2.0573	0.3326	"	2.2411	2.1054	"	0.184136
	2.0888	1.2864	-0.05663	2.2454	2.0398	-0.02169	0.0816660
	2.1853	(1)	-0.02467	2.2654	(1)	-0.01543	0.254993
	2.1942	(2)	-0.04635	2.2502	(1)	-0.01530	0.196338
	2.0916	(1)	-0.04862	2.2457	(2)	-0.02128	0.0928909
**	2.0949	(2)	-0.07426	2.2446	(2)	-0.02175	0.100208
	2.0098	(1)	-0.03894	2.2388	(3)	-0.02593	0.184192
	2.0152	(2)	-0.06191	2.2423	(3)	-0.02649	0.266388

— these R values used as starting values in the fixed-CN fit.
** — of the fixed-CN fits, this one has the best initial fit (F = 1.03127). Next best initial fit is F = 1.07154 (for Ni-S_1S_1).

Fits of CDHRD.FIL3 :

N + S :

	R_N	CN_N	c_{2N}	R_S	CN_S	c_{2S}	F
Initial	1.9	2	-0.02297	2.2	2	-0.02044	-----
	1.8700	"	"	2.2341	"	"	0.743142
	1.8713	1.1897	"	2.2363	2.1245	"	0.429883
	1.8462	1.4783	-0.02572	2.2347	3.0249	-0.02634	0.226235
	1.9439	(1)	-0.02831	2.2447	(1)	-0.01283	0.834657
	1.9502	(2)	-0.03653	2.2470	(1)	-0.01301	0.714210
	1.9532	(3)	-0.04233	2.2482	(1)	-0.01320	0.621341
**	1.8690	(1)	-0.02420	2.2369	(2)	-0.02069	0.450366
	1.8847	(2)	-0.03413	2.2416	(2)	-0.02034	0.357920
	1.8941	(3)	-0.04118	2.2445	(2)	-0.02042	0.309399
	1.8413	(1)	-0.02056	2.2324	(3)	-0.02676	0.247253
	1.8520	(2)	-0.03040	2.2371	(3)	-0.02586	0.239318
	1.8601	(3)	-0.03765	2.2408	(3)	-0.02563	0.301789

— these R values used as starting values in each of the fixed-CN fits.
** — of the fixed-CN fits, this one has the best initial fit (F = 0.463157). Next best initial fit is F = 0.743142 (for Ni-N_2S_2).

N + N' :

	R_N	CN_N	c_{2N}	$R_{N'}$	$CN_{N'}$	$c_{2N'}$	F
Initial	1.9	2	-0.02297	2.2	4	-0.02297	-----
##	1.8714	"	"	2.0719	"	"	1.06640
	1.8786	3.3869	"	2.0742	6.5165	"	0.599615
	1.9309	9.6969	-0.04838	2.1030	3.7629	-0.01922	0.382274
	1.8963	(2)	-0.01826	2.0805	(4)	-0.01744	0.831311

— these R values used as starting values in the fixed-CN fit.

S + S' :

	R_S	CN_S	c_{2S}	$R_{S'}$	$CN_{S'}$	$c_{2S'}$	F
Initial	1.9	2	-0.02044	2.2	2	-0.02044	-----
	1.9976	"	"	2.2108	"	"	2.42063
	2.0459	0.6244	"	2.2379	2.3938	"	0.512846
	1.9721	0.3346	-0.01151	2.2205	3.9545	-0.03214	0.348967
	2.1691	(1)	-0.02776	2.2596	(1)	-0.01425	0.688567
	2.1762	(2)	-0.04251	2.2543	(1)	-0.01487	0.534805
	2.1800	(3)	-0.05303	2.2513	(1)	-0.01494	0.463262
**	2.0919	(1)	-0.03247	2.2490	(2)	-0.01980	0.512119
	2.1150	(2)	-0.04741	2.2520	(2)	-0.02110	0.481359
	2.1278	(3)	-0.06086	2.2505	(2)	-0.02192	0.510134
	2.0346	(1)	-0.02847	2.2386	(3)	-0.02422	0.436179
	2.0649	(2)	-0.04307	2.2484	(3)	-0.02493	0.525038
	2.0793	(3)	-0.05639	2.2507	(3)	-0.02614	0.628742

— these R values used as starting values in each of the fixed-CN fits.

** — of the fixed-CN fits, this one has the best initial fit (F = 1.20716). Next best initial fit is F = 1.24502 (for Ni-S_1S_3).

Fits of CDHRD.FIL6 :

N + S :

	R_N	CN_N	c_{2N}	R_S	CN_S	c_{2S}	F
Initial	1.9	2	-0.02297	2.2	2	-0.02044	-----
##	1.8697	"	"	2.2346	"	"	0.799125
	1.8720	1.3047	"	2.2368	2.2096	"	0.519996
	1.9583	11.9063	-0.07304	2.2489	1.0066	-0.01325	0.400760
	1.9391	(1)	-0.02534	2.2454	(1)	-0.01173	0.856339
	1.9451	(2)	-0.03419	2.2478	(1)	-0.01194	0.738258
	1.9482	(3)	-0.04040	2.2490	(1)	-0.01216	0.650253
**	1.8734	(1)	-0.02222	2.2370	(2)	-0.01979	0.564461
	1.8851	(2)	-0.03190	2.2416	(2)	-0.01943	0.489761
	1.8926	(3)	-0.03883	2.2445	(2)	-0.01947	0.460015
	1.8470	(1)	-0.01936	2.2326	(3)	-0.02591	0.507370
	1.8550	(2)	-0.02889	2.2371	(3)	-0.02505	0.495076
	1.8613	(3)	-0.03588	2.2406	(3)	-0.02480	0.529538

— these R values used as starting values in each of the fixed-CN fits.

** — of the fixed-CN fits, this one has the best initial fit (F = 0.581252). Next best initial fit is F = 0.799125 (for Ni-N_2S_2).

Three-Wave Fits of CODH data, using N, S and Fe

(checked and corrected 1st Mar 1993) Grace Tan 25th Feb 1993

These fits are discussed in Chapter 7, Section (E.2.d).

Fits of CODHX.FIL6 :

N + S + S' :

	R_N	CN_N	c_{2N}	R_S	CN_S	c_{2S}	$R_{S'}$	$CN_{S'}$	$c_{2S'}$	F
Initial	1.9	2	-0.02297	2.2	1	-0.02044	2.3	1	-0.02044	-----
##	1.8519	"	"	2.2252	"	"	2.2253	"	"	0.552837
	1.8531	2.1949	"	2.2252	1.0693	"	2.2252	1.0747	"	0.527269
**	1.8544	2.1777	"	2.2415	8.8200	"	2.2467	-6.7720	"	0.523152
**	1.8544	2.1778	"	2.2415	9.0004	"	2.2466	-6.9521	"	0.523151
**	1.8652	(2)	-0.01966	2.2043	(1)	-0.01158	2.2885	(1)	-0.02212	0.404753
**	1.8571	(2)	-0.01955	2.2182	(2)	-0.01806	2.3784	(1)	-0.03812	0.315513
Initial	1.9	2	-0.02297	2.2	2	-0.02044	2.7	1	-0.02044	-----
	1.8505	"	"	2.2242	"	"	2.8832	"	"	0.663708
	1.8525	2.1711	"	2.2248	2.1280	"	2.8799	0.3614	"	0.455441
	1.8540	(2)	-0.02075	2.2232	(2)	-0.01924	2.9048	(1)	-0.03899	0.419662

** — Use ## as initial value, but reset $R_{S'}$ =2.3 Å

N + S + Fe :

	R_N	CN_N	c_{2N}	R_S	CN_S	c_{2S}	R_{Fe}	CN_{Fe}	c_{2Fe}	F
Initial	1.9	2	-0.02297	2.2	2	-0.02044	2.7	1	-0.01530	-----
	1.8522	"	"	2.2253	"	"	2.7153	"	"	0.781714
	1.8533	2.1387	"	2.2256	2.1073	"	2.7044	0.3085	"	0.440529
	1.8542	(2)	-0.02099	2.2239	(2)	-0.01935	2.7153	(1)	-0.03331	0.385578
Initial	1.9	2	-0.02297	2.2	2	-0.02044	2.9	1	-0.01530	-----
	1.8496	"	"	2.2236	"	"	3.0557	"	"	0.857158
	1.8529	2.1971	"	2.2250	2.1448	"	3.0620	0.1017	"	0.522017
	1.8542	(2)	-0.02077	2.2234	(2)	-0.01924	3.4961	(1)	-0.11151	0.491808

N + S + N' :

	R_N	CN_N	c_{2N}	R_S	CN_S	c_{2S}	$R_{N'}$	$CN_{N'}$	$c_{2N'}$	F
Initial	1.9	2	-0.02297	2.2	2	-0.02044	2.7	2	-0.02297	-----
	1.8526	"	"	2.2262	"	"	2.7163	"	"	0.511719
	1.8536	2.1702	"	2.2258	2.1370	"	2.7107	1.0936	"	0.402787
	1.8545	(2)	-0.02091	2.2239	(2)	-0.01926	2.7142	(2)	-0.03526	0.363383
Initial	1.9	2	-0.02297	2.2	2	-0.02044	2.9	2	-0.02297	-----
	1.8515	"	"	2.2250	"	"	3.0939	"	"	0.700905
	1.8530	2.1981	"	2.2251	2.1458	"	3.0900	0.2218	"	0.524587
	1.8542	(2)	-0.02077	2.2234	(2)	-0.01924	3.4463	(2)	-0.10371	0.491162

Fits of CODHOX.FIL6 :

N + S + S' :

	R_N	CN_N	c_{2N}	R_S	CN_S	c_{2S}	$R_{S'}$	$CN_{S'}$	$c_{2S'}$	F
Initial	1.9	2	-0.02297	2.2	1	-0.02044	2.3	1	-0.02044	-----
	1.8790	"	"	2.2103	"	"	2.2656	"	"	0.686165
	1.8838	1.7987	"	2.2385	2.1830	"	2.4289	0.6161	"	0.488493
	1.8933	(2)	-0.02808	2.2325	(1)	-0.01573	2.2968	(1)	-0.03453	0.516898
	1.8630	(1)	-0.01818	2.2251	(2)	-0.02404	2.3422	(1)	-0.04817	0.509558
	1.8801	(2)	-0.02667	2.2338	(2)	-0.02153	2.3968	(1)	-0.03784	0.427173
Initial	1.9	2	-0.02297	2.2	2	-0.02044	2.7	1	-0.02044	-----
	1.8837	"	"	2.2374	"	"	2.8981	"	"	0.790835
	1.8832	1.3832	"	2.2381	1.6815	"	2.8872	0.4474	"	0.521574
	1.8793	(2)	-0.02947	2.2413	(2)	-0.02334	2.8965	(1)	-0.03276	0.450810

N + S + Fe :

	R_N	CN_N	c_{2N}	R_S	CN_S	c_{2S}	R_{Fe}	CN_{Fe}	c_{2Fe}	F
Initial	1.9	2	-0.02297	2.2	2	-0.02044	2.7	1	-0.01530	-----
	1.9032	"	"	2.2494	"	"	2.6783	"	"	0.950351
	1.8867	1.3724	"	2.2397	1.6676	"	2.7144	0.3022	"	0.548799
	1.8817	(2)	-0.03006	2.2431	(2)	-0.02350	2.7192	(1)	-0.02733	0.391462
Initial	1.9	2	-0.02297	2.2	2	-0.02044	3.0	1	-0.01530	-----
	1.8817	"	"	2.2372	"	"	3.1012	"	"	0.932091
	1.8830	1.4218	"	2.2382	1.7050	"	3.0784	0.1483	"	0.606296
	1.8800	(2)	-0.02940	2.2417	(2)	-0.02331	3.4663	(1)	-0.10724	0.559856

N + S + N' :

	R_N	CN_N	c_{2N}	R_S	CN_S	c_{2S}	$R_{N'}$	$CN_{N'}$	$c_{2N'}$	F
Initial	1.9	2	-0.02297	2.2	2	-0.02044	2.7	2	-0.02297	-----
	1.8912	"	"	2.2422	"	"	2.6974	"	"	0.675035
	1.8870	1.4140	"	2.2402	1.7052	"	2.7092	1.1674	"	0.498797
	1.8814	(2)	-0.02970	2.2427	(2)	-0.02336	2.7197	(2)	-0.02948	0.370963
Initial	1.9	2	-0.02297	2.2	2	-0.02044	3.0	2	-0.02297	-----
	1.8843	"	"	2.2383	"	"	3.1184	"	"	0.811230
	1.8835	1.4237	"	2.2384	1.7055	"	3.1026	0.3345	"	0.610661
	1.8800	(2)	-0.02940	2.2417	(2)	-0.02331	3.4085	(2)	-0.09839	0.559161

Fits of CDHOX.FIL6 :

N + S + S' :

	R_N	CN_N	c_{2N}	R_S	CN_S	c_{2S}	$R_{S'}$	$CN_{S'}$	$c_{2S'}$	F
Initial	1.9	2	-0.02297	2.2	1	-0.02044	2.3	1	-0.02044	-----
	1.8870	"	"	2.2320	"	"	2.2320	"	"	0.623468
	1.8818	1.4035	"	2.2190	1.3286	"	2.2525	0.7842	"	0.473538
	1.9055	(2)	-0.03056	2.2309	(1)	-0.03690	2.2390	(1)	-0.01406	0.445932
Initial	1.9	2	-0.02297	2.2	2	-0.02044	2.3	1	-0.02044	-----
	1.8663	"	"	2.2022	"	"	2.3037	"	"	0.634603
	1.8913	1.5767	"	2.2372	2.2308	"	2.4802	0.3624	"	0.416485
	1.8748	(1)	-0.01880	2.2267	(2)	-0.02080	2.2904	(1)	-0.07375	0.451111
	1.8903	(2)	-0.02690	2.2320	(2)	-0.01950	2.4028	(1)	-0.05055	0.394554
Initial	1.9	2	-0.02297	2.2	2	-0.02044	2.7	1	-0.02044	-----
	1.8845	"	"	2.2305	"	"	2.9019	"	"	0.613206
	1.8831	1.3766	"	2.2308	2.0265	"	2.8983	0.5303	"	0.276810
	1.8899	(2)	-0.02902	2.2348	(2)	-0.02034	2.9040	(1)	-0.03004	0.290559

N + S + Fe :

	R_N	CN_N	c_{2N}	R_S	CN_S	c_{2S}	R_{Fe}	CN_{Fe}	c_{2Fe}	F
Initial	1.9	2	-0.02297	2.2	2	-0.02044	2.7	1	-0.01530	-----
	1.8861	"	"	2.2299	"	"	2.7472	"	"	0.747356
	1.8842	1.3305	"	2.2307	1.9893	"	2.7422	0.4263	"	0.278355
	1.8916	(2)	-0.03001	2.2358	(2)	-0.02079	2.7360	(1)	-0.02557	0.195659
Initial	1.9	2	-0.02297	2.2	2	-0.02044	3.0	1	-0.01530	-----
	1.8815	"	"	2.2298	"	"	3.0791	"	"	0.817655
	1.8831	1.4150	"	2.2311	2.0492	"	3.0732	0.2424	"	0.440239
	1.8906	(2)	-0.02880	2.2352	(2)	-0.02026	3.5570	(1)	-0.10840	0.458161

N + S + N' :

	R_N	CN_N	c_{2N}	R_S	CN_S	c_{2S}	$R_{N'}$	$CN_{N'}$	$c_{2N'}$	F
Initial	1.9	2	-0.02297	2.2	2	-0.02044	2.7	2	-0.02297	-----
	1.8905	"	"	2.2331	"	"	2.7382	"	"	0.522501
	1.8858	1.3835	"	2.2320	2.0265	"	2.7388	1.3338	"	0.245315
	1.8919	(2)	-0.02960	2.2359	(2)	-0.02059	2.7369	(2)	-0.02802	0.187309
Initial	1.9	2	-0.02297	2.2	2	-0.02044	3.0	2	-0.02297	-----
	1.8852	"	"	2.2314	"	"	3.1016	"	"	0.705976
	1.8838	1.4194	"	2.2314	2.0494	"	3.0946	0.5123	"	0.458226
	1.8907	(2)	-0.02880	2.2352	(2)	-0.02026	3.4796	(2)	-0.10393	0.457038

Fits of CODHRX.FIL6 :

N + S + S' :

	R_N	CN_N	c_{2N}	R_S	CN_S	c_{2S}	$R_{S'}$	$CN_{S'}$	$c_{2S'}$	F
Initial	1.9	2	-0.02297	2.2	2	-0.02044	2.3	1	-0.02044	-----
	1.8863	"	"	2.2392	"	"	2.2749	"	"	0.906768
	1.8886	1.9373	"	2.2511	1.8835	"	2.2512	0.9428	"	0.896653
	1.8373	(2)	-0.02378	2.1825	(2)	-0.01279	2.3168	(1)	-0.00384	0.367692
Initial	1.9	2	-0.02297	2.2	3	-0.02044	2.3	1	-0.02044	-----
	1.8765	"	"	2.2309	"	"	2.3360	"	"	1.15023
	1.8886	1.9373	"	2.2512	2.2484	"	2.2509	0.5778	"	0.896653
	1.8152	(2)	-0.02753	2.1845	(3)	-0.02364	2.3070	(1)	-0.00802	0.578308
Initial	1.9	2	-0.02297	2.2	3	-0.02044	2.7	1	-0.02044	-----
	1.8906	"	"	2.2519	"	"	2.6230	"	"	0.725640
	1.8877	1.6913	"	2.2514	2.6116	"	2.6224	0.8430	"	0.544102
	1.8765	(2)	-0.02800	2.2531	(3)	-0.02359	2.6104	(1)	-0.01857	0.444381
Initial	1.9	2	-0.02297	2.2	3	-0.02044	2.9	1	-0.02044	-----
	1.8873	"	"	2.2504	"	"	2.9466	"	"	1.02479
	1.8878	1.9341	"	2.2508	2.8243	"	2.9423	0.2933	"	0.872221
	1.8846	(2)	-0.02409	2.2509	(3)	-0.02120	3.2334	(1)	-0.02794	0.868847

N + S + Fe :

	R_N	CN_N	c_{2N}	R_S	CN_S	c_{2S}	R_{Fe}	CN_{Fe}	c_{2Fe}	F
Initial	1.9	2	-0.02297	2.2	3	-0.02044	2.7	1	-0.01530	-----
	1.8840	"	"	2.2485	"	"	2.8020	"	"	0.880066
	1.8852	1.9038	"	2.2495	2.7983	"	2.7982	0.5573	"	0.755406
	1.8799	(2)	-0.02455	2.2494	(3)	-0.02157	2.7970	(1)	-0.01838	0.825711
Initial	1.9	2	-0.02297	2.2	3	-0.02044	3.0	1	-0.01530	-----
	1.8863	"	"	2.2501	"	"	3.0907	"	"	0.860810
	1.8866	1.9567	"	2.2503	2.8376	"	3.0882	0.5898	"	0.788659
	1.8834	(2)	-0.02397	2.2503	(3)	-0.02119	3.0882	(1)	-0.01926	0.829862

N + S + N' :

	R_N	CN_N	c_{2N}	R_S	CN_S	c_{2S}	$R_{N'}$	$CN_{N'}$	$c_{2N'}$	F
Initial	1.9	2	-0.02297	2.2	3	-0.02044	2.7	2	-0.02297	-----
	1.8878	"	"	2.2506	"	"	2.8147	"	"	0.886183
	1.8875	1.9325	"	2.2507	2.8219	"	2.8120	1.1764	"	0.829866
	1.8816	(2)	-0.02443	2.2501	(3)	-0.02147	2.8078	(2)	-0.02122	0.858402
Initial	1.9	2	-0.02297	2.2	3	-0.02044	3.0	2	-0.02297	-----
	1.8884	"	"	2.2509	"	"	3.0958	"	"	0.877716
	1.8878	1.9487	"	2.2508	2.8328	"	3.0936	1.2968	"	0.841414
	1.8840	(2)	-0.02408	2.2506	(3)	-0.02121	3.0928	(2)	-0.02284	0.860931

Fits of CDHRD.FIL6 :

N + S + S' :

	R_N	CN_N	c_{2N}	R_S	CN_S	c_{2S}	$R_{S'}$	$CN_{S'}$	$c_{2S'}$	F
Initial	1.9	2	-0.02297	2.2	1	-0.02044	2.3	1	-0.02044	-----
##	1.8698	"	"	2.2345	"	"	2.2346	"	"	0.799128
	1.8492	1.2103	"	2.1561	0.6860	"	2.2554	2.0532	"	0.481828
**	1.8763	(2)	-0.02942	2.1852	(1)	-0.01066	2.3006	(1)	-0.01019	0.477713
Initial	1.9	2	-0.02297	2.2	2	-0.02044	2.3	1	-0.02044	-----
	1.8576	"	"	2.2084	"	"	2.3016	"	"	0.599538
	1.8492	1.2110	"	2.1563	0.6880	"	2.2555	2.0513	"	0.481828
	1.8747	(2)	-0.03031	2.2380	(2)	-0.01968	2.3052	(1)	-0.06122	0.422606
Initial	1.9	1	-0.02297	2.2	1	-0.02044	2.3	1	-0.02044	-----
	1.8693	"	"	2.2368	"	"	2.2368	"	"	0.573818
	1.8493	1.2117	"	2.2555	2.0495	"	2.1565	0.6890	"	0.481829
	1.8517	(1)	-0.01866	2.1682	(1)	-0.00872	2.2967	(1)	-0.00741	0.516684
Initial	1.9	2	-0.02297	2.2	2	-0.02044	2.7	1	-0.02044	-----
	1.9645	"	"	2.2671	"	"	2.5365	"	"	1.10544
	1.8492	1.2097	"	2.1559	0.6848	"	2.2554	2.0548	"	0.481828
	1.8746	(2)	-0.03031	2.2379	(2)	-0.01968	2.3051	(1)	-0.06118	0.422606
Initial	1.9	2	-0.02297	2.2	2	-0.02044	2.9	1	-0.02044	-----
	1.8661	"	"	2.2331	"	"	2.9192	"	"	0.798418
	1.8703	1.2870	"	2.2361	2.1980	"	2.9158	0.5007	"	0.375228
	1.8843	(2)	-0.03194	2.2413	(2)	-0.01945	2.9200	(1)	-0.03250	0.350360

** — Initial values in ##, except that R_S = 2.2 Å and $R_{S'}$ = 2.3 Å.

N + S + Fe :

	R_N	CN_N	c_{2N}	R_S	CN_S	c_{2S}	R_{Fe}	CN_{Fe}	c_{2Fe}	F
Initial	1.9	2	-0.02297	2.2	2	-0.02044	2.7	1	-0.01530	-----
	1.8614	"	"	2.2305	"	"	2.7706	"	"	0.905008
	1.8692	1.2500	"	2.2356	2.1686	"	2.7634	0.3787	"	0.398986
	1.8853	(2)	-0.03263	2.2419	(2)	-0.01970	2.7504	(1)	-0.02892	0.332579
Initial	1.9	2	-0.02297	2.2	2	-0.02044	3.0	1	-0.01530	-----
	1.8660	"	"	2.2334	"	"	3.0939	"	"	0.960752
	1.8712	1.3182	"	2.2365	2.2176	"	3.0912	0.2249	"	0.493907
	1.8851	(2)	-0.03190	2.2416	(2)	-0.01943	3.5213	(1)	-0.09818	0.487815

N + S + N' :

	R_N	CN_N	c_{2N}	R_S	CN_S	c_{2S}	$R_{N'}$	$CN_{N'}$	$c_{2N'}$	F
Initial	1.9	2	-0.02297	2.2	2	-0.02044	2.7	2	-0.02297	-----
	1.8689	"	"	2.2342	"	"	2.7620	"	"	0.763094
	1.8718	1.2732	"	2.2368	2.1917	"	2.7563	1.1703	"	0.383414
	1.8858	(2)	-0.03236	2.2420	(2)	-0.01957	2.7474	(2)	-0.03195	0.326899
Initial	1.9	2	-0.02297	2.2	2	-0.02044	3.0	2	-0.02297	-----
	1.8689	"	"	2.2344	"	"	3.1171	"	"	0.871425
	1.8718	1.3128	"	2.2367	2.2145	"	3.1125	0.4487	"	0.509074
	1.8852	(2)	-0.03191	2.2416	(2)	-0.01943	3.4447	(2)	-0.09193	0.485990